Justus Liebig University Giessen & Agricultural University of Tirana

Occurrence and partitioning of selected micropollutants in the Ishmi River Basin, Albania: water treatment under use of low-cost functionalized magneto clay-biochar composites for naproxen, carbamazepine, Cd(II), Cr(VI), and Cu(II) removal

Cumulative Dissertation

For obtaining the doctoral degree

Doctor rerum naturalium (Dr. rer. nat.)

at the

Faculty of Agricultural Sciences, Nutritional Sciences, and Environmental Management
Justus Liebig University Giessen

&

Doctor of Environmental Sciences (Dr.)
at the
Faculty of Agriculture and Environment
Agricultural University of Tirana

Submitted by

Aleksandër Peqini (M.Sc. Agro-environment Engineering)

Born in Belsh, Albania

Giessen, 2026

With the permission of the Faculty of Agricultural Sciences,

Nutritional Sciences and Environmental Management

Justus Liebig University Giessen

&

Faculty of Agriculture and Environment

Agricultural University of Tirana

Board of Examiners

1. Reviewer, Supervisor	Prof. Dr. Rolf-Alexander Düring
2. Reviewer, Supervisor	Prof. Dr. Ferdi Brahushi
Examiner	Prof. Dr. Susanne Jacobs
Examiner	Prof. Dr. Fatbardh Sallaku
Examiner	Prof. Dr. Lutz Breuer

Table of contents

List of Figures

List of Tables

List of Abbreviations

ACN	acetonitrile
AETM	anhydro-erythromycin
Al	aluminum
ANOVA	analysis of variance
APs	antiepileptics
ATM	azithromycin
BC	biochar
BET	brunauer-emmett-teller
Ca	calcium
$CaCl_2$	calcium chloride
$CaCO_3$	carbonates
CAFF	caffeine
CBZ	carbamazepine
Cd(II)	cadmium
C_e	equilibrium concentration of analyte
CEC	cation exchange capacity
CFC	ciprofloxacin
CMC	clindamycin
C_o	initial concentration of analyte
Cr(VI)	chromium
C_s	concentration in the sediment phase
Cu(II)	copper
C_w	concentration in the water phase
DAs	diaminopyrimidines
DCF	diclofenac
DOM	dissolved organic matter
D_{ow}	pH-dependent *n*-octanol-water partition coefficient
ECs	emerging contaminants
EDTA	ethylenediaminetetraacetic acid disodium salt dihydrate
ETM	erythromycin
EU	European Union
Fe	iron
Fe_3O_4	magnetite
FLC	feldspar clay
f_{oc}	fraction of organic carbon
FQs	fluoroquinolones
FTIR	fourier transform infrared
GCW	grape cluster waste
H_2SO_4	sulfuric acid
H_3PO_4	phosphoric acid
HCl	hydrochloric acid

HPLC-UV/FLD	high-performance liquid chromatography with ultraviolet and fluorescence detection
HPLC-MS/MS	high-performance liquid chromatography coupled with tandem mass spectrometry
IBU	ibuprofen
IC	inorganic carbon
ICP-OES	inductively coupled plasma optical emission spectroscopy
IPD	intraparticle diffusion model
IR1	Ishmi River 1
IR2	Ishmi River 2
IR3	Ishmi River 3
K	potassium
K_d	sediment-water partition coefficient
KH_2PO_4	potassium dihydrogen phosphate
K_{oc}	organic carbon-normalized partition coefficient
K_{ow}	*n*-octanol-water partition coefficient
LOD	limit of detection
LOQ	limit of quantification
LR1	Lana River 1
MBC-*x*	magneto-biochar-clay composite
Mg	magnesium
MLs	macrolides
MNP	magnetic nanoparticles
MW	molecular weight
Na	sodium
NaN_3	sodium azide
NaOH	sodium hydroxide
n.d.	not detected
NPX	naproxen
NSAIDs	non-steroidal anti-inflammatory drugs
OC	organic carbon
PFOM	pseudo-first-order model
pHpzc	pH of point zero charge
pK_a	acid dissociation constant
PSOM	pseudo-second-order model
PTFE	polytetrafluoroethylene
q_e	adsorption capacity in equilibrium
q_t	adsorption capacity at a certain time
R	universal gas constant
RMSE	root mean square error
SAs	sulfonamides
SEM	scanning electron microscope
SMs	stimulants
SMX	sulfamethoxazole

SPE	solid phase extraction
TH	total hydrogen
TMP	trimethoprim
TN	total nitrogen
TOC	total carbon
TR1	Tirana River 1
TR2	Tirana River 2
TS	total sulfur
v	volume
WP	work package
WWTPs	waste water treatment plants
XRD	x-ray diffractometer
$\Delta G°$	gibbs free energy
$\Delta H°$	enthalpy
$\Delta S°$	entropy

Summary

Water contamination by pharmaceuticals (“micropollutants”) and heavy metals represents a growing environmental challenge worldwide, particularly in regions where wastewater treatment infrastructure and environmental monitoring programs remain limited. Albania is one such case, where scientific evidence on the occurrence, environmental behaviour, and management of these contaminants is still scarce despite increasing pressures from urbanization, population growth, and pharmaceutical consumption. Addressing these knowledge gaps requires not only improved understanding of contaminant distribution in aquatic systems but also the development of sustainable and affordable treatment solutions.

This cumulative dissertation combines environmental monitoring and remediation research to investigate contaminant occurrence and their fate in the Ishmi River basin, Albania, and to develop low-cost materials for water treatment applications. The research is structured around three combined studies.

The first study provides a comprehensive assessment of the occurrence and environmental behaviour of selected pharmaceuticals in surface waters and sediments. By examining spatial and seasonal variations and evaluating sediment–water partitioning under natural environmental conditions, the study identifies the factors controlling contaminant distribution within the river system. The findings demonstrate that pharmaceutical behaviour is governed by a combination of compound-specific properties and in-situ sediment characteristics, highlighting the importance of site-specific approaches for predicting contaminant fate in aquatic environments. Furthermore, the study contributes to a valuable baseline data for a region where information on pharmaceutical contamination has previously been very limited and scarce.

Building upon the knowledge gained from environmental monitoring, the second and third studies focus on the development of innovative magneto-biochar-clay composites produced from locally available and low-cost materials. The introduce of biochar derived from grape cluster stalk waste, feldspar clay, and magnetic nanoparticles resulted in multifunctional composites with improved physico-chemical properties and magnetic recoverability. These materials were evaluated as sustainable adsorbents for the removal of both organic and inorganic contaminants from water.

The developed composites demonstrated strong potential for contaminant removal under environmentally relevant conditions. Their performance was confirmed for pharmaceuticals representing persistent organic micropollutants as well as for toxic heavy metals frequently

encountered in contaminated waters. In addition to high removal efficiencies, the composites exhibited good stability and reusability, indicating their suitability for practical water treatment applications. The use of agricultural waste as a raw material further supports principles of resource recovery, circular economy, and sustainable environmental management.

A major contribution of this dissertation is the integration of contaminant monitoring, environmental fate assessment, and remediation technology development within a single research framework. The results improve scientific understanding of selected pharmaceutical distribution and partitioning processes in riverine environments while simultaneously providing practical solutions for contaminant removal. This combined approach demonstrates how environmental observations can be translated into targeted remediation strategies tailored to local conditions.

Overall, the findings contribute new knowledge on pharmaceutical occurrence and sediment–water interactions in an understudied region of southeastern Europe and demonstrate the applicability of low-cost magneto-biochar-clay composites as sustainable water treatment materials. The outcomes support future water-quality management efforts in Albania and provide scientific evidence relevant to the implementation of European Union (EU) water protection objectives in countries undergoing environmental and regulatory transition.

Përmbledhje

Ndotja e ujërave nga produktet farmaceutike (“mikrondotësit”) dhe metalet e rënda përbën një sfidë mjedisore gjithnjë në rritje në nivel global, veçanërisht në rajonet ku infrastruktura për trajtimin e ujërave të ndotura dhe programet e monitorimit mjedisor mbeten të kufizuara. Shqipëria përfaqëson një rast të tillë, ku evidenca shkencore mbi praninë, sjelljen mjedisore dhe menaxhimin e këtyre ndotësve është ende e pakët, pavarësisht presioneve në rritje të shkaktuara nga urbanizimi, rritja e popullsisë dhe konsumi i produkteve farmaceutike. Plotësimi i këtyre boshllëqeve njohurish kërkon jo vetëm një kuptim më të mirë të shpërndarjes së ndotësve në sistemet ujore, por edhe zhvillimin e zgjidhjeve të qëndrueshme dhe ekonomikisht të përballueshme për trajtimin e tyre.

Kjo tezë kumulative kombinon monitorimin mjedisor dhe kërkimin mbi rehabilitimin e ujërave për të studiuar praninë dhe fatin mjedisor të ndotësve në basenin e lumit Ishëm në Shqipëri, si dhe për të zhvilluar materiale me kosto të ulët për aplikime në trajtimin e ujit. Kërkimi është strukturuar në tre studime të ndërlidhura.

Studimi i parë ofron një vlerësim gjithëpërfshirës të pranisë dhe sjelljes mjedisore të produkteve farmaceutike të përzgjedhura në ujërat sipërfaqësore dhe sedimente. Nëpërmjet analizës së ndryshimeve hapësinore dhe sezonale, si dhe vlerësimit të shpërndarjes sediment–ujë në kushte natyrore mjedisore, studimi identifikon faktorët që kontrollojnë shpërndarjen e ndotësve brenda sistemit lumor. Rezultatet tregojnë se sjellja e produkteve farmaceutike përcaktohet nga kombinimi i vetive specifike të komponimeve dhe karakteristikave in-situ të sedimenteve, duke theksuar rëndësinë e qasjeve të përshtatura sipas kushteve lokale për parashikimin e fatit të ndotësve në mjediset ujore. Për më tepër, studimi kontribuon me të dhëna bazë të vlefshme për një rajon ku informacioni mbi ndotjen farmaceutike ka qenë deri më tani shumë i kufizuar.

Duke u mbështetur në njohuritë e fituara nga monitorimi mjedisor, studimi i dytë dhe i tretë fokusohen në zhvillimin e kompoziteve inovative magneto-biochar-argjilë, të prodhuara nga materiale lokale dhe me kosto të ulët. Përdorimi i biochar-it të përftuar nga kërcelli i cepit të rrushit, argjilës feldspatike dhe nanogrimcave magnetike rezultoi në kompozite multifunksionale me veti fiziko-kimike të përmirësuara dhe rikuperueshmëri magnetike. Këto materiale u vlerësuan si adsorbentë të qëndrueshëm për largimin e ndotësve organikë dhe inorganikë nga uji.

Kompozitet e zhvilluara demonstruan potencial të lartë për largimin e ndotësve në kushte mjedisore reale. Efektiviteti i tyre u konfirmua si për farmaceutikët që përfaqësojnë

mikrondotës organikë persistentë, ashtu edhe për metalet e rënda toksike që gjenden shpesh në ujërat e ndotura. Përveç efikasitetit të lartë të largimit, kompozitet treguan stabilitet dhe ripërdorshmëri të mirë, duke dëshmuar përshtatshmërinë e tyre për aplikime praktike në trajtimin e ujërave. Përdorimi i mbetjeve bujqësore si lëndë e parë mbështet gjithashtu parimet e rikuperimit të burimeve, ekonomisë qarkulluese dhe menaxhimit të qëndrueshëm mjedisor.

Një nga kontributet kryesore të kësaj teze është integrimi i monitorimit të ndotësve, vlerësimit të fatit të tyre mjedisor dhe zhvillimit të teknologjive të rehabilitimit brenda një kuadri të vetëm kërkimor. Rezultatet përmirësojnë kuptimin shkencor të proceseve të shpërndarjes dhe ndarjes së produkteve farmaceutike të përzgjedhura në mjediset lumore, duke ofruar njëkohësisht zgjidhje praktike për largimin e ndotësve. Kjo qasje e integruar demonstron se si vëzhgimet mjedisore mund të shndërrohen në strategji rehabilitimi të orientuara dhe të përshtatura sipas kushteve lokale.

Në përgjithësi, gjetjet e kësaj teze kontribuojnë me njohuri të reja mbi praninë e produkteve farmaceutike dhe ndërveprimet sediment–ujë në një rajon pak të studiuar të Evropës Juglindore, si dhe demonstrojnë zbatueshmërinë e kompoziteve magneto-biochar-argjilë me kosto të ulët si materiale të qëndrueshme për trajtimin e ujit. Rezultatet mbështesin përpjekjet e ardhshme për menaxhimin e cilësisë së ujit në Shqipëri dhe ofrojnë evidencë shkencore të rëndësishme për zbatimin e objektivave të Bashkimit Evropian (BE) për mbrojtjen e ujërave në vendet që kalojnë procese transformimi mjedisor dhe rregullator.

Zusammenfassung

Die Belastung von Gewässern durch Arzneimittelrückstände („Mikroschadstoffe“) und Schwermetalle stellt weltweit eine zunehmende Umweltproblematik dar, insbesondere in Regionen mit begrenzter Abwasserinfrastruktur und unzureichenden Umweltüberwachungsprogrammen. Albanien gehört zu diesen Regionen, da wissenschaftliche Erkenntnisse über das Vorkommen, das Umweltverhalten und das Management dieser Schadstoffe bislang nur begrenzt verfügbar sind, obwohl Urbanisierung, Bevölkerungswachstum und Arzneimittelverbrauch kontinuierlich zunehmen. Die Schließung dieser Wissenslücken erfordert sowohl ein besseres Verständnis der Schadstoffverteilung in aquatischen Systemen als auch die Entwicklung nachhaltiger und wirtschaftlich tragfähiger Behandlungsverfahren.

Diese kumulative Dissertation verbindet Umweltmonitoring und Sanierungsforschung, um das Vorkommen von Schadstoffen und deren Umweltverhalten im Einzugsgebiet des Ishmi-Flusses in Albanien zu untersuchen sowie kostengünstige Materialien für Anwendungen in der Wasseraufbereitung zu entwickeln. Die Forschungsarbeit ist in drei miteinander verknüpfte Studien gegliedert.

Die erste Studie liefert eine umfassende Bewertung des Vorkommens und Umweltverhaltens ausgewählter Arzneimittel in Oberflächengewässern und Sedimenten. Durch die Untersuchung räumlicher und saisonaler Variationen sowie der Sediment-Wasser-Verteilung unter natürlichen Umweltbedingungen werden die Faktoren identifiziert, die die Schadstoffverteilung innerhalb des Flusssystems steuern. Die Ergebnisse zeigen, dass das Verhalten von Arzneimitteln durch eine Kombination substanzspezifischer Eigenschaften und In-situ-Sedimenteigenschaften bestimmt wird. Dies unterstreicht die Bedeutung standortspezifischer Ansätze zur Vorhersage des Verbleibs von Schadstoffen in aquatischen Ökosystemen. Darüber hinaus liefert die Studie wertvolle Basisdaten für eine Region, in der Informationen zur Arzneimittelbelastung bislang nur sehr begrenzt verfügbar waren.

Aufbauend auf den Erkenntnissen des Umweltmonitorings konzentrieren sich die zweite und dritte Studie auf die Entwicklung innovativer Magneto-Biokohle-Ton-Komposite aus lokal verfügbaren und kostengünstigen Ausgangsmaterialien. Die Verwendung von Biokohle aus Traubenstängeln, Feldspat-Ton und magnetischen Nanopartikeln führte zur Herstellung multifunktionaler Komposite mit verbesserten physikochemischen Eigenschaften und

magnetischer Rückgewinnbarkeit. Diese Materialien wurden als nachhaltige Adsorbentien zur Entfernung organischer und anorganischer Schadstoffe aus Wasser untersucht.

Die entwickelten Kompositen zeigten ein hohes Potenzial zur Schadstoffentfernung unter umweltrelevanten Bedingungen. Ihre Leistungsfähigkeit wurde sowohl für Arzneimittel als persistente organische Mikroschadstoffe als auch für toxische Schwermetalle nachgewiesen, die häufig in belasteten Gewässern vorkommen. Neben hohen Eliminationsraten zeichneten sich die Komposite durch gute Stabilität und Wiederverwendbarkeit aus, was ihre Eignung für praktische Anwendungen in der Wasseraufbereitung unterstreicht. Die Nutzung landwirtschaftlicher Reststoffe als Ausgangsmaterial unterstützt darüber hinaus die Prinzipien der Ressourcenschonung, der Kreislaufwirtschaft und eines nachhaltigen Umweltmanagements.

Ein wesentlicher Beitrag dieser Dissertation besteht in der Verknüpfung von Schadstoffmonitoring, Umweltverhaltensanalysen und der Entwicklung von Sanierungstechnologien innerhalb eines gemeinsamen Forschungsrahmens. Die Ergebnisse erweitern das wissenschaftliche Verständnis der Verteilungs- und Partitionierungsprozesse ausgewählter Arzneimittel in Fließgewässern und liefern gleichzeitig praxisnahe Lösungsansätze zur Schadstoffentfernung. Dieser integrierte Ansatz zeigt, wie Umweltbeobachtungen in gezielte und lokal angepasste Sanierungsstrategien überführt werden können.

Insgesamt liefern die Ergebnisse neue Erkenntnisse über das Vorkommen von Arzneimitteln und deren Sediment-Wasser-Interaktionen in einer bislang wenig untersuchten Region Südosteuropas. Gleichzeitig wird die Anwendbarkeit kostengünstiger Magneto-Biokohle-Ton-Komposite als nachhaltige Materialien für die Wasseraufbereitung aufgezeigt. Die Arbeit unterstützt zukünftige Maßnahmen zum Gewässerschutz in Albanien und liefert wissenschaftliche Grundlagen für die Umsetzung der Wasser- und Gewässerschutzziele der Europäischen Union (EU) in Ländern, die sich in einem umwelt- und regulierungspolitischen Transformationsprozess befinden.

Abstract

This cumulative study explores the occurrence, environmental behavior, and removal of heavy metals and pharmaceuticals (belonging to the group of "micropollutants") through the development of sustainable adsorbents in aquatic systems, with a focus on the Ishmi River basin, Albania. In the first component of this thesis, twelve pharmaceuticals, including caffeine (CAFF), anti-inflammatories (naproxen (NPX), ibuprofen (IBU), and diclofenac (DCF)), antibiotics (anhydro-erythromycin (AETM), azithromycin (ATM), clindamycin (CMC), ciprofloxacin (CFC), erythromycin (ETM), sulfamethoxazole (SMX), and trimethoprim (TMP)), and the antiepileptic carbamazepine (CBZ) were analyzed in surface water and sediment during seasons of the years 2023 and 2024. Highest concentrations occurred near urban areas with limited wastewater treatment, notably at site LR1. Partitioning behavior (K_d, K_{oc}) was significantly influenced by compound-specific (D_{ow}, molecular weight) and sediment-specific (pH, content of organic carbon, $CaCO_3$, and metals) properties, and regression models successfully predicted partition coefficients for NPX, IBU, CFC, AETM, and CMC. In the second component, innovative low-cost magneto-biochar-clay (MBC) composite adsorbents were prepared from the combination of magnetic nanoparticles, biochar (from grape cluster stalk), and feldspar clay and were tested for simultaneously heavy metal removal (Cd(II), Cr(VI), Cu(II)). The MBC 1:2:1 and MBC 1:3:1 showed high adsorption capacities due to enhanced surface area and functional groups. Adsorption was governed by electrostatic interactions and pore filling, with Cr(VI) showing the highest removal efficiency and strong adsorbent reusability over multiple cycles. The third component evaluated the MBC 1:2:1 composite for pharmaceutical removal, specifically NPX and CBZ. The composite demonstrated excellent adsorption performance (≥99% efficiency over five cycles), particularly at low pH values, through electrostatic and hydrophobic interactions. NPX removal remained high (≈93%) even in real Ishmi River water. Overall, the combined findings highlight the influence of environmental and sediment characteristics on pharmaceutical distribution, both the environmental risks posed by pharmaceutical and metal contaminants in under-monitored regions and the effectiveness of MBC composites as sustainable, cost-effective adsorbents for water treatment applications.

Keywords: *Emerging contaminants*; *Sediment-water partitioning*; *Adsorption*; *Magneto-biochar-clay composites*; *Organic contaminants*; *Heavy metals*; *Water treatment*

1. Extended Summary

1.1. Introduction

Pharmaceuticals are biologically active compounds developed and extensively used to prevent and treat human and veterinary diseases (Kümmerer, 2009). They include a wide range of substances such as analgesics/non-steroidal anti-inflammatory drugs (NSAIDs), antibiotics, cardiovascular pharmaceuticals, psycho-stimulants, hormones, and antiepileptic drugs (Li, 2014). Among these, compounds such as caffeine (CAFF), carbamazepine (CBZ), naproxen (NPX), and trimethoprim (TMP) are frequently detected in surface waters across multiple countries and continents, with high concentrations found in lower-middle income countries due to increasing consumption of pharmaceuticals and limited wastewater treatment infrastructure (Wilkinson et al., 2022). While pharmaceuticals are crucial for modern healthcare, their widespread use and incomplete metabolism in humans and animals result in their release into the environment. Pharmaceuticals can enter terrestrial and aquatic systems through various pathways, including excretion by humans and animals, improper disposal of unused medicines, application of sewage sludge (biosolids) to agricultural land, and runoff from pharmaceutical manufacturing (Gerba et al., 2011, Li, 2014, Heyde et al., 2025, Kümmerer, 2010, Li et al., 2022, Matesun et al., 2024, Phillips et al., 2015). The continuous input of pharmaceuticals into the environment raises concerns about their effects on non-target organisms, development of antibiotic resistance, bioaccumulation, and potential impacts on ecosystem functioning. These substances, often termed “emerging contaminants” (ECs) are currently not covered by water-quality regulations and may exert long-term effects that are still poorly understood.

Due to their physicochemical properties and possible bioaccumulation in the food chain, these compounds represent a threat to the environment and non-target organisms (Wang et al., 2021). CAFF, considered as one of the most detected and abundant pharmaceuticals in the environment, is reported to have adverse effects on different aquatic organisms such as polychaete (*Diopatra neapolitana* and *Arenicola marina*, *Hediste diversicolor)*, bivalvia (*Ruditapes philippinarum, Corbicula fluminea)*, sea urchin (*Paracentrotus lividus)*, amphipod (*Ampelisca brevicornis*), crustacean (*Daggerblade grass shrimp*), crab (*Carcinus maenas*), fish (*Neotropical freshwater teleost, Carassius auratus, Dania rerio and fathead minnow*), insects arthropods (*Megaselia. scalaris*) (Li et al., 2020). CBZ toxicity is reported and

confirmed for the parent compound and for its degradation products, which result to be more toxic than the parent compound in bacteria (*Vibrio fischeri*), algae (*Pseudokirchneriellasubcapitata*) and *Daphnia magna* (Donner et al., 2013). The acute toxicity of this compound at *Oncorhynchus mykiss* makes it a very harmful compound for aquatic systems (Li et al., 2011). NPX also can affect organisms in ecosystems through toxicity or that of its metabolites. These metabolites are reported to have more toxicity than parent/main compound to *Brachionuscalyciflorus*, *Thamnocephalusplatyurus*, *Ceriodaphniadubia*, *Vibrio fischeri* and *Daphnia magna* (Della Greca et al., 2003, Jallouli et al., 2016). NPX has adverse effects on gastrointestinal and renal activity of *Dania rerio*, and on liver of *Dania rerio* embryos (Ding et al., 2017, Li et al., 2016). The adverse effects to ecosystems and human health of IBU are attributed to IBU and its degradation products. Ellepola et al. (2020) reported that IBU can be more toxic to human gut microbiota and *Aliivibriofischeri,* meanwhile the degradation products of IBU can be more toxic to human kidney cell line and liver cell line (Cleuvers, 2004). Also IBU is reported to compromise the echinoderm *Psammechinusmiliaris* reproduction (Mohd Zanuri et al., 2017), and to cause nephrotoxicity and immunosuppressive effect on *Rhamdiaquelen* (Mathias et al., 2018). DCF has been reported to have fatal effects on wild vultures (J. Lindsay Oaks et al., 2004, Prakash et al., 2012, Cuthbert et al., 2015). DCF was tested with water species such as crustacean *Daphnia magna* in single compound toxicity tests and in combination with other anti-inflammatory drugs, resulting in higher toxicity compared to other NSAIDs (Cleuvers, 2004). Toxicity tests with *Ceriodaphniadubia sp* and vertebrates such as fish and mussels (*Mytilus spp.)* confirmed a high toxicity of DCF (Connors et al., 2022, Schmidt et al., 2011, Triebskorn et al., 2004).

Antibiotics are widely and increasingly both for human and veterinary use with a growing world population, even though there is a global action plan from the World Health Organization (WHO) on antimicrobial resistance which aims to reduce antibiotic use and their misuse in human, animal and agriculture (WHO, 2015). These compounds negatively affect nontarget species such as algae, bacteria and fish. Robinson et al. (2005) reported that the cyanobacterium *Microcystis aeruginosa* is two to three orders of magnitude more sensitive to fluoroquinolones (ciprofloxacin, lomefloxacin, ofloxacin, levofloxacin, clinafloxacin, enrofloxacin, and flumequine) than green alga *Pseudokirchneriellasubcapitata* (Robinson et al., 2005). Also, the mixture toxicity of antibiotics is reported to have additive toxicity to the green algae (Backhaus, 2016, DeLorenzo and Fleming, 2008).

This cumulative thesis examines the occurrence and environmental behavior of selected pharmaceutical compounds in the sediments and waters of the Ishmi River Basin in Albania (publication 1 or work package (WP) 1 - WP1), as well as the preparation and testing of magneto-biochar-clay composites for the removal of organic and inorganic contaminants from water with publication 2 or WP2 and publication 3 or WP3, respectively.

The first publication or WP1 of this thesis investigates the occurrence and environmental behavior of twelve selected pharmaceuticals in sediments and surface waters of the Ishmi River basin in Albania. These compounds represent different therapeutic classes, including the stimulant CAFF, the antiepileptic CBZ, NSAIDs such as NPX, ibuprofen (IBU), and diclofenac (DCF), and antibiotics including anhydro-erythromycin (AETM), azithromycin (ATM), clindamycin (CMC), ciprofloxacin (CFC), erythromycin (ETM), sulfamethoxazole (SMX), and trimethoprim (TMP). These active pharmaceutical ingredients (API) were chosen due to their environmental relevance and in the context of Albania's obligation, as a European Union (EU) candidate country, to align its water policies with the Water Framework Directive (Directive 2000/60/EC). This directive requires robust monitoring and reporting of water quality status across all water bodies. Based on the latest update of this directive watch list (Commission Implementing Decision (EU) 2025/439), only CMC remains in the watch list, due to insufficient monitoring data, while SMX and TMP were removed in 2024 (completed the four-year monitoring cycle). Other compounds (except CAFF, NPX and AETM) were included in previous versions of the watch list but no longer monitored. In this context, the chosen API belong to the much-discussed group of "micropollutants".

In the second publication or WP2, innovative low-cost magneto-biochar-clay (MBC) composites were developed and tested for the removal of organic contaminants, specifically the pharmaceuticals naproxen (NPX) and carbamazepine (CBZ). The MBC 1:2:1 composite, synthesized from grape cluster waste biochar, feldspar clay, and magnetic nanoparticles, was selected for its superior adsorption properties. Thanks to its magnetic properties, it can be easily separated from the aqueous phase and is available for reuse. Grape cluster stem from grape cultivation is a major component of agricultural waste in central Albania and was collected for this study on a local farm. Due to the favorable climatic conditions in this region, several thousand tons of this agricultural waste are produced there annually, providing a sufficient quantity for water treatment. Sorption experiments evaluated the effects of pH, adsorbent dosage, contact time, dissolved organic matter (DOM), and competition between

NPX and CBZ, as well as performance in real Ishmi River water. Results revealed that both pharmaceuticals were effectively removed through electrostatic and hydrophobic interactions, with maximum adsorption achieved at low pH values. The composite demonstrated excellent reusability, maintaining ≥99% removal efficiency over five regeneration cycles and sustaining high performance under environmentally relevant conditions, confirming its suitability for practical water treatment applications.

In the third publication or WP3, the same MBC composites (MBC 1:2:1 and MBC 1:3:1) were applied to the simultaneous removal of three toxic heavy metals: cadmium (Cd(II)), chromium (Cr(VI)), and copper (Cu(II)). Both MBC 1:2:1 and MBC 1:3:1 composites were tested to determine their adsorption capacities under varying environmental parameters, including adsorbent dosage, pH, contact time, temperature, and initial metal concentration. The results demonstrated rapid and efficient metal uptake, with adsorption primarily driven by electrostatic interactions and pore filling. Among the tested metals, Cr(VI) was removed with highest efficiency. Additionally, the composites maintained strong performance for Cr(VI) over multiple adsorption–desorption cycles, indicating high stability and reusability. These findings highlight the potential of MBC composites as cost-effective and sustainable adsorbents for heavy metal remediation in water systems.

The integration of environmental monitoring with innovative treatment strategies underscores the potential for implementing nature-based and economically viable approaches to improve water quality, especially in regions lacking advanced wastewater treatment infrastructure. The findings of this research contribute to the scientific understanding of contaminant dynamics and support the development of EU-aligned water management policies for Albania and other similar regions facing environmental and regulatory challenges.

1.2. Properties and fate of study selected pharmaceuticals

1.2.1. Physicochemical properties

The selected pharmaceutical compounds used in this study were chosen based on their environmental relevance, consumption data, frequent occurrence in wastewater treatment plants (WWTPs) and surface waters, as well as for their diverse characteristics. These compounds represent different therapeutic classes, such as stimulant (SM), antiepileptic (AP), anti-inflammatories (AMs), antibiotics (macrolides (MLs), fluoroquinolone (FQ), sulfonamide (SA), and diaminopyrimidine (DP)) and physicochemical behaviors, which are crucial for assessing environmental behavior and adsorption. Their molecular weight (MW), water solubility, hydrophobicity (Log K_{ow}), and acid dissociation constants (pK_a) significantly influence their fate in aquatic environments and interaction with sediments. Table 1 provides detailed information on the physicochemical properties of these compounds. In addition to the numerical data summarized in Table 1, the molecular structures of the selected pharmaceuticals are presented separately in Table 2. The structures allow for a clearer understanding of the solubility and polarity, aromaticity, and other structural features that play key roles in their environmental partitioning (Kümmerer, 2009), thus resulting in different sorption behaviors with solid particles such as soils and sediments. Even small changes in their chemical structure may totally change their solubility, polarity, and other properties which control their behavior in the environment (Kümmerer, 2009). Under varying pH and environmental conditions, the physicochemical properties of pharmaceuticals such as molecular structure, solubility, hydrophobicity, speciation (due to pK_a), and partition coefficients (K_d and K_{oc}) differ and govern their sorption–desorption processes, thus governing their transport and mobility between aqueous and solid phases (Patel et al., 2019). Sorption is considered to have an important role on the mobility and (bio)availability of pharmaceuticals in the environment (Tolls, 2001, Kümmerer, 2009). This process also controls their removal through solid particles such as activated carbon or biochar (Zhang et al., 2020). Sorption of pharmaceuticals in the environment is driven by the amount of suspended particles, soil organic matter, soil minerals, and partition coefficient (K_d) (Thiele-Bruhn, 2003), which itself is driven by the combination of physicochemical properties of both compound and sediment (Al-Khazrajy and Boxall, 2016, Tang et al., 2019, Zhao et al., 2016). Therefore, it is essential to investigate their partitioning behavior by

considering both the intrinsic properties of the compounds and site-specific environmental conditions, and to test biochar-based composites for their adsorption from water.

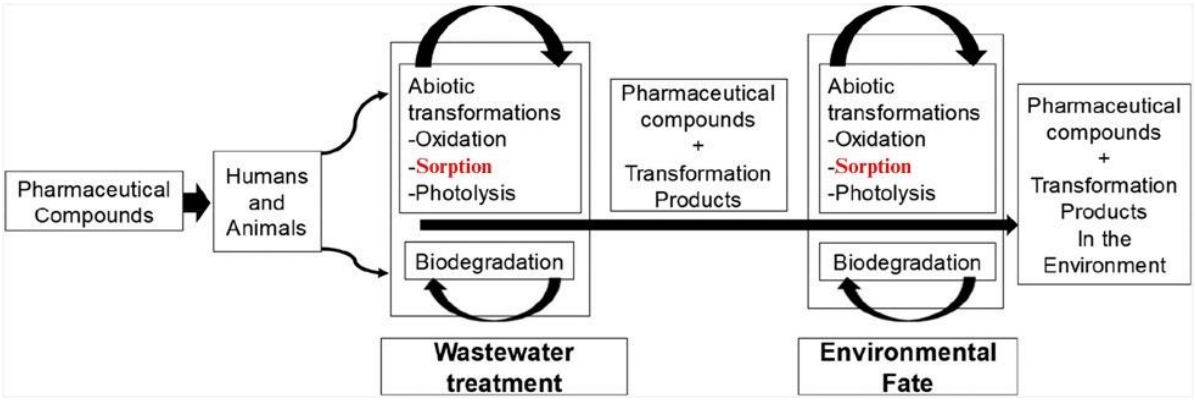

Figure 1. *Schematic illustration of pharmaceutical entry, fate, and transformation pathways in the environment, adapted from Patel et al. (2019). In the adapted figure, the original term "adsorption" was replaced with "sorption" in the adapted figure to reflect both surface and bulk phase partitioning processes that occur in environmental matrices, such as sediment in this case*

As presented in Table 2, the selected pharmaceuticals vary greatly in their functional groups and molecular structure. The presence of functional groups such as carboxylic acids (–COOH), ketones (C=O), hydroxyls (–OH), esters (–COO), ethers (C–O–C), amines ($–NH_2$), halogen atoms (–Cl and –F), and aromatic rings (benzene, pyrimidine), can strongly influence their interactions with solids (soil and suspended particles, sediments, adsorbents). These interactions may occur through electrostatic interactions, hydrogen bonding, and π–π stacking mechanisms between both pharmaceuticals functional groups with the solid matrix active sites (Xu et al., 2021, Heinrich et al., 2021, Olu-Owolabi et al., 2021, Le Guet et al., 2018).

Table 1. *Physicochemical properties of the selected pharmaceutical compounds*

Class	Compound	Acronym	CAS No.	MW	Formula	Water solubility (mg L^{-1})	Log K_{ow}	pK_a
SM	Caffeine	CAFF	58-08-2	194.2	$C_8H_{10}N_4O_2$	20,000	-0.07	10.4
AMs	Diclofenac	DCF	15307-86-5	296.15	$C_{14}H_{11}Cl_2NO_2$	2.37	4.15	4.51
	Naproxen	NPX	22204-53-1	230.26	$C_{14}H_{14}O_3$	15.9	3.18	4.2
	Ibuprofen	IBU	15687-27-1	206.28	$C_{13}H_{18}O_2$	21	3.97	4.91
AP	Carbamazepine	CBZ	298-46-4	236.27	$C_{15}H_{12}N_2O$	17.66	2.45	13.9
MLs	Anhydro-erythromycin	AETM	23893-13-2	715.9	$C_{37}H_{65}NO_{12}$		3.06	8.88
	Azithromycin	ATM	83905-01-5	748.98	$C_{38}H_{72}N_2O_{12}$	2.4	4.02	8.7
	Clindamycin	CMC	18323-49-9	425	$C_{18}H_{33}ClN_2O_5S$		2.16	7.6
	Erythromycin	ETM	114-07-8	733.9	$C_{37}H_{67}NO_{13}$	2,000	3.06	8.9
FQ	Ciprofloxacin	CFC	85721-33-1	331.3	$C_{17}H_{18}FN_3O_3$	30,000	0.28	6.09/8.76
SA	Sulfamethoxazole	SMX	723-46-6	253.3	$C_{10}H_{11}N_3O_3S$	610	0.89	1.85/5.6/5.9
DP	Trimethoprim	TMP	738-70-5	290.3	$C_{13}H_{18}N_4O_3$	400	0.91	3.23/6.76

Source: (Chen and Zhou, 2014, Li et al., 2019b, Moreno-Gonzalez et al., 2015, Zhang et al., 2013)

Table 2. *Molecular structures of the selected pharmaceutical compounds*

Compound	Structure	Compound	Structure
CAFF	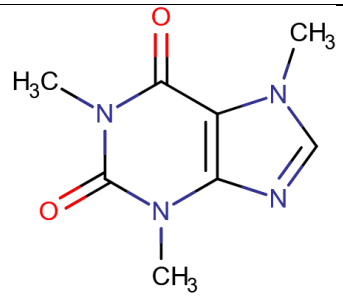	DCF	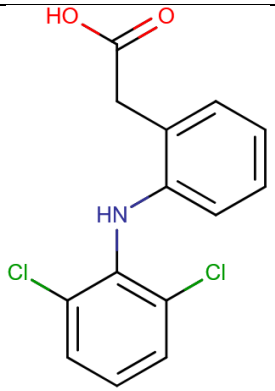
CBZ	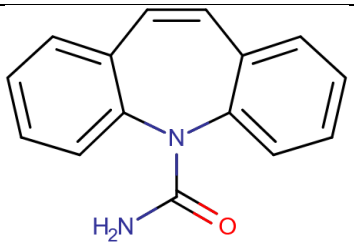	AETM	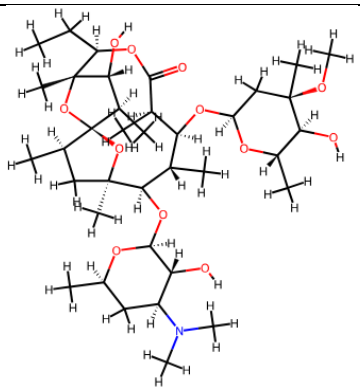

NPX	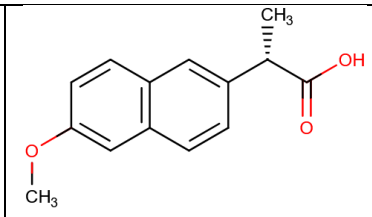	ATM	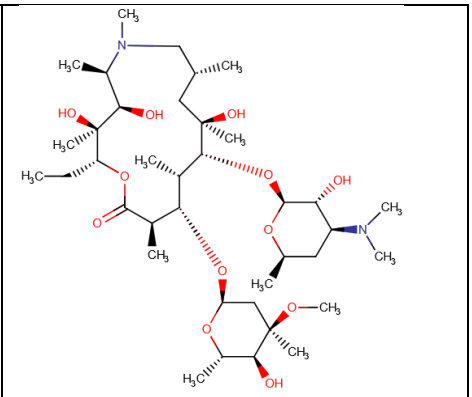
IBU	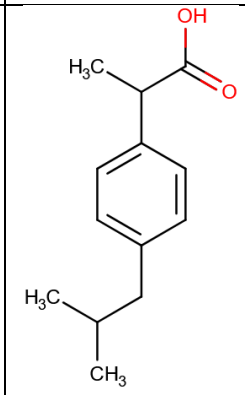	CMC	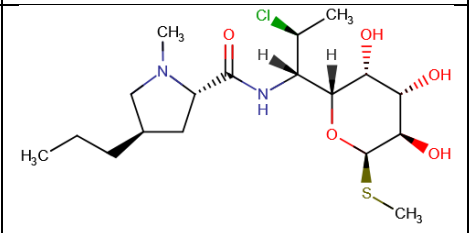
ETM	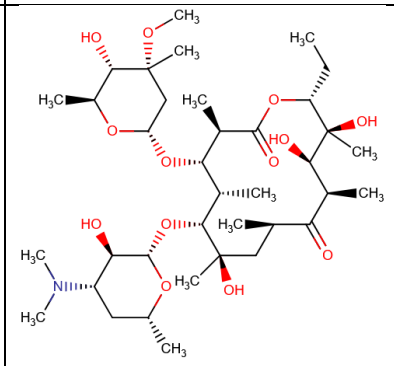	SMX	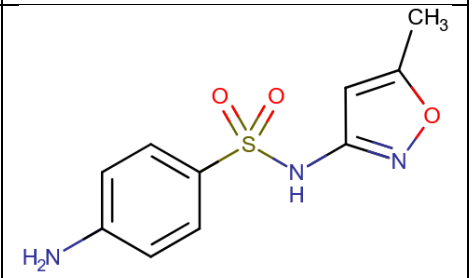
CFC	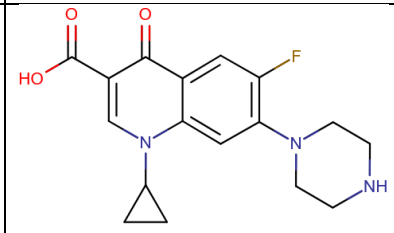	TMP	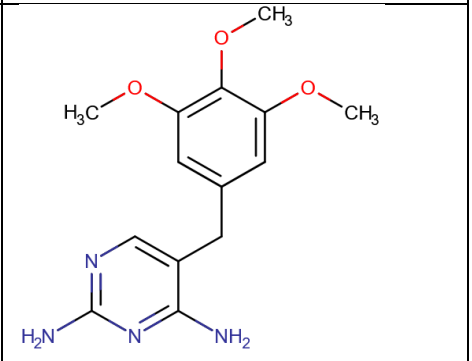

Source: https://go.drugbank.com/ and https://www.chemspider.com/search

Macrolides such as ATM, AETM, ETM, and CMC are characterized by large macrocyclic lactone rings with multiple oxygen-containing functional groups ((C–O–C), (–OH), and

(C=O)), contributing to their relatively high molecular weight and structural complexity (Jednacak et al., 2020). In contrast, compounds such as the stimulant CAFF and NSAIDs like NPX and IBU are structurally smaller and more rigid, typically featuring simpler aromatic or less complex ring systems (Hebig et al., 2017).

DCF, also an NSAID, differs from the others due to its relatively high environmental persistence, attributed largely to its halogenated aromatic structure and ecotoxicological relevance (Wojcieszyńska et al., 2023). The presence of chlorine atoms enhances hydrophobicity and reduces biodegradability, leading to reduced breakdown through hydrolysis, photodegradation, and microbial action (Wojcieszyńska et al., 2023).

Between these extremes are compounds like CBZ, CFC, SMX, and TMP, which, although not as large as macrolides, are of particular environmental concern due to their frequent detection in wastewater (Wilkinson et al., 2022) and relatively high persistence, especially CBZ. This persistence is largely attributed to their chemical stability and resistance to biodegradation (Li et al., 2013, Kodešová et al., 2016, Rilstone et al., 2025).

1.2.2. Sources of pharmaceuticals in the environment

Pharmaceutical pollution arises from two main sources: point sources (e.g., industrial, hospital, and sewage effluents) that are identifiable and measurable, and diffuse sources (e.g., agricultural and urban runoff) that occur over large areas and are harder to pinpoint (Li, 2014). These pollutants come from six major sources, such as households, industries and hospital effluents, landfills, animal waste, and aquaculture, which potentially could reach soil, groundwater, and surface water (Li et al., 2022, Li, 2014). Another pathway is the use of wastewater for irrigation or surface water impacted by wastewater effluents (Heyde et al., 2025). Among the sources mentioned above, household discharges have the highest impact because pharmaceuticals often do not undergo complete metabolism in humans or animals and are excreted unchanged, reaching the environment not through misuse but as a result of normal use (Kümmerer, 2010). Apart from this, the low or incomplete removal of pharmaceuticals in conventional WWTPs makes their release into the environment inevitable (Joss et al., 2006, Matesun et al., 2024). Additional routes occur when leftover pharmaceuticals are improperly disposed of, such as by flushing them down toilets or drains, or discarding them with regular household waste (Kümmerer, 2010). Also, septic systems can act as significant pathways for pharmaceuticals to contaminate the environment, as their discharges often introduce pharmaceuticals into nearby groundwater and surface water

systems (Phillips et al., 2015). Pets can act as a source of pharmaceuticals in the environment, directly when they are treated and spend time outdoors or through the disposal of pet feces, such as cat litter, in household waste, which is subsequently sent to municipal solid waste landfills (Gerba et al., 2011). All these sources and pathways are illustrated in Fig. 2.

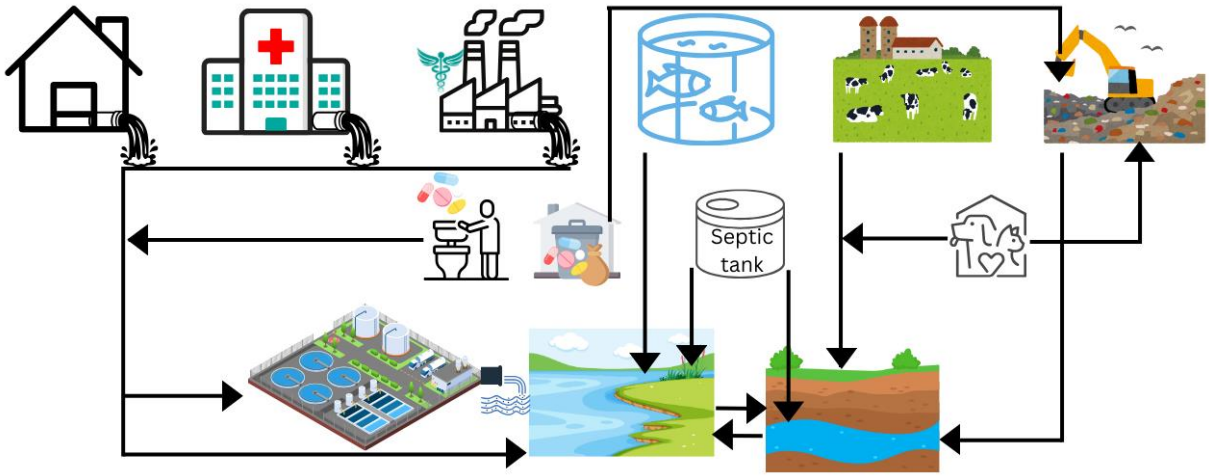

Figure 2. *Author developed schematic illustration of pharmaceutical sources and pathways in the environment, based on Gerba et al. (2011), Heyde et al. (2025), Joss et al. (2006), Kümmerer et al. (2010), Li et al. (2022), Matesun et al. (2024), and Philips et al. (2015)*

1.2.3. Removal methods of pharmaceuticals from wastewater

Wastewater is defined as a combination of water and waste produced by residential, institutional, commercial, and industrial establishments, and may also include groundwater, surface water, and storm water (Hanafi and Sapawe, 2020). Wastewater treatment is receiving increasing attention due to a better understanding of the adverse effects (toxicity) of contaminants, advances in techniques for trace determination and quantification of emerging contaminants, and the implementation of regulations.

In general, wastewater at most of conventional WWTPs is subjected of several treatment steps such as, preliminary (screeners, grit chambers, and skimming tanks), primary (sedimentation, coagulation), secondary (aerobic, anaerobic, and pond process) (Crini and Lichtfouse, 2018), and in some cases, tertiary or advanced (adsorption, chemical oxidation, membrane technology, electrochemical techniques, advanced oxidation processes) (Ranjit et al., 2021). The latter is getting more attention due to the enforcement of regulations for emerging contaminants (ECs) such as pharmaceuticals, personal care products, pesticides, and surfactants. ECs are chemicals or microorganisms not typically monitored in the environment that may harm ecosystems or human health, including newly introduced

substances, neglected existing contaminants, and legacy contaminants with newly recognized risks (Wan Ismail and Mohktar, 2020). Due to their low concentrations and their various physicochemical properties, it is reported and confirmed that the conventional WWTPs could not or do not totally remove these compounds, which in this context are referred to as "micropollutants" (Matesun et al., 2024, Bijlsma et al., 2021).

Micropollutants could be removed from water *via* different techniques, part of the tertiary or the advanced treatment step. One of these is adsorption, a surface process in which porous solids attract and concentrate solute molecules (adsorbate) from a bulk solution onto their surfaces via intermolecular forces, forming an interfacial layer (Dąbrowski, 2001). Wastewater treatment *via* adsorption, especially onto agro-organic waste has several advantages compared to the most techniques due to simplicity in handling and operation, sustainability, environmental compatibility and formation of zero-to-little harmful by-product, and cost-effectiveness (Crini and Lichtfouse, 2018, Wan Ismail and Mohktar, 2020). A comparison with other elimination techniques such as chemical oxidation, membrane technology, electrochemical techniques, and advanced oxidation processes is provided in table 3.

Table 3. *Advantages and disadvantages of ECs removal techniques*

Technique	Characteristics	Advantages	Disadvantages
Adsorption	Nondestructive process Use of a solid material	Simple and easy adaptable Wide range of products Waste valorization Environmentally sustainable (when from agro-waste) Excellent treatment quality Wide target of contaminants Effective and fast Reduce of chemical oxygen demand (COD) values	High initial capital costs Nondestructive process Non-selective Performance – material type based Physical/chemical activation (when from agro-waste) Rapid saturation – regeneration Material elimination – incineration Not efficient for some polar compounds
Chemical oxidation	Use of oxidants such as O_3, Cl_2, ClO_2, H_2O_2, $KMnO_4$	Simple, rapid, and efficient Generation of ozone on-site Elimination of color and odor Cyanide and sulfide removal Increases biodegradability Disinfection	Chemicals and pre-treatment Efficiency influenced by oxidants Short half-life (O_3) Few dyes resistant - high O_3 doses Formation of byproducts No effect on COD values (O_3) No effect on salinity (O_3) Release of volatile compounds Release of aromatic amines (ClO_2) Generates sludge

Membrane technology	Nondestructive Semipermeable barrier	Wide range of membranes Small space requirement Simple, rapid, and efficient High-quality-treated effluent No chemicals required Low solid waste generation Removes dyes, salts, minerals Wide elimination contaminant	Investment costs High energy requirements The design can differ significantly Maintenance and operation costs Rapid membrane clogging Low throughput and limited flow Elimination of the concentrate Membrane is specific application
Electrochemical techniques	Electrolysis	Recovery of valuable metals High adaptation to conditions Increases biodegradability Fast organic matter separation Efficient and pH independent In situ coagulants Economically feasible	High initial cost of the equipment Maintenance and chemicals Operation inhibition (sludge) Post-treatment for Fe and Al Filtration necessary for flocs Formation of sludge
Advanced oxidation processes	Emerging processes Destructive techniques	In situ reactive radicals No consumption of chemicals Contaminants mineralization No sludge Rapid degradation Efficient for dyes and drugs Reduce of COD and TOC Destruction of phenol	Laboratory scale Economically non-viable for small and medium plants Technical constraints Formation of by-products High-pressure and energy pH dependence

Source: (Crini and Lichtfouse, 2018, Wan Ismail and Mohktar, 2020)

Switching from activated carbon to bio-based adsorbents such as biochar is increasingly recommended due to biochar's lower production cost, renewable feedstocks, and reduced environmental impact, while still offering considerable adsorption performance (Wang et al., 2020, Alhashimi and Aktas, 2017). But, most natural and biomass-based adsorbents, including biochar, suffer from drawbacks such as relatively low adsorption efficiency, limited stability, bleeding, and difficult post-adsorption separation from water. Recent research addresses these issues by combining low-cost materials like biomass, clays, and nanoparticles to enhance surface area, porosity, adsorption sites, and reusability (Arif et al., 2021, Maged et al., 2023, Olu-Owolabi et al., 2021, Zheng et al., 2021, Zhou et al., 2018, Diagboya et al., 2022). The separation of the adsorbents from large volumes of water after the treatment process is possible with magnetized composites, simplifying handling, reducing operational costs, and avoiding labor-intensive filtration steps (Mohubedu et al., 2019, Zhang et al., 2022, Anfar et al., 2020).

1.3. Aim of the study

The main aim of this study was to assess the occurrence and environmental behavior of selected pharmaceuticals in the water and sediments of the Ishmi River basin in Albania, and to develop sustainable, low-cost composite materials for water treatment. The removal efficiency of these materials was to be quantified by selected pharmaceuticals and heavy metals.

This scientific objective was structured into three sub-areas, each of which was recognized in a publication:

1. Assessment of selected pharmaceutical occurrence and partitioning behavior.

   To investigate the occurrence of selected pharmaceuticals in water and sediments, and to evaluate their in-situ sediment-water partitioning behavior by considering both the physicochemical properties of the compounds and the site-specific environmental conditions. This study served as the basis for the development of composite adsorbents and the selection of target contaminants for removal through sorption experiments.

2. Development of cost-efficient composite adsorbents to remove pharmaceuticals from water.

   To develop cost-effective magneto-biochar-clay composites using grape cluster waste, feldspar clay, and magnetic nanoparticles, and to evaluate their removal capacity and efficiency for aqueous naproxen and carbamazepine.

3. Testing the performance and stability of adsorbents using heavy metal contamination.

   To assess the removal capacity and efficiency of the developed composites for three toxic metals, such as Cd(II), Cr(VI), and Cu(II) from water.

1.4. Materials and methods

1.4.1. Study area and sample collection

Sampling campaigns in the Ishmi River basin were carried out seasonally during 2023 and 2024 for surface water samples (n = 8). Sediment samples were collected during the spring and summer seasons of both years (n = 4). Site locations and brief site characteristics are summarized in Fig. 4 and Table 4. Sampling sites were situated at established national water monitoring stations and categorized based on their relative position in the basin: upstream (Brari Bridge – TR1), midstream/urban areas (Casa Italia Bridge – LR1, Kamza Bridge – TR2, Rinas Bridge – IR1), and downstream (Gjoles Bridge – IR2, Salmer Bridge – IR3). TR1 represented a site with minimal anthropogenic influence. In contrast, LR1, TR2, IR1, and IR2 were heavily impacted by urban activities, particularly LR1, and with some agricultural influence the other sites. IR3 was predominantly affected by agricultural activities.

Table 4. *Sampled Ishmi basin Rivers sites characteristics*

ID	River	Location	*Flow $m^3 s^{-1}$				Site characteristics
			Year 2023		Year 2024		
			Autumn	Summer	Autumn	Summer	
TR1	Tirana River	N41° 38'; E19° 86'	0.31	0.55	0.13	0.29	Light human activity; touristic attraction
LR1	Lana River	N41° 34'; E19° 77'					Wastewater discharges and urban industry
TR2	Tirana River	N41° 35'; E19° 77'					Wastewater discharges and urban industry
IR1	Ishmi River	N41° 43'; E19° 69'					Wastewater, agriculture, and industry; Airport
IR2	Ishmi River	N41° 46'; E19° 69'					Urban and agriculture activities
IR3	Ishmi River	N41° 54'; E19° 61'	4.89	3.83	4.94	3.26	Agriculture activities

*Data from Report of Environmental State of the year 2023, National Environment Agency of Albania

Grab water samples (Fig. 3) were filtered (0.45 μm), pH-adjusted (pH 2.7), and extracted using solid-phase extraction (SPE) by adapting the reported methods of (Röhricht et al., 2009, Patrolecco et al., 2013) for CAFF, CBZ, NPX, IBU, DCF, then analyzed by high-performance liquid chromatography with ultraviolet and fluorescence detection (HPLC-UV/FLD), based on (Martin et al., 2012).

AETM, ATM, CMC, CFC, ETM, SMX, and TMP were analyzed via direct injection with high-performance liquid chromatography coupled with tandem mass spectrometry (HPLC-MS/MS), based on (Dalkmann et al., 2012).

Sediments (0–5 cm depth) were sampled with a spatula (Fig. 3), frozen, lyophilized, homogenized, and sieved (<100 μm). Sediment extraction used ethylenediaminetetraacetic acid disodium salt dihydrate (EDTA) assisted solvent extraction for CBZ, NPX, IBU, followed by SPE and HPLC-UV/FLD (Martin et al., 2010). Antibiotics were extracted using phosphate buffered acetonitrile (ACN) (0.2 M KH_2PO_4:ACN (1:1, v/v)), and analyzed with HPLC-MS/MS (Dalkmann et al., 2012).

Sediment physicochemical properties such as pH, total nitrogen (TN), total hydrogen (TH), total sulfur (TS), total carbon (TOC), carbonates ($CaCO_3$), inorganic (IC) and organic carbon (OC), and metals (Al, Fe, Ca, K, Mg, Na) were extracted using standard methods and determined with CHNS analyzer, Scheibler device, and ICP-OES.

Data on pharmaceutical consumption (reimbursed amounts) in Albania were obtained from official national statistics provided by governmental health authorities in Albania (Mandatory Health Insurance Fund of Albania). For each pharmaceutical compound, the total monthly mass consumed was calculated based on the reported dosage and the number of units consumed. The monthly consumption mass (M_{month}, (mg)) was calculated using the following equation:

$$M_{month} = D \times N$$

where D (mg) is the mass of active pharmaceutical ingredient per unit dose and N is the number of units consumed per month, converted to kilograms for further analysis.

Figure 3. *Water and sediment sampling in the Ishmi River basin*

1.4.2. Data treatment: partitioning

The sediment–water partition coefficient (K_d) for the selected pharmaceuticals was calculated using equation (1) (Royano et al., 2024).

$$K_d = C_s / C_w \quad (1)$$

where (C_s) (ng g^{-1}) is concentration in the sediment phase (C_w) (ng L^{-1}) is concentration in the water phase.

This coefficient is a key factor influencing the persistence and long-term fate of contaminants in aquatic environments, as higher K_d values indicate stronger sorption to sediments, leading to enhanced binding and increased environmental persistence due to reduced photodegradation and biodegradation (Chen and Zhou, 2014).

Another parameter that describes the distribution of a compound between water and sediment is the pH-dependent *n*-octanol-water partition coefficient (D_{ow}). This parameter accounts for the compound's ionization at a given pH. To assess the distribution behavior of the selected pharmaceuticals, D_{ow} was calculated using equation (2) (Vazquez-Roig et al., 2012).

$$D_{ow} = \frac{K_{ow}}{1+(10^{pH-pK_a)}} \quad (2)$$

where K_{ow} is the *n*-octanol-water partition coefficient and pK_a is the acid dissociation constant.

The organic carbon content of sediments strongly influences the distribution of organic compounds between water and sediment phases by providing abundant adsorption sites and facilitating hydrophobic interactions, thereby enhancing the sorption of both polar and non-polar compounds. To evaluate this influence, the organic carbon-normalized partition coefficient (K_{oc}) was calculated using the equation (3) (Vulava et al., 2016).

$$K_{oc} = K_d / f_{oc} \quad (3)$$

Where f_{oc} represents the fraction of organic carbon.

Using in-situ K_d values together with sediment properties such as organic carbon content, pH, carbonate content, and cation concentrations, multiple linear regression models were developed to predict compound-specific K_d values in the environment. The predictive performance of these models was subsequently validated against the measured in-situ K_d values.

1.4.3. Statistical analysis

For CAFF, CBZ, NPX, IBU, and DCF in water samples, statistical analysis was not performed due to limited sample volume and insufficient replication; therefore, the data were evaluated descriptively to illustrate spatial and seasonal patterns. For sediment samples, the remaining pharmaceuticals in water, and the total concentrations across water and sediment

phases, two-way analysis of variance (ANOVA) was conducted, with season and location as independent variables and pharmaceutical concentration as the dependent variable. When the assumptions of normality and homogeneity of variances were not met, non-parametric Kruskal–Wallis tests were applied. In addition, single and multiple stepwise regression analyses were used to assess relationships between the distribution coefficient (K_d), sediment properties, and predicted K_d. Statistical significance was defined as $p < 0.05$. All statistical analyses were performed using OriginPro 2015 (OriginLab Corporation, USA).

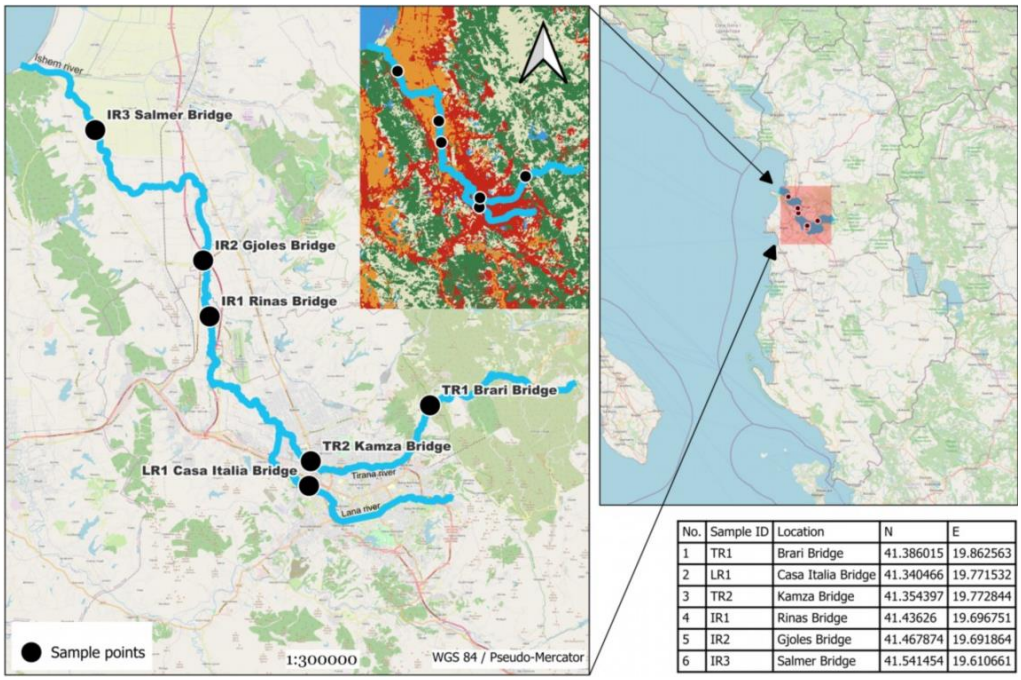

No.	Sample ID	Location	N	E
1	TR1	Brari Bridge	41.386015	19.862563
2	LR1	Casa Italia Bridge	41.340466	19.771532
3	TR2	Kamza Bridge	41.354397	19.772844
4	IR1	Rinas Bridge	41.43626	19.696751
5	IR2	Gjoles Bridge	41.467874	19.691864
6	IR3	Salmer Bridge	41.541454	19.610661

Figure 4. *Location of sampling points in the Ishmi River basin*

1.4.4. Composites preparation

Low-cost materials, including pretreated Feldspar clay (FLC) (Diagboya et al., 2022) and grape cluster stalk waste (GCW), which was collected in central Albania, were used to prepare magneto-biochar-clay composites (MBC-*x*). GCW was dried, pulverized, and calcined at 500 °C to produce biochar (BC). Magnetic nanoparticles (MNP) were synthesized by co-precipitating $FeCl_3$ and $FeSO_4 \cdot 7H_2O$ with NaOH. Two MBC variants (1:2:1 and 1:3:1 ratio of MNP:BC:FLC) were prepared by first preparing the MNP, sequentially mixing with GCW and FLC, followed by agitation, centrifugation, drying, and calcinations at 500°C for 2 hours. The composites were labeled MBC-1:2:1 and MBC-1:3:1, washed with Milli-Q, and stored for further use in sorption tests with organic and inorganic contaminants as given in the second publication or WP2 and the third publication or WP3, respectively.

1.4.5. Sorption tests

For NPX, standardized sorption experiments were performed using MBC 1:2:1 due to its strong adsorption and magnetic separation properties. Batch tests evaluated the effects of adsorbent mass, contact time, pH, temperature, and NPX concentration, as well as competition with CBZ, dissolved organic matter (DOM), and river water. Reusability was assessed over five adsorption–desorption cycles. Final applicability tests were conducted in river water spiked with environmentally relevant NPX levels. After each test, solutions were filtered and residual concentrations were quantified by HPLC-DAD.

For metals, preliminary sorption tests with single and simultaneous metal solutions showed that MBC 1:2:1 and MBC 1:3:1 composites outperformed BC, FLC, and MNP, and were therefore selected for detailed studies. Batch experiments were conducted under controlled conditions, varying adsorbent mass, contact time, pH, contaminant concentration, and temperature. Reusability was tested over five adsorption–desorption cycles. After each run, solutions were filtered and metal concentrations quantified by ICP-OES.

1.4.6. Sorption data analysis

All the sorption data analysis was performed using the respective equations given in Table 5. The amounts (mg g^{-1}) of analytes adsorbed (q_e) were calculated from Eq. 1. Kinetics of analytes sorption were evaluated using the nonlinear forms of the pseudo-first-order (PFO) (Eq. 2), pseudo-second-order (PSO) (Eq. 3), and the intra-particle diffusion (IPD) (Eq. 4) models. The Langmuir (Eq. 5), Freundlich (Eq. 6), and the Sips non-linear adsorption isotherm (Eq. 7) models were fitted to the equilibrium adsorption data and used to describe the analytes uptake process. The dimensionless equilibrium constant K^0 (L g^{-1}) was calculated from Eq. 8, while the thermodynamic parameters were determined from Eq. 9 and 10 using equilibrium adsorption data at 293.15, 303.15, and 313.15 K. The model fittings and models' parameters were obtained using the OriginPro 2015 software (OriginLab Corporation, USA).

Table 5. *Sorption data treatment equations*

Equation	Description	Parameters	Number
$q_e = (C_O - C_e)v/m$	Amount of analyte adsorbed (mg g^{-1})	m, v, q_e, C_o, C_e, are the composite mass (g), volume of analyte solution (L), equilibrium amount of analyte adsorbed (mg g^{-1}), initial and final analyte concentrations (mg L^{-1}), respectively	1
$q_t = q_e(1 - e^{-k_1 t})$	Pseudo-First Order (PFO) kinetics model (Junck et al., 2024)	t, q_t, and k_1 are time (min), analyte adsorbed at time- t (mg g^{-1}), and PFO model rate constant, respectively	2
$q_t = \frac{q_e^2 k_2 t}{1 + q_e k_2 t}$	Pseudo-Second Order (PSO) kinetics model	k_2 is the PSO model rate constant	3
$q_e = k_{IPD} t^{1/2} + C$	Weber-Morris intraparticle diffusion (IPD)	k_{IPD} and C are the IPD model rate constant, and the amount of surface adsorbed analyte (mg g^{-1}), respectively	4
$q_e = \frac{Q_O b C_e}{1 + b C_e}$	Langmuir adsorption isotherm model (Langmuir, 1916)	Q_o (mg/g) and b (L mg^{-1}) are the maximum adsorption capacity per gram (mg g^{-1}) and energy-related parameter (L mg^{-1}), respectively	5
$q_e = k_f C_e^n$	Freundlich adsorption isotherm model (Freundlich, 1906)	k_f (L g^{-1}) and n are Freundlich model constant and the Freundlich linearity parameter (dimensionless), respectively	6
$q_e = \frac{Q_o (K_S C_e)^n}{1 + (K_S C_e)^n}$	Sip's adsorption isotherm model	K_S (L mg^{-1}) and n are Sip's model constant and the Sip's exponent, respectively	7
$K^0 = K_L * 1000$	Dimensionless equilibrium constant	K_L is Langmuir constant	8
$LnK^0 = \frac{\Delta S^o}{R} - \frac{\Delta H^o}{RT}$	Thermodynamic parameters	ΔS^o, ΔH^o, T, and R are entropy change (J^{-1} mol^{-1} K^{-1}), enthalpy change (kJ mol^{-1}), Temperature (K), and ideal gas constant (J^{-1} mol^{-1} K^{-1}), respectively	9
$\Delta G^o = -RTLnK^0$	Van't Hoff equilibrium	ΔG^o is the Gibb's free energy (kJ mol^{-1})	10

1.5. Results and discussion

1.5.1. Pharmaceutical consumption in Albania

Albanian total reimbursed consumption data for selected pharmaceuticals during the period 2018–2024 (with 2020 covering only nine months) show that the highest recorded usage was for NPX, with 1,880 kg reported in 2023. This was followed by CBZ with 559 kg in 2019, IBU with 89.5 kg in 2021, and DCF with 10.8 kg in 2019 (Fig. 5a). In contrast, the consumption of antibiotics of ATM, CFC, ETM, SMX, and TMP was significantly lower (Fig. 5b). Their respective amounts for 2023 and 2024 were: ATM (0.6 kg and 0.3 kg), CFC (7.2 kg and 6.7 kg), ETM (1.0 kg and 1.05 kg), SMX (5.7 kg and 6.9 kg), and TMP (1.1 kg and 1.4 kg). Notably, AETM and CMC were not reimbursed during the reporting period. These figures represent only the reimbursed quantities covered by the Mandatory Health Insurance Fund of Albania, which account for an estimated 1-5% of total national pharmaceutical consumption. Based on these data, it can be observed and concluded that NPX consumption showed an increasing trend from 2018 to 2023, followed by a slight decline in 2024.

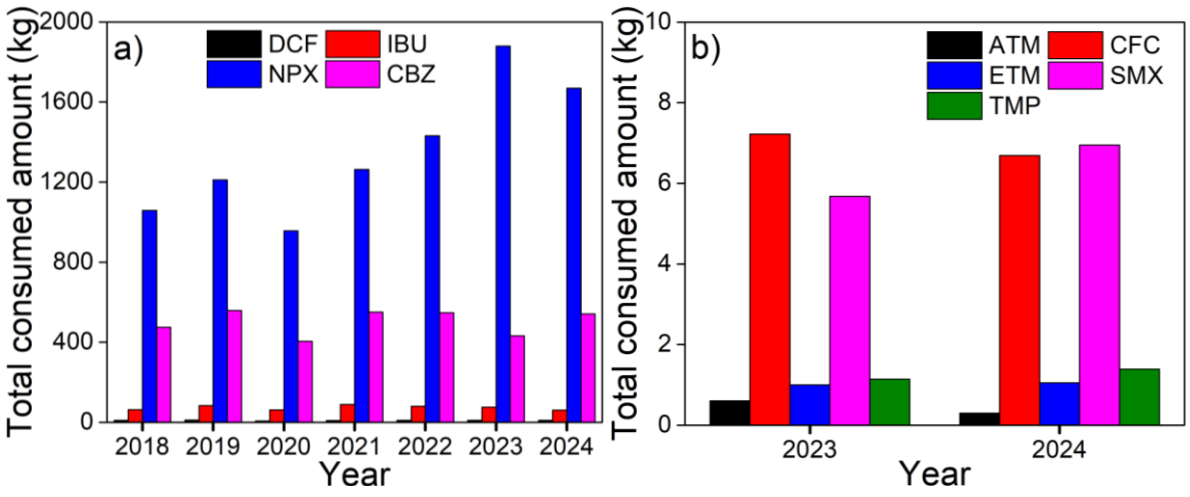

Figure 5. *(a) Total reimbursed consumed amounts of selected pharmaceuticals of CBZ, NPX, IBU, and DCF and over the period 2018-2024, and (b) of ATM, CFC, ETM, SMX, and TMP over 2023-2024 in Albania*

1.5.2. Wastewater situation in Albania

Albania is located in southeastern Europe within the Mediterranean area and has a population of 2,363,314 inhabitants (as of 01.01.2025 census, reported by Instat Albania). More than 60% of the population lives in the central and west part of Albania, such as Tirana, Fieri,

Elbasan, and Durrës districts. Based on Eurostat database, the total connected population to WWTPs has a slight increasing trend over the last decade, reaching a value of 32.4% in 2022 (Fig. 6a). From the same source, it is reported that the total amount of generated wastewater has also an increasing trend, presumably with the increase of connection, reaching a value of 78 million cubic meters (Mm^3) in 2022 (Fig. 6b). On the other hand, the percentage of safely treated wastewater regarding the total generated wastewater, remains quite low, with the maximum value of 16.8% in 2022, as reported by the Instat Albania database (Fig. 6b). Therefore, based on the annual reports for the environmental state from the National Environment Agency (NEA) of Albania, it is concluded that the most polluted rivers in Albania are Lana, Tirana, Ishmi (part of Ishmi's basin located in Tirana and Durrës districts), Gjanica and Osumi (part of Semani's basin located in Fier district), and surface waters where the population density is higher (Tirana, Durrës, Fieri, Elbasan), as a result of discharging untreated urban and industrial wastewaters. In addition to urban and industrial wastewater, a concern remains the hospital effluent. In Albania, this effluent is treated as wastewater and no on-site treatment is applied, as reported by Tahiri et al. (2023). This effluent in Albania is reported to have high content of pharmaceuticals, mainly NSAIDs such as DCF and IBU, antibiotics such as ATM and CFC, and the antiepileptic CBZ, and some other pharmaceuticals such as, amikacin, ampicillin, dexamethasone, metoprolol, and nifedipine (Tahiri et al., 2023). Therefore, considering the low rate of connected population to the WWTPs and safely treated wastewater, the presence of contaminants and pharmaceuticals in the environment in Albania remains a concern.

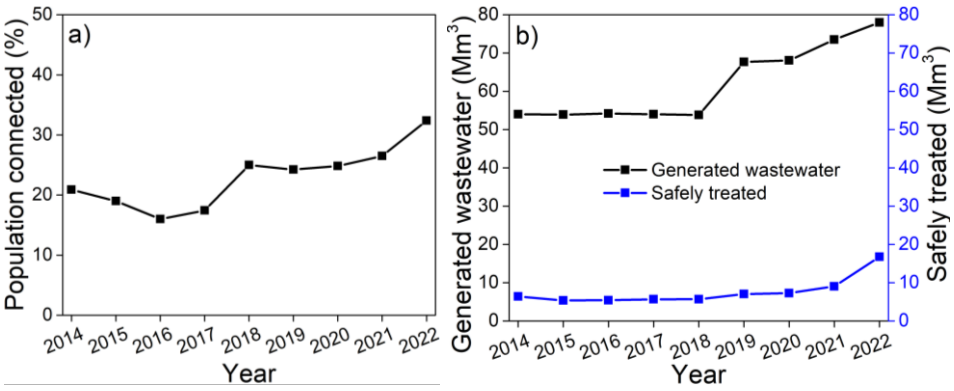

Figure 6. *(a) Population percentage connected to wastewater treatment plants, and (b) generated and safely treated wastewater over the period 2014-2022 in Albania*

Source:https://ec.europa.eu/eurostat/databrowser/view/env_ww_con/default/table?lang=en&category=env.env_wat.env_nwat and https://www.instat.gov.al/al/sdg/

1.5.3. Selected pharmaceuticals concentrations in water samples

A total of twelve pharmaceuticals were detected in the Ishmi River basin surface waters during seasonal campaigns in 2023 and 2024, CAFF, CBZ, NPX, IBU, DCF, AETM, ATM, CMC, CFC, ETM, SMX, and TMP. Concentrations varied noticeably by location, reflecting anthropogenic pressures, with the most urban-impacted site LR1, consistently showing the highest values (Fig. 7) (Table 6). Mean CAFF, IBU, NPX, and CFC concentrations at LR1 reached 10.7 µg L^{-1}, 11.3 µg L^{-1}, 2.0 µg L^{-1}, and 0.7 µg L^{-1}, respectively, with maximum recorded values of 22.5 µg L^{-1} (CAFF), 12.8 µg L^{-1} (IBU), 2.6 µg L^{-1} (NPX), and 1.8 µg L^{-1} (CFC). ATM peaked at 7.5 µg L^{-1}, while SMX and TMP reached 0.4 µg L^{-1} and 0.1 µg L^{-1}, respectively. Upstream reference site TR1 typically showed non-detectable or very low concentrations, while downstream sites exhibited dilution or reduction effects. These concentrations are within the higher range reported in other wastewater-impacted European rivers, such as in Portugal and in Spain, where CAFF, IBU, NPX, and DCF concentrations were registered at 9.4-83.9, 7.2, 6.6, and 3.5 µg L^{-1}, respectively (Paiga et al., 2019, Carmona et al., 2014), especially considering the absence of effective wastewater treatment in the study area. Regarding seasons, autumn showed the highest concentrations, followed by winter, summer, and spring; while for the year 2024, winter had the highest concentrations, followed by spring, autumn, and summer. The total concentrations of selected pharmaceuticals in water were significantly affected by both season and location across both years ($p< 0.001$), confirming the combined impact of environmental conditions and urban impact.

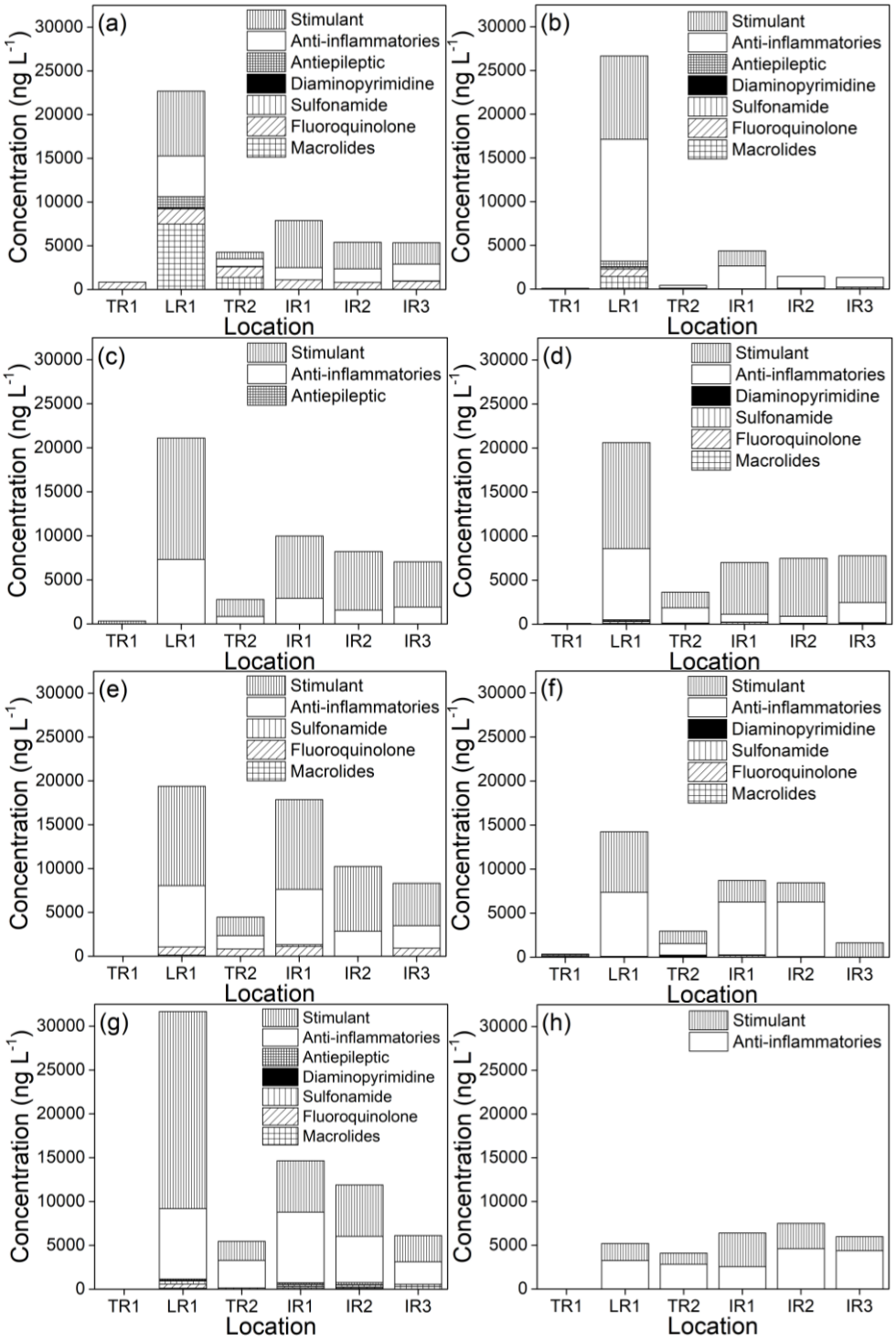

Figure 7. *Pharmaceutical concentrations in waters for (a) and (b) winter; (c) and (d) spring; (e) and (f) summer; and (g) and (h) autumn seasons of the years 2023 and 2024*

Table 6. *Summary of mean concentrations of selected pharmaceuticals in water and sediments of different locations from Ishmi River basin*

Compounds	Water (ng L^{-1}) (n = 8)						Sediment (ng g^{-1}) (n = 4)					
	Sampling Point											
	TR1	LR1	TR2	IR1	IR2	IR3	TR1	LR1	TR2	IR1	IR2	IR3
CAFF	n.d.	10,676	1,430	5,309	4,324	2,996	NM					
CBZ	41.1	260.5	n.d.	21.7	28.2	n.d.	2.5	44.1	15.2	9.7	11.5	9.6
NPX	n.d.	2,028	525	1,255	914	585	2.8	18.4	5.6	8.8	4.8	1.6
IBU	n.d.	11,297	1,037	8,384	7,926	1,450	n.d.	47.2	8.3	16.0	8.0	9.0
DCF	n.d.	278	n.d.	47.5	50.2	59.6	NM					
AETM	10.7	26.5	6.0	32.3	10.8	58.2	0.3	0.9	0.9	0.7	0.9	0.6
ATM	n.d.	1,501	n.d.	n.d.	n.d.	n.d.	n.d.	113	54.0	122	16.0	48.2
CMC	5.2	12.3	23.3	36.7	20.2	9.8	11.8	8.1	3.8	4.3	4.6	17.8
CFC	179.2	714	404	407	188	348	3.2	705	77.9	170	129	48.6
ETM	n.d.	n.d.	230	24.3	n.d.	n.d.	*Added to AETM					
SMX	23.2	126	17.8	74.2	42.0	49.8	0.8	3.6	2.7	0.9	0.8	0.1
TMP	8.0	40.5	3.0	8.2	9.0	3.8	n.d.	6.4	11.3	6.7	6.0	2.1

*Due to dominance of AETM, as dominant degradation product in acidic conditions

1.5.4. Selected pharmaceuticals concentrations in sediment samples

Pharmaceuticals were also detected in river sediments, with spatial and seasonal patterns different from those in the water samples. CFC and ATM dominated the sediment matrix, especially in spring, with maximum of 1,068 ng g^{-1} at LR1 and 396 ng g^{-1} IR2, respectively. Other compounds occurred at lower but notable concentrations, including IBU (93.7 ng g^{-1}), CBZ (60.5 ng g^{-1}), NPX (49.3 ng g^{-1}), TMP (38.3 ng g^{-1}), CMC (37.8 ng g^{-1}), SMX (13.3 ng g^{-1}), and AETM (2.7 ng g^{-1}) (detailed in Table 7).

The LR1 site again showed the highest detection frequencies (100% for most compounds except AETM and SMX), indicating sediment contamination is directly linked to urban effluent inputs. Spring seasons generally yielded the highest sediment concentrations, presumably due to higher pharmaceutical loads and cooler conditions (low temperatures - lower biodegradability), resulting in a pseudo-persistence phenomenon (Fig. 8). These findings align with global observations in wastewater-impacted rivers, where fluoroquinolones and macrolides show high sediment affinity (Zhou et al., 2011, Senta et al., 2021). Similarly to water trend, the total pharmaceutical concentrations showed strong effects of both season and location (p< 0.001), indicating that both natural and human factors substantially affect contaminant distribution in the Ishmi River basin (Fig. 8).

Table 7. *Concentrations of the selected pharmaceuticals at each sampled season of 2023 and 2024 in sediments of Ishmi River basin*

Season	Location	Concentration (ng g^{-1})								
		CBZ	NPX	IBU	AETM	ATM	CMC	CFC	SMX	TMP
Spring 2023	TR1	n.d.	n.d.	n.d.	1.05	<LOQ	5.54	n.d.	n.d.	n.d.
	LR1	34.11	12.70	93.74	0.87	144.66	5.90	782.98	13.33	5.32
	TR2	6.62	7.07	3.26	0.90	76.69	0.56	139.98	n.d.	2.29
	IR1	5.39	9.17	36.68	0.74	61.99	7.14	286.48	n.d.	4.24
	IR2	10.2	2.39	21.24	1.16	167.16	5.39	188.68	n.d.	2.72
	IR3	4.26	3.11	9.26	0.62	54.18	13.75	88.43	n.d.	2.48
Summer 2023	TR1	n.d.	n.d.	n.d.	n.d.	n.d.	9.82	2.06	0.44	n.d.
	LR1	40.4	2.76	20.34	0.86	42.82	7.19	553.54	0.44	3.68
	TR2	3.37	4.68	7.46	0.54	10.24	11.87	35.16	1.09	1.56
	IR1	2.89	0.76	9.43	n.d.	85.61	0.35	84.27	n.d.	3.28
	IR2	0.74	2.81	3.68	0.49	18.04	11.94	40.93	n.d.	0.57
	IR3	3.06	1.39	1.55	0.62	10.02	37.77	12.61	n.d.	n.d.
Spring 2024	TR1	3.47	7.16	n.d.	n.d.	n.d.	21.27	3.72	1.02	n.d.
	LR1	60.5	49.28	41.95	n.d.	212.15	18.85	1067.5	n.d.	7.84
	TR2	36.56	9.23	10.25	2.68	111.37	1.43	101.78	9.80	38.3
	IR1	20.15	22.13	17.09	n.d.	312.43	9.45	251.71	3.48	17.6
	IR2	20.43	11.51	0.41	0.74	396.20	0.32	220.24	2.97	17.8
	IR3	14.88	0.62	n.d.	0.49	87.32	5.98	65.83	n.d.	4.29
Summer 2024	TR1	6.43	4.20	n.d.	n.d.	n.d.	10.66	7.16	1.90	n.d.
	LR1	41.53	8.98	32.80	1.46	54.24	0.27	415.15	0.59	8.91
	TR2	14.24	1.48	12.09	1.54	17.71	1.45	34.55	n.d.	2.91
	IR1	10.41	3.32	0.87	n.d.	30.99	0.46	57.24	n.d.	1.68
	IR2	14.52	2.44	6.58	1.29	59.74	0.82	66.89	0.41	2.70
	IR3	16.1	1.37	n.d.	0.64	41.21	13.53	27.53	0.40	1.83

n.d. : not detected; <LOQ: below the limit of quantitation.

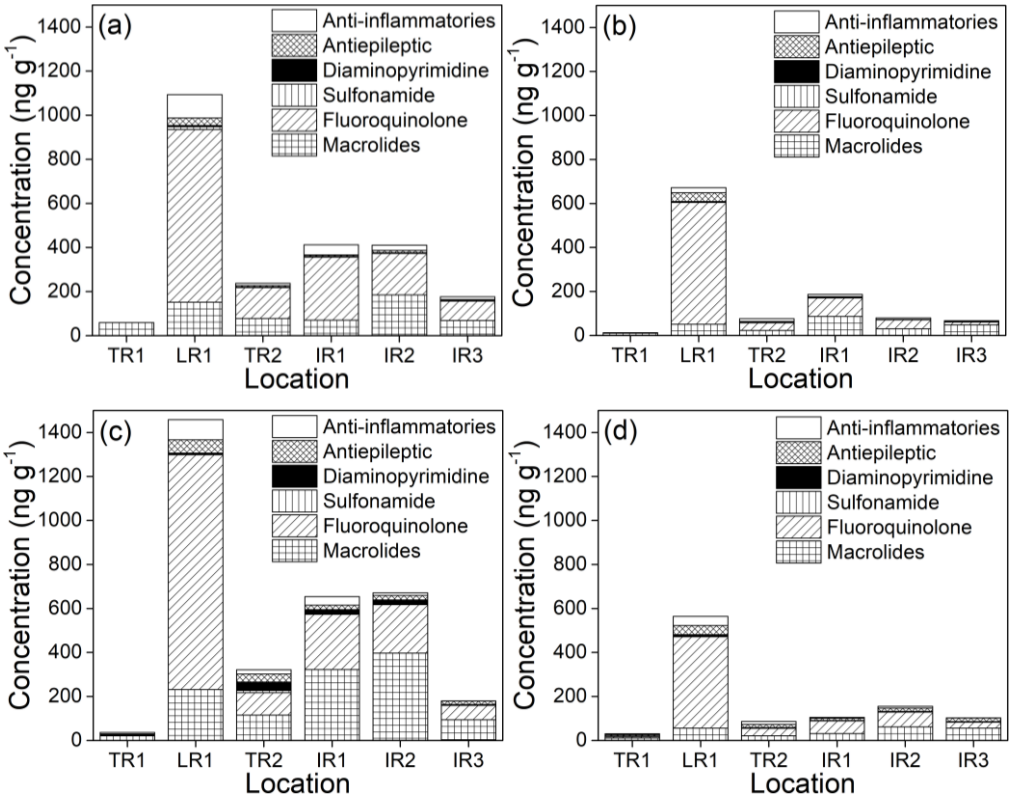

Figure 8. *Seasonal and spatial variations of selected pharmaceuticals in sediments of the Ishmi River basin for (a) spring and (b) summer of the year 2023; and (c) spring and (d) summer of the year 2024*

1.5.5. Partitioning of selected pharmaceuticals under environmental conditions

Sediment-water partition coefficients (K_d) calculated from corresponding (water and sediment sampled at the same time and at the same location) aqueous and sediment concentrations revealed high variability among compounds and sites (Table 8). Values ranged from 0.42 – 24.8 mL g^{-1} for NPX, 0.17 – 27.3 mL g^{-1} for IBU, 12.5 – 178.1 mL g^{-1} for AETM, 3.06 – 971.2 mL g^{-1} for CMC, 13.9 – 8,534.4 mL g^{-1} for CFC, 54.2 – 197.3 mL $g^{-1}$for SMX, and 39.3 – 3,142 mL g^{-1} for TMP. Organic carbon-normalized coefficients (K_{oc}) were especially high for CFC (up to 135,037 mL g^{-1} C), reflecting strong sorption potential for this compound.

Correlation analyses indicated sediment pH, organic carbon content (OC), and the pH-dependent n-octanol–water distribution coefficient (D_{ow}) as primary predictors of partitioning. From the models and the fittings data, it could be observed that for CFC, NPX, and IBU the models were accurate and could be used to predict their environmental concentrations. Meanwhile, AETM and CMC, although showing good fitting relationship

between calculated and predicted values (especially for AETM), the significance was not achieved during the multiple step fitting analysis (Fig. 9).

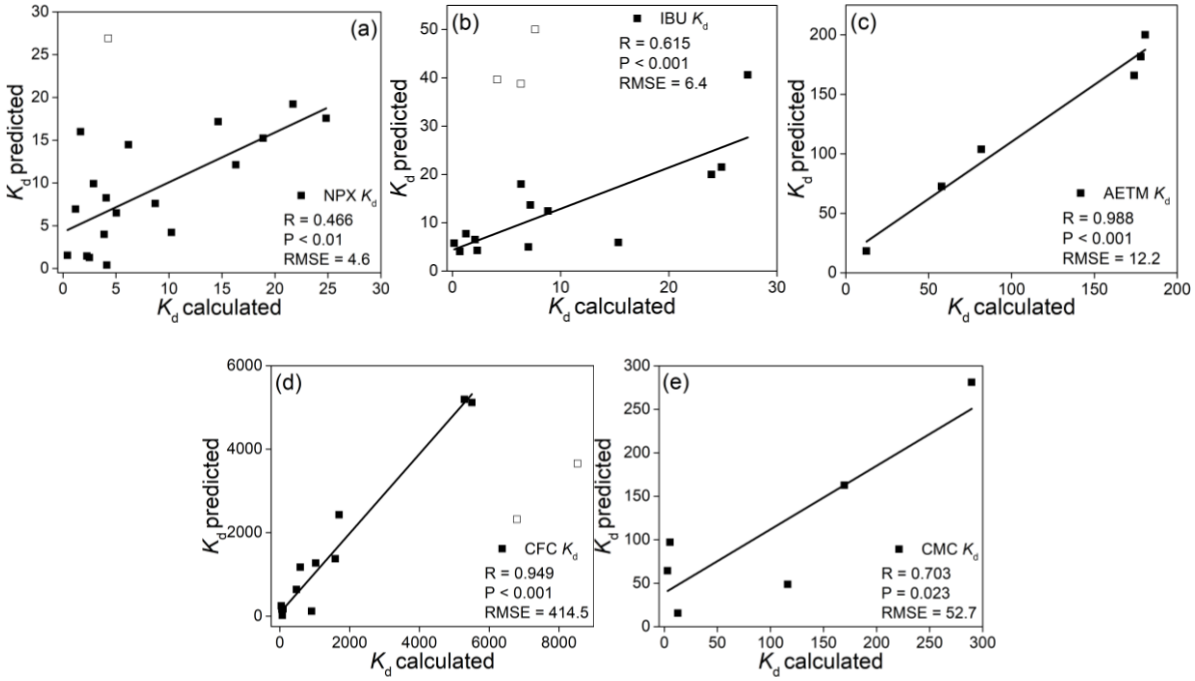

Figure 9. *The relation (model validation) between the calculated and predicted K_d of (a) NPX; (b) IBU; (c) AETM; (d) CFC; and (e) CMC*

Table 8. *K_d and K_{oc} calculated values on site compared with literature values*

Compound	K_d (mL g^{-1})			K_{oc} (mL g^{-1} C)	Literature (mL g^{-1})		Matrix	Reference
	Min	Max	Mean	Mean	K_d	K_{oc}		
ATM	369.2			3,144.7	121-1,834	17,783	Sediment	(Royano et al., 2024, Li et al., 2019a)
AETM	12.5	178.1	114.2	2,699.7	2-73; 211	-	Sediment	(Royano et al., 2024, Sung-Chul and Kenneth, 2007)
CFC	13.9	8534.4	2,180.9	42,472.9	329.3-4,664	-	Sediment	(Zhao et al., 2016)
CMC	3.06	971.2	224.0	24,276	0.7-570	125.9-25,119	Sediment	(Li et al., 2019a)
IBU	0.17	27.3	9.09	236.4	1.72-45.5	192-1,110	Soil	(Vulava et al., 2016)
NPX	0.42	24.8	8.10	209.7	3.4-356	340-7,610	Soil	(Vulava et al., 2016)
SMX	54.2	197.3	115.5	3,117.6	22-105	-	Sediment	(Hu et al., 2018)
TMP	39.3	3,142	720.5	12,854	18.8-3,126	-	Sediment	(Tang et al., 2019, Hu et al., 2018)

Sediment pH influenced compound speciation and sediment surface charge, with higher pH reducing D_{ow} and consequently the K_d. Hydrophobicity (log K_{ow}) alone was insufficient to explain sorption; ionic interactions, often dominant for ionizable pharmaceuticals, played a key role. OC content positively influenced D_{ow} and sorption, underscoring the role of organic matter in pharmaceutical retention.

In addition, the total content of major sediment cations (Al, Fe, Ca, Mg, K, Na) contributed to observed sorption patterns. Metals such as Al and Fe can promote complexation and ligand exchange with functional groups of certain pharmaceuticals, enhancing sediment binding, particularly for antibiotics with multiple ionizable moieties (IBU and NPX) (Table 9). Similarly, Ca and Mg may influence sorption indirectly by affecting sediment aggregation and surface charge, while monovalent cations such as K and Na can compete with pharmaceuticals for electrostatic binding sites. In this study, significant negative correlations were observed between K_d and certain cations (e.g., Fe, Ca, Mg for CFC), suggesting that in some cases high cation content may reduce sorption by altering electrostatic interactions or competing for active binding sites (Table 9) (Kong et al., 2024).

Table 9. *Correlation coefficients (R) between K_d and sediment properties*

Comp-ound	Adj. R^2 (%OC)	Adj. R^2 pH ($CaCl_2$)	D_{ow}	$CaCO_3$	Al (mg kg^{-1})	Fe (mg kg^{-1})	Ca (mg kg^{-1})	K (mg kg^{-1})	Mg (mg kg^{-1})	Na (mg kg^{-1})
AETM	0.734*	-0.085	-0.011	-0.369	-0.867*	-0.306	-0.308	-0.242	-0.609*	-0.605*
CFC	0.565**	-0.811***	0.837***	-0.105	-0.119	-0.636*	-0.394*	-0.389*	-0.384*	-0.113
CMC	0.678*	-0.194	0.15	-0.249	-0.335	-0.61*	-0.179	-0.477	-0.134	-0.11
IBU	0.206	-0.544**	0.609**	-0.144	0.311*	0.247	-0.129	0.133	-0.049	0.208
NPX	0.259	-0.461**	0.444**	-0.326*	0.423*	0.095	-0.029	0.259	-0.153	0.104
SMX	0.961**	-0.169	0.286	-0.04	0.687	0.351	-0.271	-0.18	-0.282	-0.077
TMP	0.227	-0.129	0.095	-0.248	0.499	-0.087	-0.249	-0.373	-0.112	-0.248

*p < 0.05, **p <0.01, ***p<0.001

1.5.6. Sorption of naproxen and carbamazepine onto MBC 1:2:1 composite

The adsorption performance of the prepared MBC 1:2:1 composite was evaluated for the removal of NPX having CBZ as a co-contaminant from aqueous solutions, focusing on solid to liquid ratio, adsorption kinetics, solution pH, temperature and concentration, dissolved organic matter (DOM), reusability, and tests with river water. The composite achieved maximum sorption at a low solution pH of ~2.5 and an individual adsorbent dose of 0.5 g L^{-1}(Fig. 10a). Equilibrium was reached within approximately 12 hours (720 minutes) (Fig.

10b). The PSO model provided a better fit to the rate data, suggesting that the adsorption process followed chemisorption, primarily controlled by valence electron sharing or exchange, which resulted in attractive interactions, such as electrostatic and hydrophobic forces, between the adsorbent surfaces and naproxen species. Sorption was endothermic and best described by the Sips isotherm model, suggesting combined monolayer adsorption and heterogeneous surface behavior (Fig. 10c).

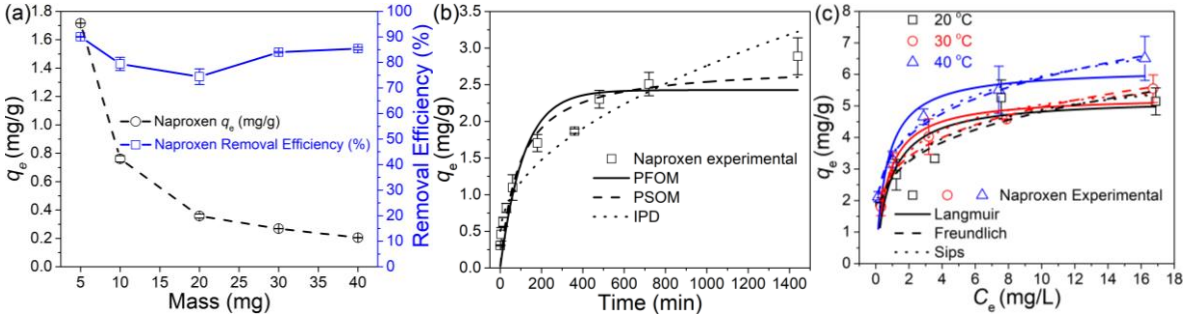

Figure 10. *(a) Adsorption trend and removal efficiency at varying MBC 1:2:1 dosage; (b) naproxen adsorption rate trend and kinetics model fittings on the naproxen adsorption rate data; (c) adsorption isotherm models at 20 °C, 30 °C, and at 40 °C*

Mechanistic insights from Fourier-transform infrared (FTIR) spectroscopy revealed that –OH functional groups of the composite played a key role in NPX sorption (Fig. 11a). A pronounced decrease in the broad absorption band between 3600–2600 cm^{-1} (centered at ~3200 cm^{-1}) after NPX adsorption indicated strong hydrogen bonding between NPX and –OH sites on the composite surface. For CBZ, the adsorption process was predominantly governed by hydrophobic interactions and π–π electron donor–acceptor interactions between CBZ's aromatic rings and the conjugated carbon structures of the composite. Under conditions where solution pH was lower than the composite's point of zero charge (pHpzc), cation–π interactions were also likely, due to a positively charged composite surface. The study examined how solution pH affects NPX and CBZ adsorption in single and binary systems (Fig. 11b). CBZ, which remains neutral across tested pH values (2.5 – 10), adsorbed mainly through hydrophobic, π–π, hydrogen bonding, and possible cation–π interactions. At low pH (<4.5), both drugs showed high sorption, with NPX adsorbing more strongly due to stronger competition. As pH increased, overall sorption decreased, but CBZ adsorption gradually surpassed NPX, indicating weaker competition at higher pH values. The MBC 1:2:1 composite thus demonstrated multifunctional sorption behavior and maintained high removal efficiency under environmentally relevant pH ranges (Fig. 11d). The effect of

dissolved organic matter (DOM) on NPX and CBZ sorption was studied using humic acid (Fig. 11c). At low DOM levels, NPX uptake slightly increased, but higher DOM concentrations reduced sorption in both single and binary systems due to electrostatic repulsion. CBZ sorption decreased more consistently with rising DOM, likely from competition between humic acid functional groups and CBZ for adsorption sites. In river water (similar DOM to 20 mg L^{-1} humic acid), sorption capacities matched this trend, confirming that DOM limits drug adsorption onto the composite. The composite retained ≥99% removal efficiency after five consecutive adsorption–desorption cycles, demonstrating exceptional reusability. In river water spiked with low levels of NPX (~50 µg L^{-1}), removal efficiency remained high (~93%), indicating the composite's applicability in environmental contexts.

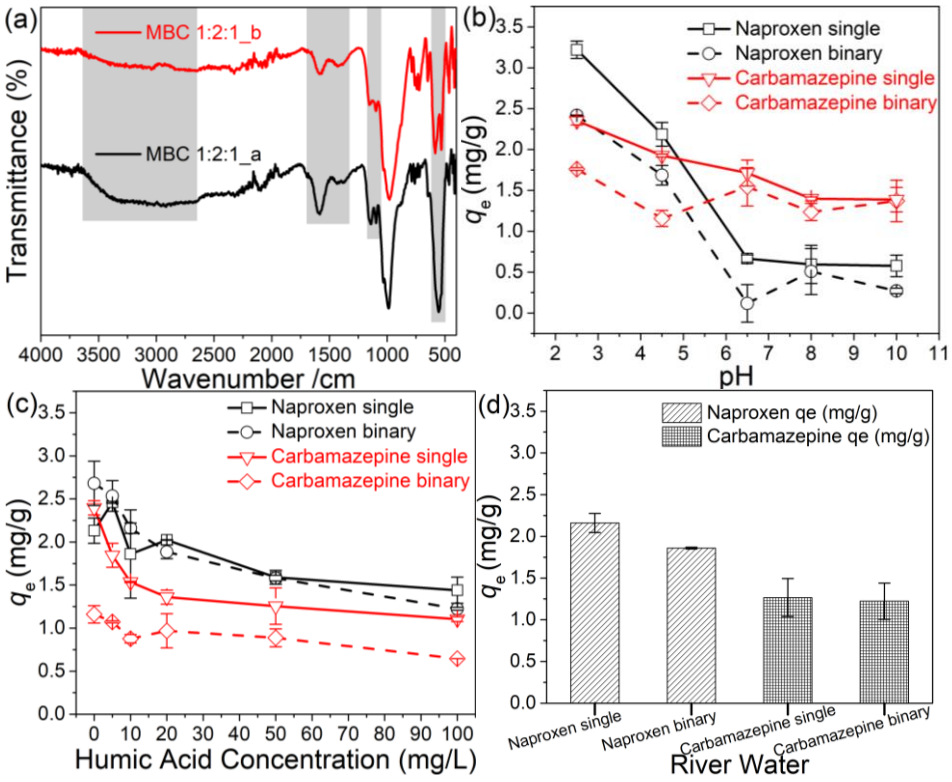

Figure 11. *(a) Comparison of pre-adsorption and post-adsorption FTIR spectra; (b) effect of pH; (c) effect of DOM; and (d) effect of river water*

1.5.7. Sorption of Cd(II), Cr(VI), and Cu(II) onto MBC 1:2:1 and MBC 1:3:1 composites

The adsorption performance of the prepared MBC 1:2:1 and MBC 1:3:1 composites was evaluated for the removal of simultaneously Cd(II), Cr(VI), and Cu(II) from aqueous solutions, focusing on solid to liquid ratio, adsorption kinetics, solution pH, temperature and

concentration, and reusability. Both composites showed optimum removal efficiency for all three cations at 0.66 g L^{-1} adsorbent dose. Rapid uptake occurred within the first 240 min, accounting for >85% of total adsorption, followed by slower diffusion driven uptake until equilibrium at 720 min (Fig. 12). Overall, comparison of the PFOM and PSOM correlation coefficients (r^2) and chi-square (χ^2) values showed that the PSOM provided a better fit, with r^2 values closer to unity and lower χ^2 values (Fig. 12). This indicates that the adsorption process was better described by PSOM kinetics, suggesting control by valence electron exchange between surface sites and metal ions, leading to electrostatic interactions. Adsorption capacity trends showed Cu(II) >Cd(II) ≈ Cr(VI). The effect of pH was significant; Cd(II) and Cu(II) adsorption maximized at pH 6 due to deprotonation of active sites, while Cr(VI) adsorption peaked at pH 3, driven by attraction of $HCrO_4^-$ to positively charged composites surfaces.

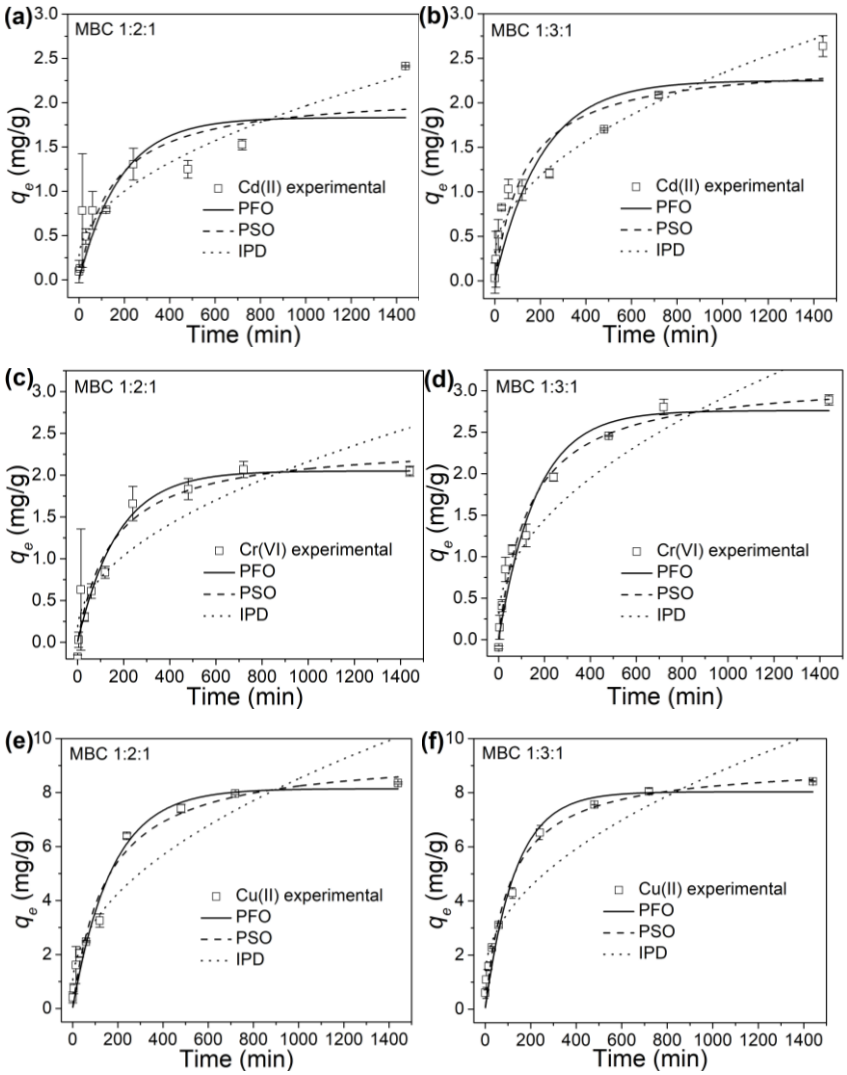

Figure 12. *Kinetics modeling of rate data for adsorption of (a) Cd(II) on MBC 1:2:1, (b) Cd(II) on MBC 1:3:1; (c) Cr(VI) on MBC 1:2:1 (d) Cr(VI) on MBC 1:3:1; (e) Cu(II) on MBC 1:2:1, (f) Cu(II) on MBC 1:3:1*

The dominant adsorption processes were electrostatic attractions and pore phase adsorption, together accounting for over 90% of total uptake. Key functional groups involved included –OH, $–COO^-$, and –C–N, which likely facilitated surface-binding and complexation interactions with metal ions (Fig. 13c).

In ternary systems, both competitive and synergistic effects were observed. Increasing Cu(II) concentration enhanced Cr(VI) adsorption efficiency by 79–86% but reduced Cd(II) uptake by 52–65% ((Fig. 13a and 13b). This suggests preferential interactions between Cu(II) and the adsorbent, facilitating additional binding of Cr(VI). FTIR spectra post-adsorption showed enhanced vibrations of –OH groups and the emergence of carboxyl peaks, suggesting participation in metal binding and partial reduction of Cr(VI) to Cr(III) (Fig. 13c). Amide groups also shifted, confirming involvement in binding. Isotherm modeling indicated that Langmuir best described Cu(II) adsorption, consistent with monolayer coverage, while Langmuir–Freundlich also fit well, suggesting surface heterogeneity. Elevated temperatures modestly improved Cd(II) adsorption, whereas Cr(VI) and Cu(II) sorption showed negligible sensitivity to temperature changes.

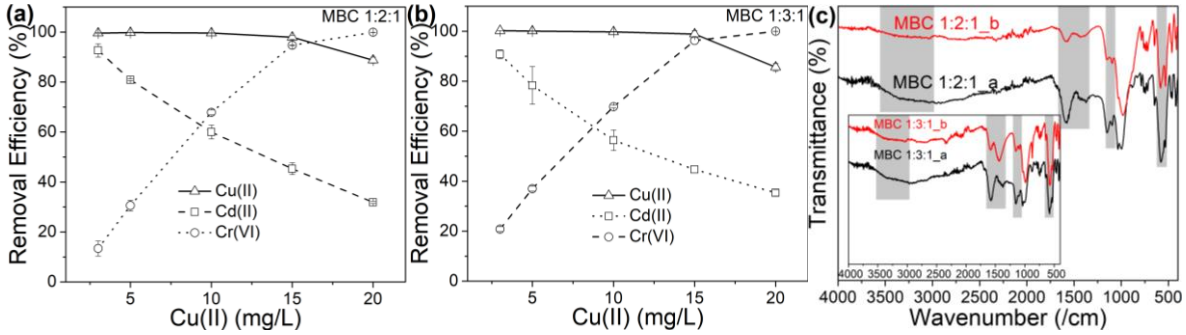

Figure 13. *(a) Effect of the initial concentration of Cu(II) on Cd(II) and Cr(VI) removal efficiency on MBC 1:2:1; (b) on MBC 1:3:1 [adsorbent mass: 20 mg in 30 mL solution using 1 mg L^{-1} Cd(II), 3 mg L^{-1} Cr(VI), and 3-20 mg L^{-1} of Cu(II), pH = 5.4 at 200 rpm]; (c) pre and post-adsorption FTIR spectra of the composites*

Reusability tests demonstrated stable Cr(VI) removal over five cycles, with 70% efficiency retained for MBC 1:2:1. In contrast, Cd(II) and Cu(II) removal dropped after the first cycle, indicating strong irreversible binding.

1.6. Conclusions

This cumulative dissertation has provided new insights into the occurrence, environmental partitioning, and remediation of pharmaceutical and heavy metal contaminants in the Ishmi River basin, Albania. By combining field monitoring with the development of sustainable composite adsorbents, the research has addressed both fundamental knowledge gaps and practical treatment challenges in regions with limited wastewater treatment infrastructure.

The first component of this thesis demonstrated that pharmaceutical pollution in the Ishmi River basin is both compound's and site-specific, with urban hotspots such as the Lana River (LR1) exhibiting the highest contamination levels. Seasonal monitoring confirmed the persistence of compounds such as azithromycin and ciprofloxacin, while regression modeling revealed that physicochemical properties of sediments (pH, organic carbon, carbonates, and metal (cations) content) are key drivers of sediment–water partitioning of selected pharmaceuticals. These findings validate the need for locally adapted predictive models in limited data regions.

The second component established the potential of grape cluster stalk waste derived biochar, combined with feldspar clay and magnetic nanoparticles, to form magneto-biochar-clay (MBC) composites with enhanced surface properties, cation exchange capacity, and recoverability. The prepared MBC 1:2:1 composite was applied to remove selected pharmaceuticals such as naproxen and carbamazepine, showing that they can be effectively removed through hydrophobic, electrostatic, and π–π interactions. The composite maintained its high performance under competitive, in the presence of dissolved organic matter, and under real river water conditions, while also demonstrating excellent reusability across multiple cycles.

The third component extended the application of MBC composites (MBC 1:2:1 and MBC 1:3:1) to heavy metal removal. These composites exhibited high efficiency for the simultaneous removal of toxic metals (Cd(II), Cr(VI), Cu(II)) under environmentally relevant conditions, with favorable kinetics and strong sorption mechanisms involving hydroxyl, carboxyl, and amide functional groups.

Taking together, the outcomes of this thesis contribute to three main advances:

1. A mechanistic understanding of pharmaceutical occurrence and partitioning in under-monitored surface water systems.

2. The development of sustainable, low-cost, magnetically separable biochar–clay composites for water remediation.
3. The demonstration of integrated approaches linking contaminant monitoring to treatment strategies, thereby bridging scientific research with practical applications.

Overall, the findings not only enhance scientific knowledge of contaminants fate in freshwater ecosystems but also offer scalable, nature-based technologies with direct relevance for Albania's environmental management and alignment with European Union water policy goals. Future work should focus on pilot-scale implementation of the developed composites, long-term performance under variable field conditions, and integration into national water quality management frameworks.

1.7. Literature

1. AL-KHAZRAJY, O. S. A. & BOXALL, A. B. A. 2016. Impacts of compound properties and sediment characteristics on the sorption behaviour of pharmaceuticals in aquatic systems. *J Hazard Mater,* 317**,** 198-209.
2. ALHASHIMI, H. A. & AKTAS, C. B. 2017. Life cycle environmental and economic performance of biochar compared with activated carbon: A meta-analysis. *Resources, Conservation and Recycling,* 118**,** 13-26.
3. ANFAR, Z., ZBAIR, M., AHSIANE AIT, H., JADA, A. & ALEM EL, N. 2020. Microwave assisted green synthesis of Fe2O3/ biochar for ultrasonic removal of nonsteroidal antiinflammatory pharmaceuticals. *The Royal Society of Chemistry,* 10**,** 11371–11380.
4. ARIF, M., LIU, G., YOUSAF, B., AHMED, R., IRSHAD, S., ASHRAF, A., ZIA-UR-REHMAN, M. & RASHID, M. S. 2021. Synthesis, characteristics and mechanistic insight into the clays and clay minerals-biochar surface interactions for contaminants removal-A review. *Journal of Cleaner Production,* 310**,** 127548.
5. BACKHAUS, T. 2016. Environmental Risk Assessment of Pharmaceutical Mixtures: Demands, Gaps, and Possible Bridges. *AAPS J,* 18**,** 804-13.
6. BIJLSMA, L., PITARCH, E., FONSECA, E., IBÁÑEZ, M., BOTERO, A. M., CLAROS, J., PASTOR, L. & HERNÁNDEZ, F. 2021. Investigation of pharmaceuticals in a conventional wastewater treatment plant: Removal efficiency, seasonal variation and impact of a nearby hospital. *Journal of Environmental Chemical Engineering,* 9**,** 105548.
7. CARMONA, E., ANDREU, V. & PICO, Y. 2014. Occurrence of acidic pharmaceuticals and personal care products in Turia River Basin: from waste to drinking water. *Sci Total Environ,* 484**,** 53-63.
8. CHEN, K. & ZHOU, J. L. 2014. Occurrence and behavior of antibiotics in water and sediments from the Huangpu River, Shanghai, China. *Chemosphere,* 95**,** 604-12.
9. CLEUVERS, M. 2004. Mixture toxicity of the anti-inflammatory drugs diclofenac, ibuprofen, naproxen, and acetylsalicylic acid. *Ecotoxicol Environ Saf,* 59**,** 309-15.
10. CONNORS, K. A., BRILL, J. L., NORBERG-KING, T., BARRON, M. G., CARR, G. & BELANGER, S. E. 2022. Daphnia magna and Ceriodaphnia dubia Have Similar Sensitivity in Standard Acute and Chronic Toxicity Tests. *Environ Toxicol Chem,* 41**,** 134-147.
11. CRINI, G. & LICHTFOUSE, E. 2018. Advantages and disadvantages of techniques used for wastewater treatment. *Environmental Chemistry Letters,* 17**,** 145-155.
12. CUTHBERT, R. J., TAGGART, M. A., SAINI, M., SHARMA, A., DAS, A., KULKARNI, M. D., DEORI, P., RANADE, S., SHRINGARPURE, R. N., GALLIGAN, T. H. & GREEN, R. E. 2015. Continuing mortality of vultures in India associated with illegal veterinary use of diclofenac and a potential threat from nimesulide. *Oryx,* 50**,** 104-112.
13. DĄBROWSKI, A. 2001. Adsorption — from theory to practice. *Advances in Colloid and Interface Science,* 93**,** 135-224.
14. DALKMANN, P., BROSZAT, M., SIEBE, C., WILLASCHEK, E., SAKINC, T., HUEBNER, J., AMELUNG, W., GROHMANN, E. & SIEMENS, J. 2012. Accumulation of pharmaceuticals, Enterococcus, and resistance genes in soils irrigated with wastewater for zero to 100 years in central Mexico. *PLoS One,* 7**,** e45397.
15. DELLA GRECA, M., BRIGANTE, M., ISIDORI, M., NARDELLI, A., PREVITERA, L., RUBINO, M. & TEMUSSI, F. 2003. Phototransformation and ecotoxicity of the drug Naproxen-Na. *Environmental Chemistry Letters,* 1**,** 237-241.

16. DELORENZO, M. E. & FLEMING, J. 2008. Individual and mixture effects of selected pharmaceuticals and personal care products on the marine phytoplankton species Dunaliella tertiolecta. *Arch Environ Contam Toxicol,* 54**,** 203-10.
17. DIAGBOYA, P. N., MTUNZI, F. M., ADEBOWALE, K. O., DÜRING, R.-A. & OLU-OWOLABI, B. I. 2022. Comparative empirical evaluation of the aqueous adsorptive sequestration potential of low-cost feldspar-biochar composites for ivermectin. *Colloids and Surfaces A: Physicochemical and Engineering Aspects,* 634**,** 127930.
18. DING, T., LIN, K., YANG, B., YANG, M., LI, J., LI, W. & GAN, J. 2017. Biodegradation of naproxen by freshwater algae Cymbella sp. and Scenedesmus quadricauda and the comparative toxicity. *Bioresour Technol,* 238**,** 164-173.
19. DONNER, E., KOSJEK, T., QUALMANN, S., KUSK, K. O., HEATH, E., REVITT, D. M., LEDIN, A. & ANDERSEN, H. R. 2013. Ecotoxicity of carbamazepine and its UV photolysis transformation products. *Sci Total Environ,* 443**,** 870-6.
20. FREUNDLICH, H. M. F. 1906. Über die adsorption in lösungen. *Zeitschrift für Physikalische Chemie,* 57A**,** 57A, 385-470.
21. GERBA, C. P., TAMIMI, A. H., PETTIGREW, C., WEISBROD, A. V. & RAJAGOPALAN, V. 2011. Sources of microbial pathogens in municipal solid waste landfills in the United States of America. *Waste Manag Res,* 29**,** 781-90.
22. HANAFI, M. F. & SAPAWE, N. 2020. A review on the current techniques and technologies of organic pollutants removal from water/wastewater. *Materials Today: Proceedings,* 31**,** A158-A165.
23. HEBIG, K. H., GROZA, L. G., SABOURIN, M. J., SCHEYTT, T. J. & PTACEK, C. J. 2017. Transport behavior of the pharmaceutical compounds carbamazepine, sulfamethoxazole, gemfibrozil, ibuprofen, and naproxen, and the lifestyle drug caffeine, in saturated laboratory columns. *Sci Total Environ,* 590-591**,** 708-719.
24. HEINRICH, A. P., ZOLTZER, T., BOHM, L., WOHDE, M., JADDOUDI, S., EL MAATAOUI, Y., DAHCHOUR, A. & DURING, R. A. 2021. Sorption of selected antiparasitics in soils and sediments. *Environ Sci Eur,* 33**,** 77.
25. HEYDE, B. J., BRAUN, M., SOUFI, L., LÜNEBERG, K., GALLEGO, S., AMELUNG, W., AXTMANN, K., BIERBAUM, G., GLAESER, S. P., GROHMANN, E., ARREDONDO-HERNÁNDEZ, R., MULDER, I., PULAMI, D., SMALLA, K., ZARFL, C., SIEBE, C. & SIEMENS, J. 2025. Transition from irrigation with untreated wastewater to treated wastewater and associated benefits and risks. *npj Clean Water,* 8.
26. HU, Y., YAN, X., SHEN, Y., DI, M. & WANG, J. 2018. Antibiotics in surface water and sediments from Hanjiang River, Central China: Occurrence, behavior and risk assessment. *Ecotoxicol Environ Saf,* 157**,** 150-158.
27. J. LINDSAY OAKS, M. G., MUNIR Z. VIRANI, RICHARD T. WATSON,, CAROL U. METEYER, B. A. R., H. L. SHIVAPRASAD,, SHAKEEL AHMED, M. J. I. C., MUHAMMAD ARSHAD, S. M., AHMAD ALI & KHAN6, A. A. 2004. Diclofenac residues as the cause of vulture population decline in Pakistan. *Nature,* 427**,** 630–633
28. JALLOULI, N., ELGHNIJI, K., HENTATI, O., RIBEIRO, A. R., SILVA, A. M. & KSIBI, M. 2016. UV and solar photo-degradation of naproxen: TiO(2) catalyst effect, reaction kinetics, products identification and toxicity assessment. *J Hazard Mater,* 304**,** 329-36.
29. JEDNACAK, T., MIKULANDRA, I. & NOVAK, P. 2020. Advanced Methods for Studying Structure and Interactions of Macrolide Antibiotics. *Int J Mol Sci,* 21.
30. JOSS, A., ZABCZYNSKI, S., GÖBEL, A., HOFFMANN, B., LÖFFLER, D., MCARDELL, C. S., TERNES, T. A., THOMSEN, A. & SIEGRIST, H. 2006. Biological degradation of pharmaceuticals in municipal wastewater treatment: Proposing a classification scheme. *Water Research,* 40**,** 1686-1696.

31. JUNCK, J., DIAGBOYA, P. N., PEQINI, A., ROHNKE, M. & DÜRING, R.-A. 2024. Mechanistic interpretation of the sorption of terbuthylazine pesticide onto aged microplastics. *Environmental Pollution,* 345**,** 123502.
32. KODEŠOVÁ, R., KOČÁREK, M., KLEMENT, A., GOLOVKO, O., KOBA, O., FÉR, M., NIKODEM, A., VONDRÁČKOVÁ, L., JAKŠÍK, O. & GRABIC, R. 2016. An analysis of the dissipation of pharmaceuticals under thirteen different soil conditions. *Sci Total Environ,* 544**,** 369-81.
33. KONG, W., WANG, W., JIANG, Y., WANG, G., MA, F. & WU, Y. 2024. Sorption of ciprofloxacin and enrofloxacin on alkaline cropland soil in semiarid regions: Roles of pH, ionic strength, and ion type. *J Environ Manage,* 365**,** 121565.
34. KÜMMERER, K. 2009. The presence of pharmaceuticals in the environment due to human use--present knowledge and future challenges. *J Environ Manage,* 90**,** 2354-66.
35. KÜMMERER, K. 2010. Pharmaceuticals in the Environment. *Annual Review of Environment and Resources,* 35**,** 57-75.
36. LANGMUIR, I. 1916. The constitution and fundamental properties of solids and liquids. *J. Amer. Chem. Soc.,* 38**,** 2221–2295.
37. LE GUET, T., HSINI, I., LABANOWSKI, J. & MONDAMERT, L. 2018. Sorption of selected pharmaceuticals by a river sediment: role and mechanisms of sediment or Aldrich humic substances. *Environ Sci Pollut Res Int,* 25**,** 14532-14543.
38. LI, J., DODGEN, L., YE, Q. & GAN, J. 2013. Degradation Kinetics and Metabolites of Carbamazepine in Soil. *Environmental Science & Technology,* 47**,** 3678-3684.
39. LI, J., LI, W., LIU, K., GUO, Y., DING, C., HAN, J. & LI, P. 2022. Global review of macrolide antibiotics in the aquatic environment: Sources, occurrence, fate, ecotoxicity, and risk assessment. *J Hazard Mater,* 439**,** 129628.
40. LI, Q., WANG, P., CHEN, L., GAO, H. & WU, L. 2016. Acute toxicity and histopathological effects of naproxen in zebrafish (Danio rerio) early life stages. *Environ Sci Pollut Res Int,* 23**,** 18832-41.
41. LI, S., HE, B., WANG, J., LIU, J. & HU, X. 2020. Risks of caffeine residues in the environment: Necessity for a targeted ecopharmacovigilance program. *Chemosphere,* 243**,** 125343.
42. LI, S., ZHANG, R., HU, J., SHI, W., KUANG, Y., GUO, X. & SUN, W. 2019a. Occurrence and removal of antibiotics and antibiotic resistance genes in natural and constructed riverine wetlands in Beijing, China. *Sci Total Environ,* 664**,** 546-553.
43. LI, W. C. 2014. Occurrence, sources, and fate of pharmaceuticals in aquatic environment and soil. *Environ Pollut,* 187**,** 193-201.
44. LI, Y., DING, J., ZHANG, L., LIU, X. & WANG, G. 2019b. Occurrence and ranking of pharmaceuticals in the major rivers of China. *Sci Total Environ,* 696**,** 133991.
45. LI, Z. H., ZLABEK, V., VELISEK, J., GRABIC, R., MACHOVA, J., KOLAROVA, J., LI, P. & RANDAK, T. 2011. Acute toxicity of carbamazepine to juvenile rainbow trout (Oncorhynchus mykiss): effects on antioxidant responses, hematological parameters and hepatic EROD. *Ecotoxicol Environ Saf,* 74**,** 319-27.
46. MAGED, A., ELGARAHY, A. M., HLAWITSCHKA, M. W., HANEKLAUS, N. H., GUPTA, A. K. & BHATNAGAR, A. 2023. Synergistic mechanisms for the superior sorptive removal of aquatic pollutants via functionalized biochar-clay composite. *Bioresour Technol,* 387**,** 129593.
47. MARTIN, J., CAMACHO-MUNOZ, D., SANTOS, J. L., APARICIO, I. & ALONSO, E. 2012. Occurrence of pharmaceutical compounds in wastewater and sludge from wastewater treatment plants: removal and ecotoxicological impact of wastewater discharges and sludge disposal. *J Hazard Mater,* 239-240**,** 40-7.

48. MARTIN, J., SANTOS, J. L., APARICIO, I. & ALONSO, E. 2010. Multi-residue method for the analysis of pharmaceutical compounds in sewage sludge, compost and sediments by sonication-assisted extraction and LC determination. *J Sep Sci,* 33**,** 1760-6.
49. MATESUN, J., PETRIK, L., MUSVOTO, E., AYINDE, W. & IKUMI, D. 2024. Limitations of wastewater treatment plants in removing trace anthropogenic biomarkers and future directions: A review. *Ecotoxicol Environ Saf,* 281**,** 116610.
50. MATHIAS, F. T., FOCKINK, D. H., DISNER, G. R., PRODOCIMO, V., RIBAS, J. L. C., RAMOS, L. P., CESTARI, M. M. & SILVA DE ASSIS, H. C. 2018. Effects of low concentrations of ibuprofen on freshwater fish Rhamdia quelen. *Environ Toxicol Pharmacol,* 59**,** 105-113.
51. MOHD ZANURI, N. B., BENTLEY, M. G. & CALDWELL, G. S. 2017. Assessing the impact of diclofenac, ibuprofen and sildenafil citrate (Viagra((R))) on the fertilisation biology of broadcast spawning marine invertebrates. *Mar Environ Res,* 127**,** 126-136.
52. MOHUBEDU, R. P., DIAGBOYA, P. N. E., ABASI, C. Y., DIKIO, E. D. & MTUNZI, F. 2019. Magnetic valorization of biomass and biochar of a typical plant nuisance for toxic metals contaminated water treatment. *Journal of Cleaner Production,* 209**,** 1016-1024.
53. MORENO-GONZALEZ, R., RODRIGUEZ-MOZAZ, S., GROS, M., BARCELO, D. & LEON, V. M. 2015. Seasonal distribution of pharmaceuticals in marine water and sediment from a Mediterranean coastal lagoon (SE Spain). *Environ Res,* 138**,** 326-44.
54. OLU-OWOLABI, B. I., DIAGBOYA, P. N., MTUNZI, F. M. & DURING, R. A. 2021. Utilizing eco-friendly kaolinite-biochar composite adsorbent for removal of ivermectin in aqueous media. *J Environ Manage,* 279**,** 111619.
55. PAIGA, P., RAMOS, S., JORGE, S., SILVA, J. G. & DELERUE-MATOS, C. 2019. Monitoring survey of caffeine in surface waters (Lis River) and wastewaters located at Leiria Town in Portugal. *Environ Sci Pollut Res Int,* 26**,** 33440-33450.
56. PATEL, M., KUMAR, R., KISHOR, K., MLSNA, T., PITTMAN, C. U., JR. & MOHAN, D. 2019. Pharmaceuticals of Emerging Concern in Aquatic Systems: Chemistry, Occurrence, Effects, and Removal Methods. *Chem Rev,* 119**,** 3510-3673.
57. PATROLECCO, L., ADEMOLLO, N., GRENNI, P., TOLOMEI, A., BARRA CARACCIOLO, A. & CAPRI, S. 2013. Simultaneous determination of human pharmaceuticals in water samples by solid phase extraction and HPLC with UV-fluorescence detection. *Microchemical Journal,* 107**,** 165-171.
58. PHILLIPS, P. J., SCHUBERT, C., ARGUE, D., FISHER, I., FURLONG, E. T., FOREMAN, W., GRAY, J. & CHALMERS, A. 2015. Concentrations of hormones, pharmaceuticals and other micropollutants in groundwater affected by septic systems in New England and New York. *Sci Total Environ,* 512-513**,** 43-54.
59. PRAKASH, V., BISHWAKARMA, M. C., CHAUDHARY, A., CUTHBERT, R., DAVE, R., KULKARNI, M., KUMAR, S., PAUDEL, K., RANADE, S., SHRINGARPURE, R. & GREEN, R. E. 2012. The population decline of Gyps vultures in India and Nepal has slowed since veterinary use of diclofenac was banned. *PLoS One,* 7**,** e49118.
60. RANJIT, P., JHANSI, V. & REDDY, K. V. 2021. Conventional Wastewater Treatment Processes. *In:* MADDELA, N. R., GARCÍA CRUZATTY, L. C. & CHAKRABORTY, S. (eds.) *Advances in the Domain of Environmental Biotechnology: Microbiological Developments in Industries, Wastewater Treatment and Agriculture.* Singapore: Springer Singapore.
61. RILSTONE, V., FILION, Y. & CHAMPAGNE, P. 2025. Study on the persistence of ciprofloxacin and sulfamethoxazole in simulated drinking water systems. *Environ Syst Res (Heidelb),* 14**,** 7.

62. ROBINSON, A. A., BELDEN, J. B. & LYDY, M. J. 2005. TOXICITY OF FLUOROQUINOLONE ANTIBIOTICS TO AQUATIC ORGANISMS. *Enviro Toxic and Chemistry* 24**,** 423-430.
63. RÖHRICHT, M., KRISAM, J., WEISE, U., KRAUS, U. R. & DÜRING, R.-A. 2009. Elimination of Carbamazepine, Diclofenac and Naproxen from Treated Wastewater by Nanofiltration. *CLEAN - Soil, Air, Water,* 37**,** 638-641.
64. ROYANO, S., NAVARRO, I., TORRE, A. & MARTINEZ, M. A. 2024. Investigating the presence, distribution and risk of pharmaceutically active compounds (PhACs) in wastewater treatment plants, river sediments and fish. *Chemosphere,* 368**,** 143759.
65. SCHMIDT, W., O'ROURKE, K., HERNAN, R. & QUINN, B. 2011. Effects of the pharmaceuticals gemfibrozil and diclofenac on the marine mussel (Mytilus spp.) and their comparison with standardized toxicity tests. *Mar Pollut Bull,* 62**,** 1389-95.
66. SENTA, I., TERZIC, S. & AHEL, M. 2021. Analysis and occurrence of macrolide residues in stream sediments and underlying alluvial aquifer downstream from a pharmaceutical plant. *Environ Pollut,* 273**,** 116433.
67. SUNG-CHUL, K. & KENNETH, C. 2007. Temporal and Spatial Trends in the Occurrence of Human and Veterinary Antibiotics in Aqueous and River Sediment Matrices. *Environmental Science & Technology,* 41**,** 50-57.
68. TAHIRI, V., DENAJ, A. & PRENGA, D. 2023. Assessment of the Presence of Pharmaceutical Compounds in Wastewaters and in Aquatic Environment. *Journal of Human, Earth, and Future,* 4.
69. TANG, J., WANG, S., FAN, J., LONG, S., WANG, L., TANG, C., TAM, N. F. & YANG, Y. 2019. Predicting distribution coefficients for antibiotics in a river water-sediment using quantitative models based on their spatiotemporal variations. *Sci Total Environ,* 655**,** 1301-1310.
70. THIELE-BRUHN, S. 2003. Pharmaceutical antibiotic compounds in soils – a review. *Journal of Plant Nutrition and Soil Science,* 166**,** 145-167.
71. TOLLS, J. 2001. Sorption of Veterinary Pharmaceuticals in Soils: A Review. *Environmental Science & Technology,* 35**,** 3397-3406.
72. TRIEBSKORN, R., CASPER, H., HEYD, A., EIKEMPER, R., KOHLER, H. R. & SCHWAIGER, J. 2004. Toxic effects of the non-steroidal anti-inflammatory drug diclofenac. Part II: cytological effects in liver, kidney, gills and intestine of rainbow trout (Oncorhynchus mykiss). *Aquat Toxicol,* 68**,** 151-66.
73. VAZQUEZ-ROIG, P., ANDREU, V., BLASCO, C. & PICO, Y. 2012. Risk assessment on the presence of pharmaceuticals in sediments, soils and waters of the Pego-Oliva Marshlands (Valencia, eastern Spain). *Sci Total Environ,* 440**,** 24-32.
74. VULAVA, V. M., CORY, W. C., MURPHEY, V. L. & ULMER, C. Z. 2016. Sorption, photodegradation, and chemical transformation of naproxen and ibuprofen in soils and water. *Sci Total Environ,* 565**,** 1063-1070.
75. WAN ISMAIL, W. N. & MOHKTAR, S. U. 2020. Various Methods for Removal, Treatment, and Detection of Emerging Water Contaminants. *In:* NURO, A. (ed.) *Emerging Contaminants.* Rijeka: IntechOpen.
76. WANG, H., XI, H., XU, L., JIN, M., ZHAO, W. & LIU, H. 2021. Ecotoxicological effects, environmental fate and risks of pharmaceutical and personal care products in the water environment: A review. *Sci Total Environ,* 788**,** 147819.
77. WANG, X., GUO, Z., HU, Z. & ZHANG, J. 2020. Recent advances in biochar application for water and wastewater treatment: a review. *PeerJ,* 8**,** e9164.
78. WHO 2015. Global Action Plan on Antimicrobial Resistance.
79. WILKINSON, J. L., BOXALL, A. B. A., KOLPIN, D. W., LEUNG, K. M. Y., LAI, R. W. S., GALBÁN-MALAGÓN, C., ADELL, A. D., MONDON, J., METIAN, M.,

MARCHANT, R. A., BOUZAS-MONROY, A., CUNI-SANCHEZ, A., COORS, A., CARRIQUIRIBORDE, P., ROJO, M., GORDON, C., CARA, M., MOERMOND, M., LUARTE, T., PETROSYAN, V., PERIKHANYAN, Y., MAHON, C. S., MCGURK, C. J., HOFMANN, T., KORMOKER, T., INIGUEZ, V., GUZMAN-OTAZO, J., TAVARES, J. L., GILDASIO DE FIGUEIREDO, F., RAZZOLINI, M. T. P., DOUGNON, V., GBAGUIDI, G., TRAORÉ, O., BLAIS, J. M., KIMPE, L. E., WONG, M., WONG, D., NTCHANTCHO, R., PIZARRO, J., YING, G. G., CHEN, C. E., PÁEZ, M., MARTÍNEZ-LARA, J., OTAMONGA, J. P., POTÉ, J., IFO, S. A., WILSON, P., ECHEVERRÍA-SÁENZ, S., UDIKOVIC-KOLIC, N., MILAKOVIC, M., FATTA-KASSINOS, D., IOANNOU-TTOFA, L., BELUŠOVÁ, V., VYMAZAL, J., CÁRDENAS-BUSTAMANTE, M., KASSA, B. A., GARRIC, J., CHAUMOT, A., GIBBA, P., KUNCHULIA, I., SEIDENSTICKER, S., LYBERATOS, G., HALLDÓRSSON, H. P., MELLING, M., SHASHIDHAR, T., LAMBA, M., NASTITI, A., SUPRIATIN, A., POURANG, N., ABEDINI, A., ABDULLAH, O., GHARBIA, S. S., PILLA, F., CHEFETZ, B., TOPAZ, T., YAO, K. M., AUBAKIROVA, B., BEISENOVA, R., OLAKA, L., MULU, J. K., CHATANGA, P., NTULI, V., BLAMA, N. T., SHERIF, S., ARIS, A. Z., LOOI, L. J., NIANG, M., TRAORE, S. T., OLDENKAMP, R., OGUNBANWO, O., ASHFAQ, M., IQBAL, M., ABDEEN, Z., O'DEA, A., MORALES-SALDAÑA, J. M., CUSTODIO, M., DE LA CRUZ, H., NAVARRETE, I., CARVALHO, F., GOGRA, A. B., et al. 2022. Pharmaceutical pollution of the world's rivers. *Proc Natl Acad Sci U S A*.

80. WOJCIESZYŃSKA, D., ŁAGODA, K. & GUZIK, U. 2023. Diclofenac Biodegradation by Microorganisms and with Immobilised Systems—A Review. *Catalysts* [Online], 13.
81. XU, Y., YU, X., XU, B., PENG, D. & GUO, X. 2021. Sorption of pharmaceuticals and personal care products on soil and soil components: Influencing factors and mechanisms. *Science of The Total Environment,* 753**,** 141891.
82. ZHANG, B., MEI, M., LI, K., LIU, J., WANG, T., CHEN, S. & LI, J. 2022. One-pot synthesis of MnFe2O4 functionalized magnetic biochar by the sol-gel pyrolysis method for diclofenac sodium removal. *Journal of Cleaner Production,* 381**,** 135210.
83. ZHANG, D. Q., HUA, T., GERSBERG, R. M., ZHU, J., NG, W. J. & TAN, S. K. 2013. Carbamazepine and naproxen: fate in wetland mesocosms planted with Scirpus validus. *Chemosphere,* 91**,** 14-21.
84. ZHANG, M., SHEN, J., ZHONG, Y., DING, T., DISSANAYAKE, P. D., YANG, Y., TSANG, Y. F. & OK, Y. S. 2020. Sorption of pharmaceuticals and personal care products (PPCPs) from water and wastewater by carbonaceous materials: A review. *Critical Reviews in Environmental Science and Technology,* 52**,** 727-766.
85. ZHAO, S., LIU, X., CHENG, D., LIU, G., LIANG, B., CUI, B. & BAI, J. 2016. Temporal-spatial variation and partitioning prediction of antibiotics in surface water and sediments from the intertidal zones of the Yellow River Delta, China. *Sci Total Environ,* 569-570**,** 1350-1358.
86. ZHENG, L., GAO, Y., DU, J., ZHANG, W., HUANG, Y., ZHAO, Q., DUAN, L., LIU, Y., NAIDU, R. & PAN, X. 2021. Single and Binary Adsorption Behaviour and Mechanisms of Cd2+, Cu2+ and Ni2+ onto Modified Biochar in Aqueous Solutions. *Processes,* 9**,** 1829.
87. ZHOU, L. J., YING, G. G., ZHAO, J. L., YANG, J. F., WANG, L., YANG, B. & LIU, S. 2011. Trends in the occurrence of human and veterinary antibiotics in the sediments of the Yellow River, Hai River and Liao River in northern China. *Environ Pollut,* 159**,** 1877-85.

88. ZHOU, Q., LIAO, B., LIN, L., QIU, W. & SONG, Z. 2018. Adsorption of Cu(II) and Cd(II) from aqueous solutions by ferromanganese binary oxide-biochar composites. *Sci Total Environ,* 615**,** 115-122.

2. Publication 1: Integrated analysis of the occurrence and in situ sediment-water partitioning of selected pharmaceuticals in a riverine system

Published in *Environmental Sciences Europe* as: Integrated analysis of the occurrence and in situ sediment-water partitioning of the selected pharmaceuticals in a riverine system

DOI: 10.1186/s12302-025-01264-w

Main Text of Publication 1 from page 43

Supplementary Material of Publication 1 from page 59

2.1. Main Text of Publication 1

Peqini *et al. Environmental Sciences Europe* (2025) 37:212
https://doi.org/10.1186/s12302-025-01264-w

Environmental Sciences Europe

RESEARCH Open Access

Integrated analysis of the occurrence and in situ sediment–water partitioning of selected pharmaceuticals in a riverine system

Aleksandër Peqini[1,2,4*], Benjamin Justus Heyde[1,3], Ferdi Brahushi[2] and Rolf-Alexander Düring[1,4]

Abstract

Twelve pharmaceuticals, including stimulant caffeine (CAFF), anti-inflammatories (naproxen (NPX), ibuprofen (IBU), and diclofenac (DCF)), antibiotics (anhydro-erythromycin (AETM), azithromycin (ATM), erythromycin (ETM), clindamycin (CMC), ciprofloxacin (CFC), sulfamethoxazole (SMX), and trimethoprim (TMP)), and the antiepileptic carbamazepine (CBZ), were analyzed in surface waters and sediments in the Ishmi River basin, Albania, across seasons during 2023 and 2024. This basin is characterized by limited wastewater treatment infrastructure, varying degrees of urban impact, and different environmental conditions. All targeted compounds were detected in water, with the highest concentrations observed near urban areas, particularly at the wastewater-impacted location LR1 for CAFF, IBU, NPX, and CFC with 22.5, 12.8, 2.7, and 1.8 µg L^{-1}, respectively. Sediment concentrations showed high levels of CFC and ATM, notably during spring with the highest concentrations of 1068 (LR1) and 396 ng g^{-1} (IR2), respectively, suggesting strong seasonal and spatial variability. Partitioning behavior (K_d and K_{oc}) was investigated in relation to compound-specific (D_{ow}) and sediment-specific (pH, organic carbon, $CaCO_3$ and metal content) properties. Significant correlations were found, and multiple regression models successfully predicted in situ K_d values for NPX, IBU, CFC, AETM, and CMC. These findings underline the influence of environmental and sediment characteristics on environmental pharmaceutical distribution.

Keywords Emerging contaminants, Sediment physico-chemical properties, D_{ow}, K_d modeling, Spatial–temporal pattern

Introduction

Pharmaceuticals are extensively used in treating humans or animal diseases because of their biological activity [26]. The global pharmaceutical market has expanded significantly over the past two decades; in 2019, its value reached approximately USD 1.25 trillion, compared to USD 390 billion in 2001 [16], indicating their increasing trend over the years. Pharmaceuticals may enter the environment through various pathways such as pharmaceutical factories and hospital effluents, household wastewater, livestock farm wastewater (feces and urine), wastewater treatment plant effluents, aquaculture, farmlands (sludge reuse as fertilizer), and solid waste disposal (unused and expired pharmaceuticals) [27], as well as wastewater irrigation [17]. In the environment,

*Correspondence:
Aleksandër Peqini
aleksander.peqini@umwelt.uni-giessen.de
[1] Institute of Soil Science and Soil Conservation, iFZ Research Centre for BioSystems, Land Use and Nutrition (iFZ), Justus Liebig University Giessen, Heinrich-Buff-Ring 26, 35392 Giessen, Germany
[2] Department of Environment and Natural Resources, Faculty of Agriculture and Environment, Agricultural University of Tirana, 1029 Tirana, Albania
[3] Present Address: Institute of Geography, Unit Soil Sciences and Soil Resources, Ruhr University Bochum, Bochum, Germany
[4] Kompetenzzentrum Wasser Hessen, Max-Von-Laue Straße 13, 60438 Frankfurt Am Main, Germany

pharmaceuticals are subject of abiotic and biotic processes such as biotransformation, biodegradation, photolysis, and sorption to suspended solids [3, 30]. The latter is getting more focus because of better assessment of their environmental behavior and potential effects on sediment-dwelling organisms. It is reported that the partitioning of pharmaceuticals is driven by the combination of physico-chemical properties of both compound and sediment [1, 49, 59]. At the same time, models considering these properties simultaneously are developed in order to predict their partitioning between environmental media [49]. But, as environmental conditions and certain site characteristics differ, these models still have weaknesses in predicting the distribution behavior of pharmaceuticals in the environment. Therefore, it is necessary to assess pharmaceutical partitioning through in situ developed models, considering the physico-chemical properties of the compounds and sediments under environmental conditions.

In this study, caffeine (CAFF), carbamazepine (CBZ), naproxen (NPX), ibuprofen (IBU), diclofenac (DCF), anhydro-erythromycin (AETM), azithromycin (ATM), erythromycin (ETM), clindamycin (CMC), ciprofloxacin (CFC), sulfamethoxazole (SMX), and trimethoprim (TMP) were chosen due to their environmental relevance and in the context of Albania's obligation, as a European Union (EU) candidate country, to align its water policies with the Water Framework Directive (Directive 2000/60/EC). This directive requires robust monitoring and reporting of water quality status across all water bodies. Based on the latest update of this directive watch list (Commission Implementing Decision (EU) 2025/439), only CMC remains in the watch list, due to insufficient monitoring data, while SMX and TMP were removed in 2024 (completed the four year monitoring cycle). Other compounds such as CBZ, IBU, DCF, ATM, ETM, and CFC (except CAFF, NPX and AETM) have been proposed for inclusion in the list of priority substances in surface waters. However, CAFF is particularly relevant to this study, as wastewater discharges into the Ishmi River are untreated and high CAFF inputs can therefore be assumed. NPX is the painkiller with the highest prescription rates in Albania. AETM as a transformation product of the antibiotic ETM frequently occurs in waste water and surface waters.

Pharmaceutical concentrations in aquatic environments typically range from below detection to the low μg L^{-1} level in developed countries [38, 42], while data from developing countries, such Albania in this case, remain limited. In this regard, there is only one study in Albania which detected only two compounds (caffeine at 45 ng L^{-1} and citalopram at 6–8 ng L^{-1}) in a northern Albanian River (Buna River) [57]. High concentrations of pharmaceuticals are found in lower-middle income countries due to increasing consumption of pharmaceuticals and limited wastewater treatment infrastructure [57].

Albania, classified as a middle-income country (World Bank, 2022), has over 30% of its population concentrated in the central-western region, where the Ishmi River is located. This area is notably lacking in functional wastewater treatment infrastructure, raising significant concerns regarding pharmaceutical contamination and broader environmental pollution. Albanian monthly average consumption data for 2023 and 2024 reported that CBZ, NPX, IBU, and DCF were used in quantities of 36.01 and 45.13 kg, 156.6 and 139.2 kg, 6.25 and 5.08 kg, and 0.82 and 0.85 kg, respectively. In contrast, the usage of antibiotics ATM, CFC, ETM, SMX, and TMP was considerably lower, with average monthly amounts of 0.05 and 0.02 kg, 0.60 and 0.56 kg, 0.08 and 0.09 kg, 0.47 and 0.58 kg, and 0.10 and 0.12 kg, respectively. Notably, AETM and CMC were not reimbursed during the reporting period. These values represent only the reimbursed quantities covered by the Mandatory Health Insurance Fund of Albania, accounting for an estimated 1–5% of total national pharmaceutical consumption. The study area lacks wastewater treatment, indicating high input of pharmaceuticals and that it is worthwhile investigating their partitioning behavior under environmental conditions. Therefore, the objective of this study was to assess the occurrence of the selected pharmaceuticals in water and sediments and their partitioning behavior by considering both compound properties and site-specific environmental conditions.

Materials and methods

Study area, sample collection and pretreatment

Sampling campaigns in the Ishmi River basin were carried out seasonally during 2023 and 2024 for surface water samples. For certain pharmaceuticals (AETM, ATM, CMC, CFC, ETM, SMX, and TMP), sampling was limited to three seasons, due to technical constraints in the analytical system, which prevented complete seasonal coverage for these compounds (Fig. 1; SM Table 1). Sediment samples were collected during the spring and summer seasons of both years (Fig. 1; SM Table 2). Site locations and brief site characteristics are summarized in Table 1. The Ishmi River basin includes several tributaries, such as the Tirana, Lana, Terkuzë, Gjoles, and Zeza Rivers, and discharges into the Adriatic Sea. The main stem of the Ishmi River spans 74 km, with the entire basin extending to approximately 152 km including its tributaries. Sampling sites were situated at established national water monitoring stations and categorized based on their relative position in the basin: upstream (Brari Bridge – TR1), midstream/urban areas (Casa Italia

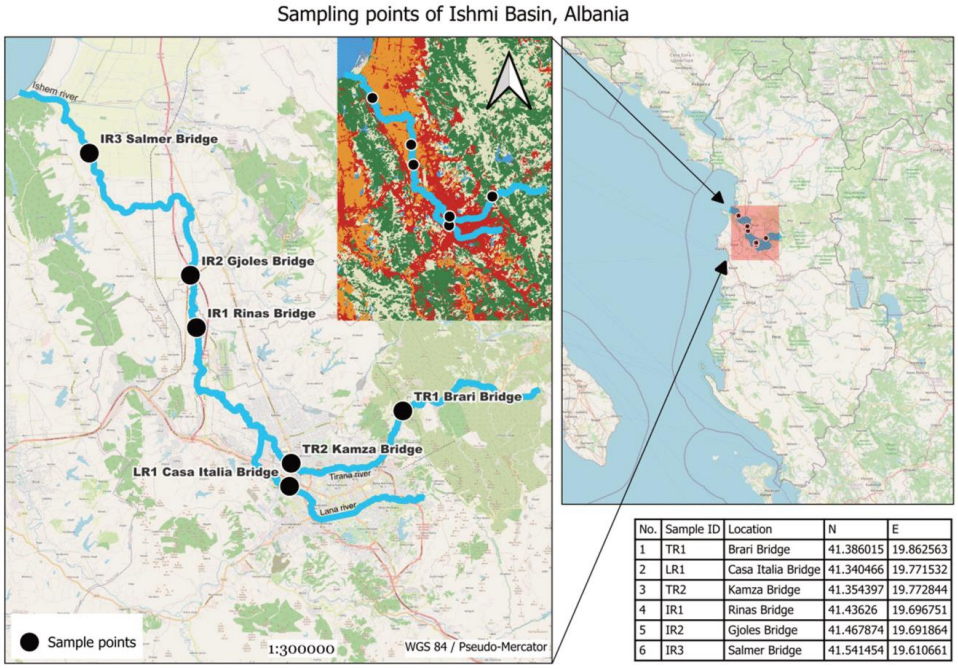

Fig. 1 Location of sampling points in the Ishmi River basin

Table 1 Sampled Ishmi basin Rivers sites characteristics

ID	River	Location	*Flow $m^3 s^{-1}$		Site characteristics
			Year 2023		
			Autumn	Summer	
TR1	Tirana River	N41° 38′; E19° 86′	0.31	0.55	Light human activity; touristic attraction
LR1	Lana River	N41° 34′; E19° 77′			Wastewater discharges and urban industry
TR2	Tirana River	N41° 35′; E19° 77′			Wastewater discharges and urban industry
IR1	Ishmi River	N41° 43′; E19° 69′			Wastewater discharges, agriculture, and urban industry; Tirana International Airport
IR2	Ishmi River	N41° 46′; E19° 69′			Urban and agriculture activities
IR3	Ishmi River	N41° 54′; E19° 61′	4.89	3.83	Agriculture activities

* Data from Report of Environmental State of the year 2023, National Environment Agency of Albania

Bridge – LR1, Kamza Bridge – TR2, Rinas Bridge – IR1), and downstream (Gjoles Bridge – IR2, Salmer Bridge – IR3). TR1 represented a site with minimal anthropogenic influence. In contrast, LR1, TR2, IR1, and IR2 were heavily impacted by urban activities, particularly LR1, and with some agricultural influence. IR3 was predominantly affected by agricultural activities (see Fig. 1, where red and orange indicate urban and agricultural land use, respectively).

The reported procedures to collect water and sediment samples were used [34, 39]. Surface water samples (grab samples) were collected in pre-cleaned (acetone and Milli-Q water) glass bottles. In the event of precipitation, sampling was delayed for approximately one week to

Table 2 Summary of mean concentrations of selected pharmaceuticals in the water and sediments of different locations from Ishmi River basin

Compounds	Water (ng L^{-1}) ($n=8$)						Sediment (ng g^{-1}) ($n=4$)					
	Sampling Point											
	TR1	LR1	TR2	IR1	IR2	IR3	TR1	LR1	TR2	IR1	IR2	IR3
CAFF	n.d	10,676	1,430	5,309	4,324	2,996	NM					
CBZ	41.1	260.5	n.d	21.7	28.2	n.d	2.5	44.1	15.2	9.7	11.5	9.6
NPX	n.d	2,028	525	1,255	914	585	2.8	18.4	5.6	8.8	4.8	1.6
IBU	n.d	11,297	1,037	8,384	7,926	1,450	n.d	47.2	8.3	16.0	8.0	9.0
DCF	n.d	278	n.d	47.5	50.2	59.6	NM					
AETM	10.7	26.5	6.0	32.3	10.8	58.2	0.3	0.9	0.9	0.7	0.9	0.6
ATM	n.d	1,501	n.d	n.d	n.d	n.d	n.d	113	54.0	122	16.0	48.2
CMC	5.2	12.3	23.3	36.7	20.2	9.8	11.8	8.1	3.8	4.3	4.6	17.8
CFC	179.2	714	404	407	188	348	3.2	705	77.9	170	129	48.6
ETM	n.d	n.d	230	24.3	n.d	n.d	*Added to AETM					
SMX	23.2	126	17.8	74.2	42.0	49.8	0.8	3.6	2.7	0.9	0.8	0.1
TMP	8.0	40.5	3.0	8.2	9.0	3.8	n.d	6.4	11.3	6.7	6.0	2.1

NM not measured, *Due to dominance of AETM, as dominant degradation product in acidic conditions

avoid dilution effects. Samples were immediately placed in a cooler, transported to the laboratory, and stored at 4 °C until extraction (within 48 h). Prior to extraction, samples were filtered using 0.45 µm cellulose acetate filters, and the filtrate pH was adjusted to 2.7 using concentrated HCl (37%).

Sediment samples were collected using a stainless steel stirring spatula (1 m length) from 0–5 cm depth, immediately cooled, and transported to the laboratory. Samples were frozen at − 28 °C and subsequently lyophilized. Dried sediments were homogenized using a mortar and pestle, sieved to < 100 µm, and stored at − 28 °C in glass containers until analysis. The processed sediment samples were analyzed for pH (the Association of German Agricultural Inspection and Research Insitutes (VDLUFA 1991) method was used), total nitrogen (TN) (the German Institute for Standardization (DIN EN 16168–2012-11) method was used), total hydrogen (TH), total sulfur (TS) (DIN ISO 15178:02–2001), total carbon (TOC) (DIN EN 15936:2012–11), carbonates ($CaCO_3$) (calculated from TOC and organic carbon), inorganic (IC) and organic carbon (OC) (VDLUFA (1991)), Al, Fe, Ca, K, Mg, Na (DIN ISO 11466/DIN EN 16174), and for the selected pharmaceutical concentrations based on reported validated methods [10, 34]. Sediment pH was determined in a 1:2.5 (w/v) suspension of sediment in 0.01 M $CaCl_2$, after shaking for 60 min at 150 rpm. The TN, TH, TS, and TOC were determined through thermal conductivity detection method with a CHNS elemental analyzer (UNICUBE®, Elementar, Langenselbold, Germany). Carbonates were determined with a Scheibler device, first dissolving the $CaCO_3$ with 10% HCl and then measuring the emitted CO_2. The IC was calculated by multiplying the carbonates with 0.1199 factor, while the OC was calculated by subtracting the carbonates from the TOC. Total metal concentrations were determined using inductively coupled plasma–optical emission spectrometry (ICP-OES, Varian 720-ES).

Chemicals

Pharmaceutical compounds were primarily selected based on their usage in Albania. Standards of CAFF, CBZ, NPX, IBU, and DCF were obtained from Sigma-Aldrich GmbH (Germany). Standard stock solutions (1000 mg L^{-1}) were prepared in methanol and stored at -20 °C. Working solutions were prepared monthly from the stock solutions. Antibiotic standards of AETM, ATM, CMC, CFC, ETM, SMX, and TMP, as well as internal standards, were purchased from HPC Standards GmbH (Cunnersdorf, Germany). Stock solutions of antibiotics were prepared in methanol containing 0.01% HCl. Organic solvents (acetone, methanol, and ACN, all HPLC grade) were obtained from VWR International (Radnor, PA, USA). Formic acid (99.6%) and sulfuric acid were obtained from VWR International (France). Potassium dihydrogen phosphate was purchased from Merck GmbH & Co. KG (Darmstadt, Germany). Orthophosphoric acid (H_3PO_4, 85%), hydrochloric acid (HCl, 37%), and ethylenediaminetetraacetic acid disodium salt dihydrate (EDTA, ≥ 99%) were purchased from Carl Roth GmbH & Co. KG (Karlsruhe, Germany). Membrane filters (cellulose acetate, 0.45 µm) and PTFE syringe filters

(0.45 µm) were obtained from OTTO E. KOBE KG (Marburg, Germany). C18-E (55 µm, 70 Å, 500 mg / 6 mL) Strata® cartridges were purchased from Phenomenex (USA). A Mettler Toledo balance (ME 204), Milli-Q water (18.2 MΩ·cm, Purelab, UK), and a pH meter (inoLab® pH 7110) were used throughout the study.

Water sample extraction

For the analysis CAFF, CBZ, NPX, IBU, and DCF, solid-phase extraction (SPE) was performed following the reported methods [39, 43]. The filtrate (500 mL, pH 2.7) was passed through C-18 SPE cartridges (Strata®, Phenomenex) via a Teflon tube at a flow rate of 3 mL min^{-1} by using an ISMATEC (ISM915A) peristaltic pump. Cartridges were pre-conditioned with 10 mL of acetonitrile (ACN) and 10 mL of acidified Milli-Q water (pH 2.7, adjusted with HCl) by using a 12-port vacuum manifold system (Macherey Nagel), connected to a vacuum pump. After extraction, analytes were eluted with a total of 14 mL of ACN: 2×5 mL under gravity flow and 4 mL of 0.1% HCl in ACN under vacuum. The combined solvent was evaporated to dryness under a gentle flow of nitrogen and reconstituted in 0.25 mL of 50:50 (v/v) ACN/Milli-Q water (pH 2.7), then filtered (0.45 µm PTFE) and measured using HPLC with UV and fluorescence detection (HPLC–UV/FLD) based on the reported method [33]. Meanwhile, AETM, ATM, CMC, CFC, ETM, SMX, and TMP were analyzed by direct injection (only filtered, pH-adjusted to 2.7, spiked with internal standards, and measured using high-performance liquid chromatography coupled with tandem mass spectrometry (HPLC–MS/MS) based on the reported method [10].

Sediment sample extraction

Sediment samples were analyzed for anti-inflammatories (NPX, IBU), the antiepileptic (CBZ), and selected antibiotics (AETM, ATM, CMC, CFC, SMX, TMP). CAFF and DCF were excluded from sediment analysis due to high matrix interference. For CBZ, NPX, and IBU, extraction was performed according to a previously reported method [34]. Briefly, replicate sediment samples (2 g) were treated with EDTA (0.2 g g^{-1} sediment) and subjected to a three-step extraction using 5 mL + 5 mL of methanol (0.1% formic acid), and 5 mL of acetone (0.1% formic acid), in 15 mL centrifuge tubes. Each step involved shaking at 350 rpm for 45 min, ultrasonication at room temperature for 30 min, and centrifugation at 3565 RCF for 20 min. The supernatants were combined and evaporated to dryness under a gentle nitrogen flow. The dried extracts were reconstituted in 0.22 mL of ACN, diluted to 250 mL with Milli-Q water acidified to pH 2 (50% H_2SO_4), passed through C18 SPE cartridges, and processed as the water extraction procedure above. Standard addition was performed using 0.5, 1.0, and 2.5 mg L^{-1} for calibration. Both unspiked and spiked samples were analyzed using HPLC–UV/FLD based on the reported method [33].

For AETM, ATM, CMC, CFC, SMX, and TMP (with ETM included in AETM), the extraction followed a previously published method [10]. Shortly, replicate sediment samples (2 g) were extracted with 26 mL of 0.2 M KH_2PO_4:ACN (1:1, v/v) in 50 mL glass vials. An aliquot (1 mL) of the extract was evaporated under nitrogen, reconstituted in 1 mL of 50 mM H_3PO_4:ACN (80:20, v/v), spiked with internal standards, and analyzed by HPLC–MS/MS based on the reported method [10].

Determination of pharmaceuticals

Compounds with available isotopically labeled internal standards were analyzed by LC–MS/MS, while others were quantified using HPLC–UV/FLD with standard addition to correct for matrix effects, thus ensuring reliable results while balancing analytical feasibility and costs.

An analytical method previously reported for the determination of CAFF, CBZ, NPX, IBU, and DCF was applied [33]. Briefly, compounds were analyzed by liquid chromatography using an Agilent 1200 HPLC system (Agilent Technologies Inc., USA) equipped with a column oven (G1316A), autosampler (G1329A), quaternary pump (G1311A), diode array detector (DAD, G1315B), and fluorescence detector (FLD). Separation was performed on a reverse-phase C18 column (3 µm, 120 Å, 2.1×150 mm). The DAD was set at 285 nm for CAFF and CBZ, and 220 nm for IBU and DCF. NPX was detected using the FLD, with excitation and emission wavelengths of 230 nm and 420 nm, respectively. Chromatographic separation was achieved within 57 min using a mobile phase consisting of ACN containing 0.5% H_2O (solvent A) and a 25 mM potassium dihydrogen phosphate buffer at pH 2.7 (solvent B). The gradient program was as follows: 15% A (0–4.5 min), 20% A (4.5–12.5 min), 25% A (12.5–18 min), 45% A (18–38 min), 80% A (38–45 min), and re-equilibration at 15% A (45–57 min). The column temperature was maintained at 40 °C, with an injection volume of 20 µL and a flow rate of 0.3 mL min^{-1}. Instrument control, data acquisition, and processing were performed using ChemStation software. The limits of quantification (LOQs) were established from matrix-matched SPE calibrations in Ishmi River water (IR1). Calibration curves were prepared by spiking IR1 and Milli-Q water (0.1–10 µg L^{-1}) and processing 500 mL samples through SPE (0.25 mL final extract). LOQs (ng L^{-1}) were 2.3 (CAFF), 97.0 (CBZ), 30.5 (NPX), 42.4 (IBU), and 188.6 (DCF). Based on these values, sediment-equivalent LOQs were derived according to the ratio of extract volume to sediment mass. Quantification was performed by

standard addition to multiple sample aliquots to correct for matrix effects; although the formal LOQs were established from the validated calibration range (12.1 ng g^{-1} for CBZ, 3.8 ng g^{-1} for NPX, and 5.3 ng g^{-1} for IBU), signals below these levels were occasionally visible due to the enhanced sensitivity of the standard addition approach. Recoveries (%) in water (IR1water spiked at 2 µg L^{-1}) were 24.4 (CAFF), 111.7 (CBZ), 107.6 (NPX), 108.8 (IBU), and 108.4 (DCF), while in sediments (IR1 sediment spiked at 300 ng g^{-1}) they were 92.8 (CBZ), 83.6 (NPX), and 92.9 (IBU).

For AETM, ATM, CMC, CFC, ETM, SMX, and TMP the reported analytical method was applied [10]. Analyses were performed with a Sciex™ ExionLC™ separations module, equipped with an auto sampler unit, a gradient pump, a column oven and a sample heater. The chromatographic device was connected via Peek capillary (0.18 mm ID) to a Sciex™ triple quadrupole mass spectrometer (QTRAP 4500™). The method used a Waters Bridge™ C18 Column (150 mm length, 2.1 mm ID, 3.5 µm particle size) and a column guard of the same material. Eluents were A: Milli-Q-water (0.1% formic acid) and B: ACN (0.1% formic acid). The flow was 0.4 mL min^{-1} and the sample cooler was set to 20 °C. The MS–MS measurement was performed in positive mode with 2500 V on the source capillary and 500 °C desolvation temperature. Nitrogen was used as curtain and collision gas (further MS parameters are provided in SM Table 3). The LOQs in µg L^{-1} for the analyzed antibiotics were as follows: 0.01 (SMX), 0.09 (TMP), 0.12 (CFC), 0.02 (CMC), 0.16 (AETM/ETM), and 0.47 (ATM). The corresponding LOQs in µg kg^{-1} were 0.01 (SMX), 0.09 (TMP), 0.12 (CFC), 0.02 (CMC), 0.16 (AETM/ETM), and 0.47 (ATM). Isotope-labeled internal standards were applied during measurement to ensure data integrity and analytical quality. The standards used were SMX-$^{13}C_6$, CMC-$^{13}Cd_6$, ATM-$^{13}Cd_3$, CFC-d_8, and TMP-d_9, each assigned to its corresponding analyte. For ETM, TMP-d_9 was used as a class-matched surrogate standard. LOQ values were determined as the mean concentrations measured in blank samples plus five times their standard deviation. When the calculated LOQ was lower than the lowest calibration level, one-half of the lowest calibration concentration was adopted as the LOQ. Extraction recoveries of the sediments extraction method varied between 50–120% for antibiotics. LC–MS/MS recovery in water samples was not tested separately, but internal standards were used to calculate the matrix effect and monitor the analytical process. If the recovered signal deviates significantly (50–120%) from the expected signal, this is considered a trigger.

Data treatment

The sediment–water partition coefficient (K_d) for the selected pharmaceuticals was calculated using their concentrations in the sediment phase (C_s) (ng g^{-1}) and the water phase (C_w) (ng L^{-1}), according to Eq. (1), as reported by [44].

This coefficient is considered as one of the key factors influencing the persistence and long-term fate of contaminants in aquatic environments. A higher K_d value indicates greater sorption to sediments, suggesting stronger binding and higher environmental persistence due to reduced photodegradation and biodegradation processes [7].

$$K_d = C_s / C_w \tag{1}$$

Another parameter that describes the distribution of a compound between water and sediment is the pH-dependent *n*-octanol–water partition coefficient (D_{ow}). This parameter accounts for the compound's ionization at a given pH. To assess the distribution behavior of the selected pharmaceuticals, D_{ow} was calculated using Eq. (2), as reported by [54].

Table 3 K_d and K_{oc} calculated values on site compared with literature values

Compound	K_d (mL g^{-1})			K_{oc} (mL g^{-1})			Literature (mL g^{-1})		Matrix	References
	Min	Max	Mean	Min	Max	Mean	K_d	K_{oc}		
ATM	369.2			3,144.7			121–1,834	17,783	Sediment	[29, 44]
AETM	12.5	178.1	114.2	678.8	4,340.5	2,699.7	2–73; 211	–	Sediment	[44, 47]
CFC	13.9	8534.4	2,180.9	828.8	135,037	42,472.9	329.3–4,664	–	Sediment	[59]
CMC	3.06	971.2	224.0	132.8	157,148	24,276	0.7–570	125.9–25,119	Sediment	[29]
IBU	0.17	27.3	9.09	7.49	784.9	236.4	1.72–45.5	192–1,110	Soil	[56]
NPX	0.42	24.8	8.10	10.91	762.9	209.7	3.4–356	340–7,610	Soil	[56]
SMX	54.2	197.3	115.5	623.3	4,555.6	3,117.6	22–105	–	Sediment	[18]
TMP	39.3	3,142	720.5	1,076.9	4,9726	12,854	18.8–3,126	–	Sediment	[18, 49]

$$D_{ow} = \frac{K_{ow}}{1 + (10^{pH - pK_a})} \quad (2)$$

where K_{ow} is the *n*-octanol–water partition coefficient and pK_a is the acid dissociation constant.

The organic carbon content in sediments significantly influences the distribution of organic compounds between the water and sediment phases. Organic carbon provides abundant adsorption sites and facilitates hydrophobic interactions, enhancing the sorption of both polar and non polar compounds. To evaluate this influence, the organic carbon-normalized partition coefficient (K_{oc}) was calculated using the Eq. (3), as reported by [56].

$$K_{oc} = K_d / f_{oc} \quad (3)$$

where f_{oc} represents the fraction of organic carbon.

Statistical analysis

For CAFF, CBZ, NPX, IBU, and DCF in water samples, statistical analysis was not performed due to limited sample volume and lack of replication. Instead, concentration data were summarized descriptively to illustrate spatial and seasonal patterns. In contrast, for sediment samples, the remaining pharmaceuticals in water samples, and the total concentrations across water and sediment phases, a two-way analysis of variance (ANOVA) was conducted. Season and location were considered as independent variables, while pharmaceutical concentration served as the dependent variable. When the assumptions of ANOVA (normality and homogeneity of variances) were not met, non-parametric Kruskal–Wallis tests were applied as an alternative. In addition, single and multiple stepwise regression analyses were used to examine relationships between the calculated distribution coefficient (K_d) and sediment properties, as well as with the predicted K_d. Statistical significance was set at $p < 0.05$. All analyses were performed using OriginPro 2015 (OriginLab Corporation, USA).

Results and discussion

Occurrence of the studied pharmaceuticals in surface waters and sediments

A summary of mean values of selected pharmaceuticals detected in water and sediment samples from the Ishmi River basin is presented in Table 2. Full datasets of concentrations in surface water samples at each sampling location and during seasons of 2023 and 2024 are shown in SM Table 1. All 12 investigated pharmaceuticals were detected. In general, the highest concentrations were observed at location LR1, in line with urban impact, then a decreasing trend with lowering the urban impact was observed, while concentrations at TR1 were typically low or below detection limits. CAFF, IBU, NPX, and CFC exhibited the highest environmental concentrations at almost all locations (except TR1), significantly at location LR1 with mean concentrations of 10.7, 11.3, 2, and 0.7 μg L^{-1}, respectively. CAFF is considered as one of the water treatment tracers [11], due to its limited use only to humans and high removal rates mainly during the biological treatment at the wastewater treatment plants [60]. In the continent of Europe (where Albania is part of), daily intake of CAFF was reported at 288.58 mg/person/day [24], although Albania encourages pregnant and lactating women to reduce CAFF product consumption (≤200–300 mg caffeine/day), and discourages CAFF containing products intake from childrens [41], the detected concentrations were up to 22.5 μg L^{-1} (considering a comparably low recovery rate of 24.4%), comparing only to urban impacted waters and wastewater influent concentrations such as in Brazil, in Portugal, and Hungary with 16.5, 9.4–83.9, and 221.4 μg L^{-1}, respectively [11, 22, 37]. Anti-infammatories such as IBU and NPX, were also detected in relatively high concentrations, especially at location LR1, with maximum of 12.8 and 2.6 μg L^{-1}, respectively. DCF was also detected, with the highest concentration of 1.8 μg L^{-1}at the same location, but lower frequency was observed compared to IBU and NPX. Under environmental surface water pH > 6, IBU, NPX, and DCF exist as ionized molecules, due to their pK_a values of 4.9, 4.2, and 4.5, respectively. Therefore, these compounds tend to remain in the aqueous phase. These concentrations are in agreement with those reported in the Turia River in Valencia [5], where the highest concentrations for IBU, NPX, and DCF were 7.2, 6.6, and 3.5 μg L^{-1}, respectively. The antiepileptic CBZ concentrations ranged from n.d. to 1.3 μg L^{-1} as maximum value at location LR1. This compound is relatively stable under environmental conditions, but the detection frequency was not consistent along all sites, possibly due to dilution from basin tributaries in the downstream locations (after LR1). Similar patterns are reported from Lis River, Portugal [38] and in the main Rivers of Madrid, Spain [51]. The fluoroquinolone CFC, similarly, to CAFF, IBU, and NPX, showed high frequency and relatively high concentrations, with a maximum of 1.8 μg L^{-1} again at location LR1. This compound is characterized by a low Henry's constant (< 10^{-15} atm*m^3 mol^{-1}) and, at pH values of 6.1–8.7 in the sediment samples, behaves mainly as zwitterionic but could also be positively or negatively charged (pK_a of 6.09 and 8.76), therefore it remains in aqueous phase [52]. CFC levels were comparable to those reported in studies in River waters and wastewater effluents such as in Iran (0.2–0.7 μg L^{-1}) [35], in Portugal (0.2–0.5 μg L^{-1}), in Spain (0.2 μg L^{-1}), in Ireland (0.2–0.3 μg L^{-1}), in Cyprus (0.3 μg L^{-1}), in Germany (0.2 μg L^{-1}), and in Norway (0.2 μg L^{-1}) [42]. Macrolides such as AETM, ATM, ETM,

and CMC, were also detected but showed different patterns. AETM and CMC were more frequently detected with levels ranging from n.d.–0.3 to n.d.–0.2 µg L^{-1}, respectively. ETM, is reported to be unstable and has a fast conversion rate to AETM [46]. Our results are in line with this behavior as ETM was detected only in two locations with 0.2 µg $L^{-1}$and 1.4 µg L^{-1}, similarly to trends reported in China (0.2 µg L^{-1}) [19] and in Spain (0.3–3.9 µg L^{-1}) [40, 51]. ATM was frequently detected only at location LR1, with the highest concentration of 7.5 µg L^{-1}. This pattern indicates that the main source of ATM was from high urban input and a relatively higher resistance to biodegradation [46, 55]. The sulfonamide SMX and diaminopyrimidine TMP exhibited high frequency with the highest concentrations registered at location LR1 with 0.4 µg L^{-1} and 0.1 µg L^{-1}, respectively, which are comparable with concentrations of 0.2 µg L^{-1} (SMX) and 0.3 µg L^{-1} (TMP) reported in surface waters [36].

For sediments, concentrations of selected pharmaceuticals in sediment samples at each sampling location during seasons of the years 2023 and 2024 are given in SM Table 2. Compared to water sample trends, CFC and ATM were detected in significantly higher concentrations during spring seasons ($p < 0.05 - 0.001$), with maximum of 1068 and 396 ng g^{-1}, respectively, followed by IBU (93.7 ng g^{-1}) > CBZ (60.5 ng g^{-1}) > NPX (49.3 ng g^{-1}) > TMP (38.3 ng g^{-1}) > CMC (37.8 ng g^{-1}) > SMX (13.3 ng g^{-1}) > AETM (2.7 ng g^{-1}). Similarly to water samples pattern, location LR1 showed a detection frequency of 100% for most compounds (except AETM and SMX with 50%), indicating that high input from urban discharge is the main source of contaminants in the surface waters. Under similar environment and anthropogenic impact conditions, maximum concentrations for CFC are reported at 1287 ng g^{-1} [62], for ATM at 8.1–14,680 ng g^{-1} [46], for IBU, CBZ, NPX at 66–340, 38–519, 3–96 ng g^{-1}, respectively [6], for TMP at 11–90 ng g^{-1} [20], for CMC at 87.7 ng g^{-1} [25], for SMX at 10 ng g^{-1} [2], and for AETM at 0.86–185 ng g^{-1} [46].

Partitioning of the studied pharmaceuticals in the sediment–water system

Having the concentrations of both aqueous and sediment phases, in situ K_d values of pharmaceuticals were calculated and the minimum, maximum, and the mean values, as well as all in situ calculated K_d values, are presented in Table 3 and SM Table 6, respectively. The K_d values varied highly for most of the compounds, as from 0.42 to 24.8 mL g^{-1} for NPX, from 0.17 to 27.3 mL g^{-1} for IBU, from 12.5 to 178.1 mL g^{-1} for AETM, from 3.06 to 971 mL g^{-1} for CMC, from 13.9 to 8534 mL g^{-1} for CFC, from 54.2 to 197 mL g^{-1} for SMX, and from 39.3 to 3,142 mL g^{-1} for TMP. For all compounds, similar trends were reported in the literature under comparable conditions, with wastewater discharge concluded as predominant factor (Table 3) [18, 29, 44, 47, 49, 56, 59]. The K_d is a very important parameter for understanding not only the behavior and matrix affinity of pharmaceuticals, but also for uptake and sorption mechanisms from sediments, through multiple linear correlations mainly with pH, OC (%), D_{ow}, cation exchange capacity (CEC), clay content (%), and selected sediment cations content (Al, Fe, K, Ca, Mg, Na), as reported in similar studies [1, 49, 59]. In this study, the calculated K_d of both detected water and sediment compounds, was correlated with sediment pH, OC (%), calculated D_{ow}, $CaCO_3$, and total content of selected sediment cations (Al, Fe, K, Ca, Mg, Na) in single and multiple linear regressions, with respective data given in SM Table 7 and SM Table 8, respectively. From the single linear correlations, it was observed that sediment pH, D_{ow}, and OC content had the highest impact on selected pharmaceuticals partitioning.

Of the seven compounds of which K_d was calculated, only five (NPX, IBU, AETM, CFC, CMC) were included in the multiple linear regression modeling. This judgement was based on the statistical significance of correlations and the ability to generate robust regression models with acceptable Adj. R^2 and root mean square error (RMSE) values (Fig. 2). SMX and TMP were excluded as they did not meet the criteria for reliable model development, due to weak or non-significant relationships with the sediment properties. Based on developed models of NPX, IBU, AETM, CFC, and CMC, their respective predicted values of K_d at all locations and seasons, and graphs with linear fittings are presented in SM Table 9 and Fig. 2, respectively. From the models and the fittings data, it could be observed that for CFC, NPX, and IBU the models were accurate and could be used to predict their environmental concentrations. Meanwhile, AETM and CMC, although showing good fitting relationship between calculated and predicted values (especially for AETM), the significance was not achieved during the multiple step fitting analysis.

The calculated D_{ow} values of each compound at each sediment pH showed a significant relationship with the increase of OC (SM Fig. 1). The K_{oc} values also varied from 10.9 to 763 mL g^{-1} C for NPX, from 7.5 to 785 mL g^{-1} C for IBU, from 679 to 4,341 mL g^{-1} C for AETM, from 133 to 157,148 mL g^{-1} C for CMC, from 829 to 135,037 mL g^{-1} C for CFC, from 623 to 4,556 mL g^{-1} C for SMX, and from 1,077 to 49,727 mL g^{-1} C for TMP.

The effect of sediment properties on selected pharmaceutical distribution in sediments

In general, sorption of pharmaceuticals in sediments is influenced by the physico-chemical properties of the

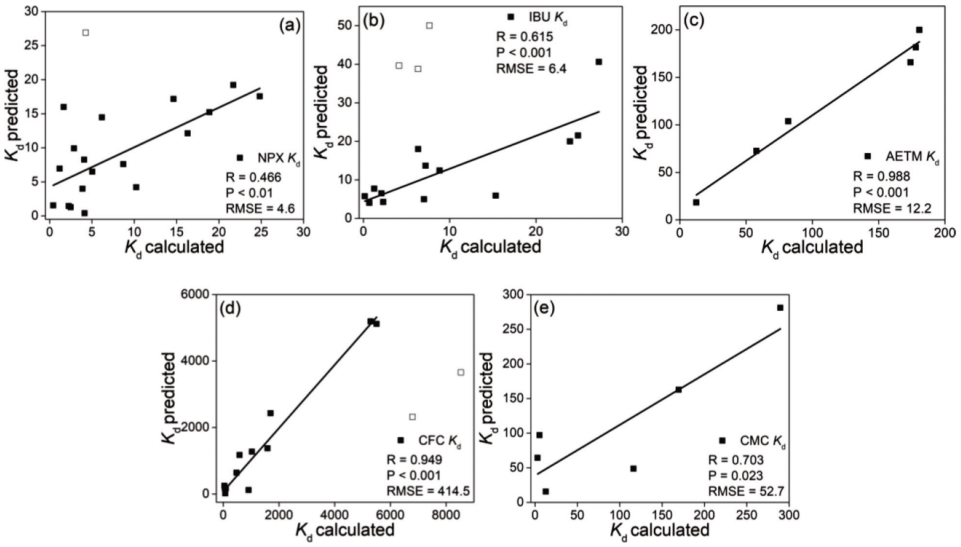

Fig. 2 The relation (model validation) between the calculated and predicted K_d of (**a**) NPX; (**b**) IBU; (**c**) AETM; (**d**) CFC; and (**e**) CMC

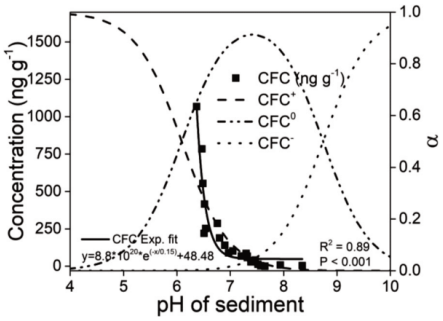

Fig. 3 The effect of sediment pH on CFC detected concentrations in sediments

compounds (hydrophobicity and chemical charge) as well as the properties of the sediment itself, mainly, OC content, CEC, cation content, and surface charge [15, 18]. These factors (including compounds properties) are all pH-dependent. At first, the effect of sediment pH on CFC concentrations in sediments followed an exponential trend, highlighting the prominent role of pH (Fig. 3).

Apart from influencing the compound speciation, sediment pH also governs the surface charge of sediments. As sediment pH increases, the net negative charge of the sediment also increases due to the deprotonation of surface functional groups (–OH) [4]. To evaluate the isolated effect of sediment pH on each pharmaceutical detected in the sediment phase, taking into account compound speciation, the corresponding data are presented in SM Fig. 3. The observed effect of sediment pH on compound concentrations was consistent with trends in the calculated distribution coefficient D_{ow} for most compounds (except CBZ which remains neutral under environment pH). Under these conditions, hydrophobic partitioning (K_{ow}) alone is not sufficient to assess the sorption behavior of pharmaceuticals in sediments due to their polar functional groups and their ionic nature [58]. For the selected pharmaceuticals, a significant negative relationship was observed between log K_{ow} and log K_{oc}, suggesting that compounds with higher hydrophobicity exhibited lower affinity for sediment organic matter, potentially due to other physico-chemical interactions influencing their sorption behavior (Fig. 4a). In addition to hydrophobic interactions, pharmaceutical sorption is largely driven by ionic interactions, which are pH dependent [50]. Therefore, their sorption assessment should not consider only K_{ow} but also the D_{ow}, which accounts for compound ionization at environmental pH. The calculated D_{ow} (using sediments pH) for each compound,

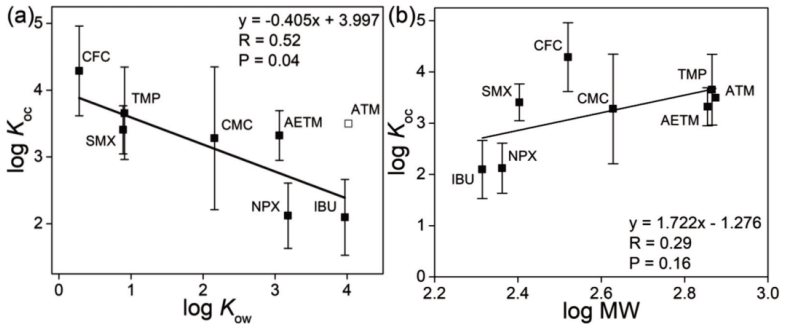

Fig. 4 (**a**) Relationship between the calculated log K_{oc} with log K_{ow} and (**b**) with log MW of the selected pharmaceuticals

showed an exponential decrease with increasing sediment pH, indicating a strong influence of pH on the ionic state of the compounds (SM Fig. 2). The molecular weight (MW) of the pharmaceuticals appeared to influence their presence in sediments. Although the relationship was not statistically significant, a positive linear trend between log K_{oc} and log MW was observed (Fig. 4b), which is consistent with findings from previous studies [7, 61].

Another important factor influencing the uptake of organic compounds in sediments is the OC content, which showed a significant positive linear correlation with the calculated D_{ow} values of the compounds (SM Fig. 1). Accordingly, by considering the physicochemical properties of pharmaceuticals, such as pK_a (SM Table 4), the relationship between calculated log K_{oc} and compound speciation (α, derived using Henderson-Hasselbalch equation) with sediment pH was examined for NPX, IBU, AETM, CMC, CFC, TMP, and SMX (both detected sediment and water matrix compounds, sampled at each time), and shown in Fig. 5a-g. In addition, based on data from both sediment and water phases under environmental sediment conditions (Table 3), sediment properties (SM Table 5), as well as their impact (SM Table 7), certain sorption trends can be identified.

The antiepileptic CBZ was detected mainly in sediment samples, indicating a higher affinity for sediments rather than waters. This pattern may be attributed to its environment persistence [38], resulting in an accumulation in the sediment over time. CBZ has a low K_{ow} and a relatively high water solubility but is not ionizable at water pH (pK_a 13.9) [54]. Therefore, the uptake mechanism is mainly through hydrophobic interactions between CBZ benzene rings and the hydrophobic organic carbon fractions of the sediments [32, 48], confirmed in this study with the fact that higher CBZ concentrations were detected at location LR1 where its content is the highest (OC ≈ 10%) (SM Fig. 1).

Anti-inflammatories such as NPX and IBU exhibited higher affinity for water compared to sediments, likely due to their acidic nature and predominant anionic speciation within the environmental pH range (6.4–8.4). Sorption of both compounds increased at lower sediment pH, with a decreasing trend observed as pH increased (Fig. 5a, b). As sediment pH increased, NPX (pK_a = 4.2) and IBU (pK_a = 4.9) exist predominantly in anionic forms, resulting in reduced sorption due to enhanced electrostatic repulsion with negatively charged sediment sites. This is supported by the significant negative correlations between K_d values and both pH and D_{ow} (SM Table 7). K_d values showed a significant positive correlation with Al ($p < 0.05$) and positive, though not statistically significant, correlations with OC, Fe, K, and Na. These findings indicate that NPX and IBU sorption under the studied pH conditions is primarily driven by electrostatic interactions between their deprotonated carboxylic groups and positively charged mineral oxide surfaces (Al, Fe, K, Na) and protonated amines of sediment organic matter [56].

Macrolides, such as AETM, ATM, and CMC, especially ATM, showed a higher affinity for sediments than for the aqueous phase. Within the studied sediment pH range (6.4–8.4), ATM (pK_a = 8.7) existed mainly in its protonated form, and the higher sorption was under low pH values (≈6.5) (SM Fig. 3e). The higher prevalence of ATM can be related with its higher biodegradation resistance [55] compared to AETM and CMC, and higher electrostatic interactions due to the presence of basic amine-N ligands (positively charged) of ATM with the negatively charged sites of the sediments, mainly of organic matter [46]. AETM (including ETM) also existed mainly in its cationic form ($AETM^+$) within this pH range (Fig. 5c).

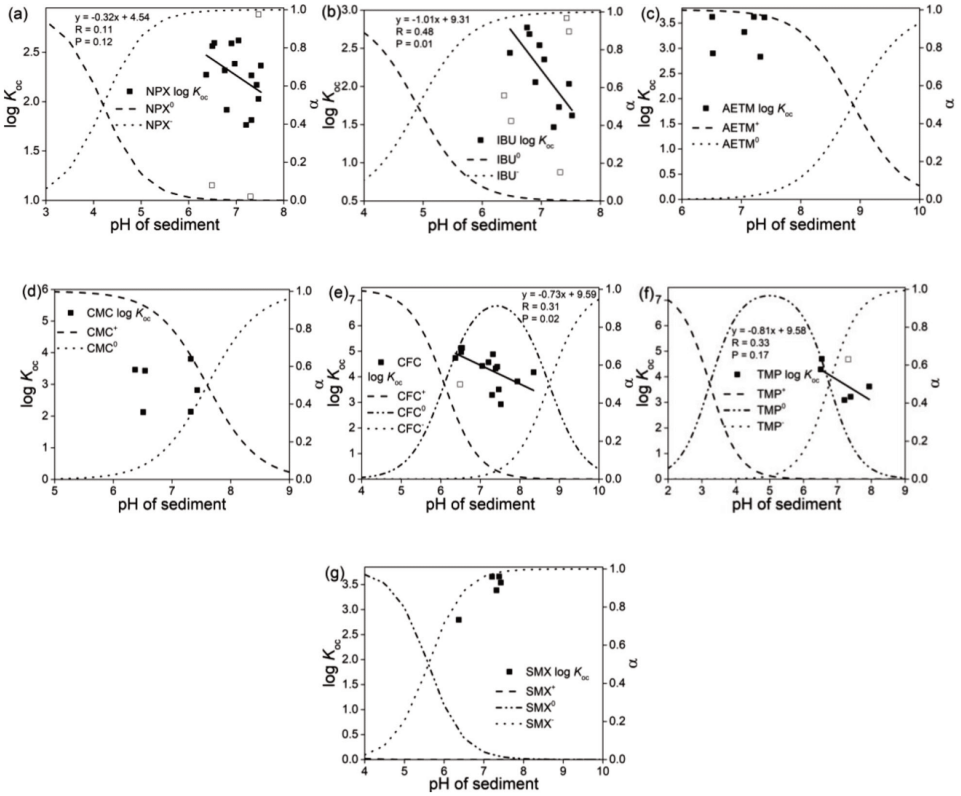

Fig. 5 The effect of sediment pH on log K_{oc} of (**a**) NPX; (**b**) IBU; (**c**) AETM; (**d**) CMC; (**e**) CFC; (**f**) TMP; and (**g**) SMX

Sorption of AETM was driven by electrostatic attraction to negatively charged functional groups of sediment organic matter and hydrogen bonding [12, 31], as can be seen from the significant positive correlation of K_d with OC and the negative correlation with sediment pH, D_{ow}, and other parameters including $CaCO_3$, Al ($p < 0.05$), Fe, Ca, K, Mg ($p < 0.05$), and Na ($p < 0.05$) (SM Table 7). CMC, with a pK_a of 7.6, in the pH range (6.4–8.4) of the studied sediments, existed predominantly in its cationic form (CMC^+) at pH values under 7.6, and mostly in its neutral form (CMC^0) at pH values above 7.6 (Fig. 5d). Generally, CMC was detected mostly and slightly in higher concentrations in sediments with a pH lower than 7, after which a decreasing trend was observed (SM Fig. 3f). Considering the negatively charged sediments, and predominantly occurring cationic CMC^+, cation-exchange is the responsible mechanism for CMC uptake from sediments, as reported under similar pH conditions [21, 45]. This is further supported by its similar K_d behavior to AETM with respect to sediment properties (SM Table 7).

The fluoroquinolone CFC, has two pK_a values (6.09 and 8.76) and within the relevant pH (6.4–8.4) of the sediments of the current study, can be mainly zwitterionic but at the same time, can be charged positively, negatively, or uncharged (Fig. 5e). The highest CFC concentrations were achieved at the lowest pH values (≈6.4) and with high OC of sediments (≈ 10%), then a decreasing trend in CFC was observed at higher sediment pH locations (electrostatic repulsion with the increase of CFC^-). Interestingly, the increase of sediment pH resulted in a significant exponential decrease of CFC sediment concentrations (Fig. 3), thus confirming that the sediment CFC uptake mechanism is through electrostatic

interactions between cationic CFC^+ with sediment surface negatively charged sediment functional groups, such as –OH, –COOH (OC, $p < 0.05$), C–O, and Si–O–Si [23, 53]. This is supported by the fact that the detected concentrations are similar to the percentage of CFC^+ (Fig. 3), and a significant negative correlation of CFC K_d with sediment pH and D_{ow} ($p < 0.001$) (SM Table 7). In addition, CFC K_d showed negative correlation with $CaCO_3$, Al, Fe ($p < 0.05$), Ca ($p < 0.05$), K ($p < 0.05$), Mg ($p < 0.05$), and Na, thus neutralizing sediment negative charges, resulting in an inhibitory effect on CFC sorption [23].

Diaminopyrimidines, such as TMP, though in lower concentrations show a higher affinity for sediments. TMP has two pK_a values (3.23 and 6.76), and can be zwitterionic (pH < 6.76) or negatively charged (pH > 6.76) under the sediment pH values of this study. The highest TMP sorption to sediments was observed at around pH 6.4 and with high OC content (positive correlation of TMP K_d with OC), suggesting hydrophobic interactions as the main sorption mechanism (SM Table 7 and Fig. 5f), as reported in a similar study with sediments [28]. With the increase in sediment pH, a decrease in TMP sorption was observed, due to the progressively increasing anionic TMP^- (pH > pK_a = 6.76) and the negative net charge of sediments, thus decreasing hydrophobic partitioning. Under these conditions, TMP uptake mechanism into the sediment is through electrostatic interactions, possibly between positively charged sites of sediment aluminium oxides with the anionic TMP^-, supported by the positive correlation of TMP K_d with sediment Al content [28, 56].

Sulfonamides, such as SMX, showed a higher tendency for the aqueous phase than for sediments, although low concentrations have also been detected in sediments (0.4 – 13.3 ng g^{-1}). Within the pH range of the studied sediments (6.4–8.4), SMX mainly exists in its anionic form (SMX^-), due to its low pK_a values (1.7, 5.6, and 5.9). Under these conditions, the affinity of sediments for SMX^- is not that high (electrostatic repulsion) as would be for SMX^0 (hydrophobic interactions), and the mechanism of sorption to the sediments, is by cation bridging between SMX^- with aluminium and iron oxides (SMX K_d positively correlated with Al and Fe sediment content, SM Table 7), and minor contributions from van der Waals forces [8].

Spatial and seasonal variations

Total concentrations of the selected pharmaceuticals for each sampled season in 2023 and 2024, in both water and sediment phases, are presented in SM Fig. 4 and in Fig. 6, respectively. The effects of location and season on the distribution of selected pharmaceuticals in both water and sediment phases of the basin were assessed using two-way ANOVA and non-parametric Kruskal–Wallis tests, with the results presented in SM Tables 10 and 11, respectively.

For waters, concentrations of selected pharmaceuticals varied significantly across sampling locations and seasons. Overall, levels were highest at LR1, followed by a decreasing trend along IR1 > IR2 > IR3, in line with reduced urban influence downstream. TR2, though aligned in parallel with LR1, exhibited lower concentrations due to less urban input. TR1 showed the lowest detection frequency and concentrations, indicating no urban impact. Regarding seasons, winter had the highest concentrations for the year 2024, followed by spring, autumn, and summer (for the year 2023, autumn > winter > summer > spring). ATM, CFC, TMP and SMX were strongly influenced by location ($p < 0.05$—0.001), while CFC also showed significant seasonal effects ($p < 0.001$). Notably, interaction effects (season × location) were significant for CFC, SMX and TMP, indicating that spatial differences in pharmaceutical concentrations were influenced by seasonal changes, including input rate or consumption, water flow rate or dilution, temperature and microbial activity [9, 13, 62]. In most of the cases the pharmaceutical concentrations in water were significantly affected by both season and location, confirming the combined impact of urban impact and environment conditions, such as changes in drug consumption as well as hydrological and degradation conditions, as similarly reported [14].

For sediments, location had a consistently significant effect on the distribution of most compounds (except SMX), including CBZ, NPX, IBU, AETM (2024), ATM, CFC, and TMP ($p < 0.05$ – 0.001), indicating strong site specific influence, potentially related to urban discharge input and site-specific conditions (pH, OC and metal content), especially for location LR1. Seasonal variation was also significant for spring compared to summer samples for several compounds, particularly CBZ (2024), NPX, IBU (2023), ATM, CFC, SMX (2024), and TMP, suggesting fluctuations in consumption (input rate) and possibly environmental factors such as precipitation and temperature. Notably, the interaction between season and location was significant for CBZ, AETM, and CFC in at least one of the study years, pointing to complex spatial seasonal dynamics. The total pharmaceutical concentration, similarly, as water samples, showed strong effects of both season and location ($p < 0.001$), indicating that both natural and human factors substantially affect contaminant distribution in the Ishmi River basin.

Conclusions

The selected pharmaceuticals were detected at all locations within the Ishmi River basin, with higher concentrations at urban impacted locations. In water, CAFF,

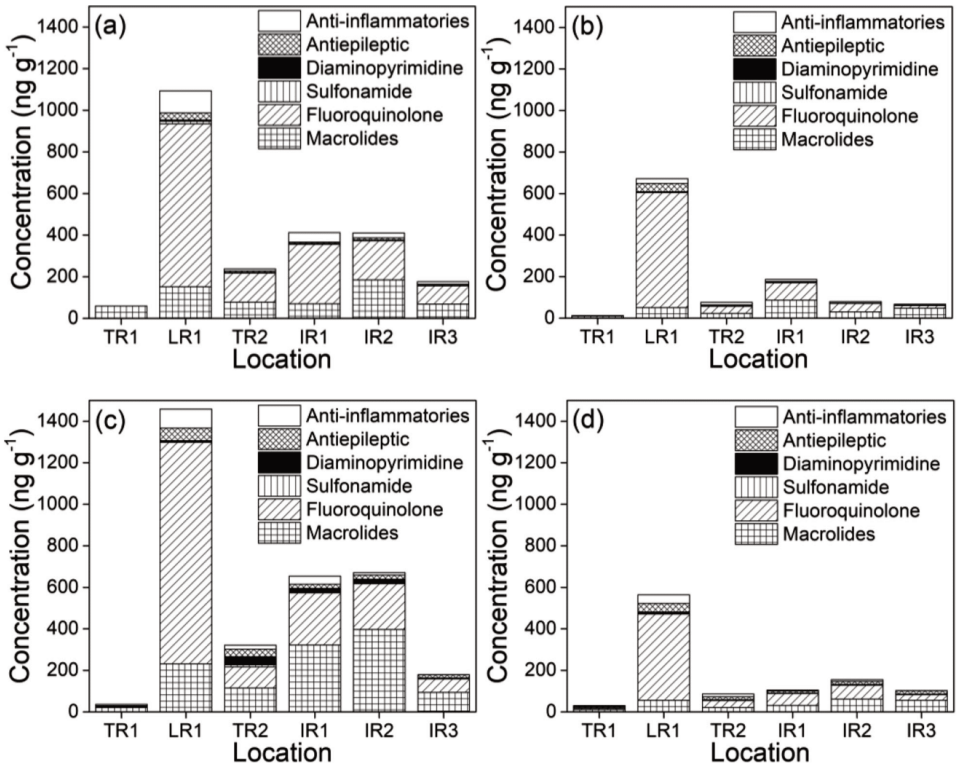

Fig. 6 Seasonal and spatial variations of selected pharmaceuticals in sediments of the Ishmi River basin for (**a**) spring and (**b**) summer of the year 2023; and (**c**) spring and (**d**) summer of the year 2024

IBU, NPX, and CFC were mostly detected, especially during winter, reflecting seasonal usage and environmental factors influence. In sediments, CFC and ATM dominated, with higher concentrations in spring, particularly at locations with low pH values and high organic carbon content. In situ partition coefficient like K_d and K_{oc} were derived from sediment and water concentrations of some frequently detected pharmaceuticals and the influence of intrinsic properties of the compounds and extrinsic environmental conditions were assessed by regression analysis. These analysis revealed that partitioning behavior was significantly influenced by compound-specific properties such as D_{ow}, as well as sediment-specific properties. These findings highlight the role of both intrinsic and extrinsic factors in controlling pharmaceutical distribution between water and sediment.

Abbreviations

CAFF	Caffeine
CBZ	Carbamazepine
NPX	Naproxen
IBU	Ibuprofen
DCF	Diclofenac
AETM	Anhydro-erythromycin
ATM	Azithromycin
CMC	Clindamycin
CFC	Ciprofloxacin
ETM	Erythromycin
SMX	Sulfamethoxazole
TMP	Trimethoprim
NSAIDs	Non-steroidal anti-inflammatory drugs
EU	European Union
TR1	Tirana river 1
LR1	Lana river 1
TR2	Tirana river 2
IR1	Ishmi river 1
IR2	Ishmi river 2
IR3	Ishmi river 3
C_s	Concentration in the sediment phase
C_w	Concentration in the water phase

K_d	Sediment–water partition coefficient
f_{oc}	Fraction of organic carbon
K_{oc}	Organic carbon-normalized partition coefficient
pK_a	Acid dissociation constant
K_{ow}	*n*-Octanol–water partition coefficient
D_{ow}	PH-dependent *n*-octanol–water partition coefficient
IC	Inorganic carbon
OC	Organic carbon
$CaCO_3$	Carbonates
TOC	Total carbon
SPE	Solid phase extraction
ACN	Acetonitrile
EDTA	Ethylenediaminetetraacetic acid disodium salt dihydrate
ANOVA	Analysis of variance
RMSE	Root mean square error
MW	Molecular weight

Supplementary Information

The online version contains supplementary material available at https://doi.org/10.1186/s12302-025-01264-w.

Supplementary file 1.

Acknowledgements
We acknowledge the support of Deutsche Bundesstiftung Umwelt (DBU), Germany, and the Erasmus+ program for the support of the research fellowships to A Peqini. Also, we acknowledge the support of E Müller and E Schneidenwind, J Junck, and A P Heinrich, iFZ, JLU Giessen, for technical assistance with HPLC and characterization of sediments.

Author contributions
AP executed the experiments, carried out the investigation and data curation, performed formal analysis, developed methodology, validated results, and prepared the initial draft. He was also responsible for resource collection (water and sediment sampling) and securing funding. BJH contributed to conceptualization, methodology development, data analysis, and validation. He also provided software support and was actively involved in reviewing and editing the manuscript. FB contributed to conceptualization and methodology, supervised the work, supported funding acquisition, and assisted in reviewing and editing the manuscript. RAD was involved in conceptualization, methodology, and validation, provided resources, supervised the research, administered the project, supported funding acquisition, and contributed to reviewing and editing the manuscript.

Funding
Not applicable.

Data availability
All data generated or analysed during this study are included in this published article [and its supplementary information files].

Declarations

Ethics approval and consent to participate
Not applicable.

Consent for publication
Not applicable.

Competing interests
The authors declare no competing interests.

Received: 29 August 2025 Accepted: 30 October 2025
Published online: 24 November 2025

References

1. Al-Khazrajy OSA, Boxall ABA (2016) Impacts of compound properties and sediment characteristics on the sorption behaviour of pharmaceuticals in aquatic systems. J Hazard Mater 317:198–209
2. Ashfaq M, Li Y, Rehman MSU, Zubair M, Mustafa G, Nazar MF, Yu CP, Sun Q (2019) Occurrence, spatial variation and risk assessment of pharmaceuticals and personal care products in urban wastewater, canal surface water, and their sediments: a case study of Lahore, Pakistan. Sci Total Environ 688:653–663
3. Bavumiragira JP, Ge J, Yin H (2022) Fate and transport of pharmaceuticals in water systems: a processes review. Sci Total Environ 823:153635
4. Borgnino L, Garcia MG, del Hidalgo MV, Avena M, De Pauli CP, Blesa MA, Depetris PJ (2009) Modeling the acid-base surface properties of aquatic sediments. Aquat Geochem 16:279–291
5. Carmona E, Andreu V, Pico Y (2014) Occurrence of acidic pharmaceuticals and personal care products in Turia River Basin: from waste to drinking water. Sci Total Environ 484:53–63
6. Chakraborty P, Mukhopadhyay M, Sampath S, Ramaswamy BR, Katsoyiannis A, Cincinelli A, Snow D (2019) Organic micropollutants in the surface riverine sediment along the lower stretch of the transboundary river Ganga: occurrences, sources and ecological risk assessment. Environ Pollut 249:1071–1080
7. Chen K, Zhou JL (2014) Occurrence and behavior of antibiotics in water and sediments from the Huangpu River, Shanghai, China. Chemosphere 95:604–612
8. Chen KL, Liu LC, Chen WR (2017) Adsorption of sulfamethoxazole and sulfapyridine antibiotics in high organic content soils. Environ Pollut 231:1163–1171
9. Da Silva BF, Jelic A, Lopez-Serna R, Mozeto AA, Petrovic M, Barcelo D (2011) Occurrence and distribution of pharmaceuticals in surface water, suspended solids and sediments of the Ebro river basin, Spain. Chemosphere 85:1331–1339
10. Dalkmann P, Broszat M, Siebe C, Willaschek E, Sakinc T, Huebner J, Amelung W, Grohmann E, Siemens J (2012) Accumulation of pharmaceuticals, Enterococcus, and resistance genes in soils irrigated with wastewater for zero to 100 years in central Mexico. PLoS ONE 7:e45397
11. de Souza RC, Godoy AA, Kummrow F, Dos Santos TL, Brandao CJ, Pinto E (2021) Occurrence of caffeine, fluoxetine, bezafibrate and levothyroxine in surface freshwater of Sao Paulo State (Brazil) and risk assessment for aquatic life protection. Environ Sci Pollut Res Int 28:20751–20761
12. Deng X, Jiang Y, Ma Z, Nan Z, Liang X, Wang G (2022) Sorption properties and mechanisms of erythromycin and ampicillin in loess soil: Roles of pH, ionic strength, and temperature. Chem Eng J 434:134694
13. Dong D, Zhang L, Liu S, Guo Z, Hua X (2016) Antibiotics in water and sediments from Liao River in Jilin Province, China: occurrence, distribution, and risk assessment. Environ Earth Sci. https://doi.org/10.1007/s12665-016-6008-4
14. Ebele AJ, Oluseyi T, Drage DS, Harrad S, Abou-Elwafa Abdallah M (2020) Occurrence, seasonal variation and human exposure to pharmaceuticals and personal care products in surface water, groundwater and drinking water in Lagos State, Nigeria. Emerg Contam 6:124–132
15. Feo ML, Bagnati R, Passoni A, Riva F, Salvagio Manta D, Sprovieri M, Traina A, Zuccato E, Castiglioni S (2020) Pharmaceuticals and other contaminants in waters and sediments from Augusta Bay (southern Italy). Sci Total Environ 739:139827
16. Gonzalez Pena OI, Lopez Zavala MÁ, Cabral Ruelas H (2021) Pharmaceuticals market, consumption trends and disease incidence are not driving the pharmaceutical research on water and wastewater. Int J Environ Res Public Health. https://doi.org/10.3390/ijerph18052532
17. Heyde BJ, Braun M, Soufi L, Lüneberg K, Gallego S, Amelung W, Axtmann K, Bierbaum G, Glaeser SP, Grohmann E, Arredondo-Hernández R, Mulder I, Pulami D, Smalla K, Zarfl C, Siebe C, Siemens J (2025) Transition from irrigation with untreated wastewater to treated wastewater and associated benefits and risks. NPJ Clean Water. https://doi.org/10.1038/s41545-025-00438-6
18. Hu Y, Yan X, Shen Y, Di M, Wang J (2018) Antibiotics in surface water and sediments from Hanjiang River, Central China: occurrence, behavior and risk assessment. Ecotoxicol Environ Saf 157:150–158
19. Jia J, Guan Y, Cheng M, Chen H, He J, Wang S, Wang Z (2018) Occurrence and distribution of antibiotics and antibiotic resistance genes in Ba River, China. Sci Total Environ 642:1136–1144

20. Kairigo P, Ngumba E, Sundberg L-R, Gachanja A, Tuhkanen T (2020) Contamination of surface water and river sediments by antibiotic and antiretroviral drug cocktails in low and middle-income countries: occurrence, risk and mitigation strategies. Water 12:1376
21. Kodesova R, Grabic R, Kocarek M, Klement A, Golovko O, Fer M, Nikodem A, Jaksik O (2015) Pharmaceuticals' sorptions relative to properties of thirteen different soils. Sci Total Environ 511:435–443
22. Kondor AC, Molnar E, Jakab G, Vancsik A, Filep T, Szeberenyi J, Szabo L, Maasz G, Pirger Z, Weiperth A, Ferincz A, Staszny A, Dobosy P, Horvathne Kiss K, Hatvani IG, Szalai Z (2022) Pharmaceuticals in water and sediment of small streams under the pressure of urbanization: concentrations, interactions, and risks. Sci Total Environ 808:152160
23. Kong W, Wang W, Jiang Y, Wang G, Ma F, Wu Y (2024) Sorption of ciprofloxacin and enrofloxacin on alkaline cropland soil in semiarid regions: roles of pH, ionic strength, and ion type. J Environ Manage 365:121565
24. Korekar G, Kumar A, Ugale C (2020) Occurrence, fate, persistence and remediation of caffeine: a review. Environ Sci Pollut Res Int 27:34715–34733
25. Kucharski D, Nalecz-Jawecki G, Drzewicz P, Skowronek A, Mianowicz K, Strzelecka A, Giebultowicz J (2022) The assessment of environmental risk related to the occurrence of pharmaceuticals in bottom sediments of the Odra River estuary (SW Baltic Sea). Sci Total Environ 828:154446
26. Kümmerer K (2009) The presence of pharmaceuticals in the environment due to human use–present knowledge and future challenges. J Environ Manage 90:2354–2366
27. Li J, Li W, Liu K, Guo Y, Ding C, Han J, Li P (2022) Global review of macrolide antibiotics in the aquatic environment: sources, occurrence, fate, ecotoxicity, and risk assessment. J Hazard Mater 439:129628
28. Li J, Zhang H (2017) Factors influencing adsorption and desorption of trimethoprim on marine sediments: mechanisms and kinetics. Environ Sci Pollut Res Int 24:21929–21937
29. Li S, Zhang R, Hu J, Shi W, Kuang Y, Guo X, Sun W (2019) Occurrence and removal of antibiotics and antibiotic resistance genes in natural and constructed riverine wetlands in Beijing, China. Sci Total Environ 664:546–553
30. Li WC (2014) Occurrence, sources, and fate of pharmaceuticals in aquatic environment and soil. Environ Pollut 187:193–201
31. Liu Z, Delgado-Moreno L, Lu Z, Zhang S, He Y, Gu X, Chen Z, Ye Q, Gan J, Wang W (2019) Inhibitory effects of dissolved organic matter on erythromycin bioavailability and possible mechanisms. J Hazard Mater 375:255–263
32. Maoz A, Chefetz B (2010) Sorption of the pharmaceuticals carbamazepine and naproxen to dissolved organic matter: role of structural fractions. Water Res 44:981–989
33. Martin J, Camacho-Munoz D, Santos JL, Aparicio I, Alonso E (2012) Occurrence of pharmaceutical compounds in wastewater and sludge from wastewater treatment plants: removal and ecotoxicological impact of wastewater discharges and sludge disposal. J Hazard Mater 239–240:40–47
34. Martin J, Santos JL, Aparicio I, Alonso E (2010) Multi-residue method for the analysis of pharmaceutical compounds in sewage sludge, compost and sediments by sonication-assisted extraction and LC determination. J Sep Sci 33:1760–1766
35. Mirzaei R, Yunesian M, Nasseri S, Gholami M, Jalilzadeh E, Shoeibi S, Mesdaghinia A (2018) Occurrence and fate of most prescribed antibiotics in different water environments of Tehran. Iran Sci Total Environ 619–620:446–459
36. Nguyen Dang Giang C, Sebesvari Z, Renaud F, Rosendahl I, Hoang Minh Q, Amelung W (2015) Occurrence and dissipation of the antibiotics sulfamethoxazole, sulfadiazine, trimethoprim, and enrofloxacin in the Mekong Delta, Vietnam. PLoS ONE 10:e0131855
37. Paiga P, Ramos S, Jorge S, Silva JG, Delerue-Matos C (2019) Monitoring survey of caffeine in surface waters (Lis River) and wastewaters located at Leiria Town in Portugal. Environ Sci Pollut Res Int 26:33440–33450
38. Paiga P, Santos L, Ramos S, Jorge S, Silva JG, Delerue-Matos C (2016) Presence of pharmaceuticals in the Lis river (Portugal): sources, fate and seasonal variation. Sci Total Environ 573:164–177
39. Patrolecco L, Ademollo N, Grenni P, Tolomei A, Barra Caracciolo A, Capri S (2013) Simultaneous determination of human pharmaceuticals in water samples by solid phase extraction and HPLC with UV-fluorescence detection. Microchem J 107:165–171
40. Perez RA, Albero B, Ferriz M, Tadeo JL (2017) Analysis of macrolide antibiotics in water by magnetic solid-phase extraction and liquid chromatography-tandem mass spectrometry. J Pharm Biomed Anal 146:79–85
41. Reyes CM, Cornelis MC (2018) Caffeine in the diet: country-level consumption and guidelines. Nutrients. https://doi.org/10.3390/nu10111772
42. Rodriguez-Mozaz S, Vaz-Moreira I, Varela Della Giustina S, Llorca M, Barcelo D, Schubert S, Berendonk TU, Michael-Kordatou I, Fatta-Kassinos D, Martinez JL, Elpers C, Henriques I, Jaeger T, Schwartz T, Paulshus E, O'Sullivan K, Parnanen KMM, Virta M, Do TT, Walsh F, Manaia CM (2020) Antibiotic residues in final effluents of European wastewater treatment plants and their impact on the aquatic environment. Environ Int 140:105733
43. Röhricht M, Krisam J, Weise U, Kraus UR, Düring R-A (2009) Elimination of carbamazepine, diclofenac and naproxen from treated wastewater by nanofiltration. CLEAN - Soil, Air, Water 37:638–641
44. Royano S, Navarro I, Torre A, Martinez MA (2024) Investigating the presence, distribution and risk of pharmaceutically active compounds (PhACs) in wastewater treatment plants, river sediments and fish. Chemosphere 368:143759
45. Schmidtova Z, Kodesova R, Grabicova K, Kocarek M, Fer M, Svecova H, Klement A, Nikodem A, Grabic R (2020) Competitive and synergic sorption of carbamazepine, citalopram, clindamycin, fexofenadine, irbesartan and sulfamethoxazole in seven soils. J Contam Hydrol 234:103680
46. Senta I, Terzic S, Ahel M (2021) Analysis and occurrence of macrolide residues in stream sediments and underlying alluvial aquifer downstream from a pharmaceutical plant. Environ Pollut 273:116433
47. Sung-Chul K, Kenneth C (2007) Temporal and spatial trends in the occurrence of human and veterinary antibiotics in aqueous and river sediment matrices. Environ Sci Technol 41:50–57
48. Svahn O, Bjorklund E (2015) Describing sorption of pharmaceuticals to lake and river sediments, and sewage sludge from UNESCO biosphere reserve Kristianstads Vattenrike by chromatographic asymmetry factors and recovery measurements. J Chromatogr A 1415:73–82
49. Tang J, Wang S, Fan J, Long S, Wang L, Tang C, Tam NF, Yang Y (2019) Predicting distribution coefficients for antibiotics in a river water-sediment using quantitative models based on their spatiotemporal variations. Sci Total Environ 655:1301–1310
50. Thiele-Bruhn S (2003) Pharmaceutical antibiotic compounds in soils – a review. J Plant Nutr Soil Sci 166:145–167
51. Valcarcel Y, Gonzalez Alonso S, Rodriguez-Gil JL, Gil A, Catala M (2011) Detection of pharmaceutically active compounds in the rivers and tap water of the Madrid Region (Spain) and potential ecotoxicological risk. Chemosphere 84:1336–1348
52. Van Doorslaer X, Dewulf J, Van Langenhove H, Demeestere K (2014) Fluoroquinolone antibiotics: an emerging class of environmental micropollutants. Sci Total Environ 500–501:250–269
53. Vasudevan D, Bruland GL, Torrance BS, Upchurch VG, MacKay AA (2009) pH-dependent ciprofloxacin sorption to soils: interaction mechanisms and soil factors influencing sorption. Geoderma 151:68–76
54. Vazquez-Roig P, Andreu V, Blasco C, Pico Y (2012) Risk assessment on the presence of pharmaceuticals in sediments, soils and waters of the Pego-Oliva Marshlands (Valencia, eastern Spain). Sci Total Environ 440:24–32
55. Vermillion Maier ML, Tjeerdema RS (2018) Azithromycin sorption and biodegradation in a simulated California river system. Chemosphere 190:471–480
56. Vulava VM, Cory WC, Murphey VL, Ulmer CZ (2016) Sorption, photodegradation, and chemical transformation of naproxen and ibuprofen in soils and water. Sci Total Environ 565:1063–1070
57. Wilkinson JL, Boxall ABA, Kolpin DW, Leung KMY, Lai RWS, Galbán-Malagón C et al (2022) Pharmaceutical pollution of the world's rivers. Proc Natl Acad Sci U S A 119:e21139
58. Ying G-G, Zhao J-L, Zhou L-J, Liu S (2013) Fate and Occurrence of Pharmaceuticals in the Aquatic Environment (Surface Water and Sediment). 62: 453-557
59. Zhao S, Liu X, Cheng D, Liu G, Liang B, Cui B, Bai J (2016) Temporal-spatial variation and partitioning prediction of antibiotics in surface water and sediments from the intertidal zones of the Yellow River Delta, China. Sci Total Environ 569–570:1350–1358
60. Zhou H, Wu C, Huang X, Gao M, Wen X, Tsuno H, Tanaka H (2010) Occurrence of selected pharmaceuticals and caffeine in sewage

treatment plants and receiving rivers in Beijing, China. Water Environ Res 82:2239–2248
61. Zhou J, Broodbank N (2014) Sediment-water interactions of pharmaceutical residues in the river environment. Water Res 48:61–70
62. Zhou LJ, Ying GG, Zhao JL, Yang JF, Wang L, Yang B, Liu S (2011) Trends in the occurrence of human and veterinary antibiotics in the sediments of the Yellow River, Hai River and Liao River in northern China. Environ Pollut 159:1877–1885

2.2. Supplementary Material of Publication 1

Supplementary Material

Integrated analysis of the occurrence and in situ sediment-water partitioning of selected pharmaceuticals in a riverine system

Aleksandër Peqini[a,b,d*], Benjamin Justus Heyde[a,c†], Ferdi Brahushi[b], Rolf-Alexander Düring[a,d]

[a]Institute of Soil Science and Soil Conservation, iFZ Research Centre for BioSystems, Land Use and Nutrition (iFZ), Justus Liebig University Giessen, Heinrich-Buff-Ring 26, 35392 Giessen, Germany

[b]Department of Environment and Natural Resources, Faculty of Agriculture and Environment, Agricultural University of Tirana, 1029 Tirana, Albania

[c]Ruhr University Bochum, Institute of Geography, Unit Soil Sciences and Soil Resources, Bochum, Germany

[d]Kompetenzzentrum Wasser Hessen, Max-Von-Laue Straße 13, 60438, Frankfurt Am Main, Germany

[*]Corresponding author. E-mail: aleksander.peqini@umwelt.uni-giessen.de

[†]Current address

SM Table 1. Concentrations of the selected pharmaceuticals in the water of Ishmi River basin for the year 2023

Season	Site	Concentration (ng L^{-1})											
		CAFF	CBZ	NPX	IBU	DCF	AETM	ATM	CMC	CFC	ETM	SMX	TMP
Winter 2023	TR1	n.d.	n.d.	n.d.	n.d.	n.d.	n.d.	n.d.	n.d.	836.57	n.d.	n.d.	n.d.
	LR1	7403.8	1321.5	1793.7	2849.4	n.d.	n.d.	7472.6	n.d.	1752.0	n.d.	82.6	n.d.
	TR2	754.7	n.d.	459.2	395.3	n.d.	n.d.	n.d.	n.d.	1198.5	1380.8	63.796	n.d.
	IR1	5402.5	n.d.	670.8	720.6	n.d.	n.d.	n.d.	n.d.	1096.4	n.d.	n.d.	n.d.
	IR2	3043.2	n.d.	554.7	671.5	325.0	n.d.	n.d.	n.d.	808.77	n.d.	n.d.	n.d.
	IR3	2436.8	n.d.	696.4	760.0	476.7	n.d.	n.d.	n.d.	935.64	n.d.	33.1	n.d.
Spring 2023	TR1	n.d.	328.9	n.d.	n.d.	n.d.							
	LR1	13789.4	n.d.	2056.0	3435.5	1818.2							
	TR2	1928.0	n.d.	326.0	513.4	n.d.				NM			
	IR1	7061.7	n.d.	1053.0	1474.7	379.7							
	IR2	6661.5	n.d.	585.7	887.2	<LOQ							
	IR3	5160.6	n.d.	618.4	1283.4	n.d.							
Summer 2023	TR1	n.d.	n.d.	n.d.	n.d.	n.d.	n.d.	n.d.	n.d.	n.d.	n.d.	n.d.	n.d.
	LR1	11346.5	n.d.	1653.6	4919.3	409.6	n.d.	115.5	n.d.	942.8	n.d.	n.d.	n.d.
	TR2	2108.7	n.d.	457.0	1060.0	n.d.	n.d.	n.d.	n.d.	828.4	n.d.	n.d.	n.d.
	IR1	10238.2	n.d.	1793.4	4511.6	n.d.	n.d.	n.d.	n.d.	1124.3	n.d.	203.4	n.d.
	IR2	7389.6	n.d.	1240.4	1602.7	n.d.	n.d.	n.d.	n.d.	n.d.	n.d.	n.d.	n.d.
	IR3	4826.4	n.d.	357.6	2224.2	n.d.	n.d.	n.d.	n.d.	906.5	n.d.	n.d.	n.d.
Autumn 2023	TR1	n.d.	n.d.	n.d.	n.d.	n.d.	n.d.	n.d.	n.d.	n.d.	n.d.	n.d.	n.d.
	LR1	22479.3	118.2	2540.9	5490.3	n.d.	n.d.	113.5	n.d.	466.2	n.d.	352.0	101.5
	TR2	2182.8	n.d.	749.2	2378.6	n.d.	3.4	n.d.	n.d.	146.6	n.d.	n.d.	n.d.
	IR1	5868.9	174.0	1330.1	6711.9	n.d.	161.8	n.d.	n.d.	159.5	n.d.	210.8	27.8
	IR2	5851.1	225.8	1503.4	3770.1	n.d.	54.4	n.d.	49.3	154.9	n.d.	237.9	37.2
	IR3	2984.6	n.d.	943.5	1615.2	n.d.	310.2	n.d.	n.d.	n.d.	n.d.	255.7	3.3

2

Continued SM Table 1. Concentrations of the selected pharmaceuticals in the water of Ishmi River basin for the year 2024

Season	Site	Concentration (ng L^{-1})											
		CAFF	CBZ	NPX	IBU	DCF	AETM	ATM	CMC	CFC	ETM	SMX	TMP
Winter 2024	TR1	n.d.	n.d.	n.d.	n.d.	n.d.	n.d.	n.d.	8.6	82.0	n.d.	n.d.	n.d.
	LR1	9533.6	644.6	1144.6	12794.9	n.d.	106.5	1305.2	9.1	869.6	n.d.	199.6	60.2
	TR2	n.d.	n.d.	<LOQ	222.6	n.d.	n.d.	n.d.	26.7	79.9	n.d.	n.d.	4.2
	IR1	1742.9	n.d.	943.5	1667.0	n.d.	n.d.	n.d.	15.3	n.d.	n.d.	n.d.	8.9
	IR2	n.d.	n.d.	303.2	1052.0	n.d.	n.d.	n.d.	11.5	82.0	n.d.	n.d.	4.5
	IR3	n.d.	n.d.	165.4	952.1	n.d.	n.d.	n.d.	7.9	172.2	n.d.	10.1	19.7
Spring 2024	TR1	n.d.	n.d.	n.d.	n.d.	n.d.	16.2	2.8	21.9	40.1	n.d.	n.d.	n.d.
	LR1	12047.0	n.d.	2608.9	5479.7	n.d.	28.1	n.d.	65.1	193.9	n.d.	124.7	73.5
	TR2	1774.5	n.d.	565.9	1160.9	n.d.	32.8	n.d.	n.d.	98.8	n.d.	n.d.	n.d.
	IR1	5876.0	n.d.	891.4	n.d.	n.d.	3.5	n.d.	55.7	29.5	146.4	n.d.	1.1
	IR2	6577.4	n.d.	786.2	n.d.	n.d.	4.2	n.d.	60.5	41.6	n.d.	n.d.	3.8
	IR3	5314.3	n.d.	518.7	1774.9	n.d.	39.2	n.d.	51.4	74.5	n.d.	n.d.	n.d.
Summer 2024	TR1	n.d.	n.d.	n.d.	n.d.	n.d.	47.9	n.d.	n.d.	115.8	n.d.	138.6	48.5
	LR1	6869.1	n.d.	2101.5	5174.5	n.d.	25.3	n.d.	n.d.	61.1	n.d.	n.d.	7.5
	TR2	1419.2	n.d.	512.7	788.5	n.d.	n.d.	n.d.	113.5	72.4	n.d.	43.0	13.9
	IR1	2457.0	n.d.	804.3	5199.2	n.d.	27.7	n.d.	149.4	33.6	n.d.	31.0	10.5
	IR2	2189.9	n.d.	973.9	5217.9	n.d.	7.1	n.d.	n.d.	42.0	n.d.	13.8	7.8
	IR3	1636.9	n.d.	n.d.	n.d.	n.d.	10.8	n.d.	112.6	40.1	n.d.	7.5	5.4
Autumn 2024	TR1	n.d.	n.d.	n.d.	n.d.	n.d.	NM						
	LR1	1942.8	n.d.	2329.1	919.4	n.d.							
	TR2	1275.8	n.d.	1049.1	1778.6	n.d.							
	IR1	3830.6	n.d.	2558.1	n.d.	n.d.							
	IR2	2883.1	n.d.	1368.9	3248.3	n.d.							
	IR3	1613.8	n.d.	1384.2	2990.7	n.d.							

n.d. : not detected; <LOQ: below the limit of quantitation; NM: not measured.

3

SM Table 2. Concentrations of the selected pharmaceuticals in sediments of Ishmi River basin

Season	Location	Concentration (ng g^{-1})								
		CBZ	NPX	IBU	AETM	ATM	CMC	CFC	SMX	TMP
Spring 2023	TR1	n.d.	n.d.	n.d.	1.05	<LOQ	5.54	n.d.	n.d.	n.d.
	LR1	34.11	12.70	93.74	0.87	144.66	5.90	782.98	13.33	5.32
	TR2	6.62	7.07	3.26	0.90	76.69	0.56	139.98	n.d.	2.29
	IR1	5.39	9.17	36.68	0.74	61.99	7.14	286.48	n.d.	4.24
	IR2	10.2	2.39	21.24	1.16	167.16	5.39	188.68	n.d.	2.72
	IR3	4.26	3.11	9.26	0.62	54.18	13.75	88.43	n.d.	2.48
Summer 2023	TR1	n.d.	n.d.	n.d.	n.d.	n.d.	9.82	2.06	0.44	n.d.
	LR1	40.4	2.76	20.34	0.86	42.82	7.19	553.54	0.44	3.68
	TR2	3.37	4.68	7.46	0.54	10.24	11.87	35.16	1.09	1.56
	IR1	2.89	0.76	9.43	n.d.	85.61	0.35	84.27	n.d.	3.28
	IR2	0.74	2.81	3.68	0.49	18.04	11.94	40.93	n.d.	0.57
	IR3	3.06	1.39	1.55	0.62	10.02	37.77	12.61	n.d.	n.d.
Spring 2024	TR1	3.47	7.16	n.d.	n.d.	n.d.	21.27	3.72	1.02	n.d.
	LR1	60.5	49.28	41.95	n.d.	212.15	18.85	1067.5	n.d.	7.84
	TR2	36.56	9.23	10.25	2.68	111.37	1.43	101.78	9.80	38.31
	IR1	20.15	22.13	17.09	n.d.	312.43	9.45	251.71	3.48	17.61
	IR2	20.43	11.51	0.41	0.74	396.20	0.32	220.24	2.97	17.83
	IR3	14.88	0.62	n.d.	0.49	87.32	5.98	65.83	n.d.	4.29
Summer 2024	TR1	6.43	4.20	n.d.	n.d.	n.d.	10.66	7.16	1.90	n.d.
	LR1	41.53	8.98	32.80	1.46	54.24	0.27	415.15	0.59	8.91
	TR2	14.24	1.48	12.09	1.54	17.71	1.45	34.55	n.d.	2.91
	IR1	10.41	3.32	0.87	n.d.	30.99	0.46	57.24	n.d.	1.68
	IR2	14.52	2.44	6.58	1.29	59.74	0.82	66.89	0.41	2.70
	IR3	16.1	1.37	n.d.	0.64	41.21	13.53	27.53	0.40	1.83

n.d. : not detected; <LOQ: below the limit of quantitation.

SM Table 3. MS Parameters fort the analysis of the antibiotics

Antibiotic	Q1	Q2	DP Volts	CE Volts	CXP Volts
Azithromycin_1	749.458	83.1	166	87	8
Azithromycin_2	749.458	591.5	151	43	22
Ciprofloxacin_1	332.087	231.1	96	53	10
Ciprofloxacin_2	332.087	288.1	96	25	16
Clindamycin_1	425.119	126.2	31	47	6
Clindamycin_2	425.119	377	86	29	16
Erythromycin_1	734.352	83.121	31	87	4
Erythromycin_2	734.352	158.149	31	87	4
Trimethoprim_1	291.028	230.2	81	33	6
Trimethoprim_2	291.028	261.2	71	35	10
Anhydro- Erythromycin_1	716.312	83.1	16	81	6
Anhydro- Erythromycin_2	716.312	158.2	21	39	8
Sulfamethoxazole_1	254.272	92.1	66	43	6
Sulfamethoxazole_2	254.272	108.1	61	31	8
Clindamycin-d3	428.131	85.1	91	105	4
Clindamycin-d3	428.131	129.2	51	39	8
Sulfamethoxazole-13C6	259.91	98.1	66	37	8
Clindamycin-13Cd6	429.187	86.2	81	113	4
Azithromycin-13Cd3	753.431	595.5	141	41	10
Ciprofloxacin-D8	340.071	235.1	31	55	10
Trimethoprim-D9	300.08	234.2	101	35	6

SM Table 4. Physico-chemical properties of the selected pharmaceuticals

Class	Compound	Acronym	CAS No.	MW	Formula	Solubility in water (mg/L)	Log K_{ow}	pK_a
Stimulants (SMs)	Caffeine	CAFF	58-08-2	194.2	$C_8H_{10}N_4O_2$	20,000	-0.07	10.4
Anti-inflammatories (AMs)	Diclofenac	DCF	15307-86-5	296.15	$C_{14}H_{11}Cl_2NO_2$	2.37	4.15	4.51
	Naproxen	NPX	22204-53-1	230.26	$C_{14}H_{14}O_3$	15.9	3.18	4.2
	Ibubrofen	IBU	15687-27-1	206.28	$C_{13}H_{18}O_2$	21	3.97	4.91
Antiepileptics (APs)	Carbamazepine	CBZ	298-46-4	236.27	$C_{15}H_{12}N_2O$	17.66	2.45	13.9
Macrolides (MLs)	Anhydro-erythromycin	AETM	23893-13-2	715.9	$C_{37}H_{65}NO_{12}$		3.06	8.88
	Azithromycin	ATM	83905-01-5	748.98	$C_{38}H_{72}N_2O_{12}$	2.4	4.02	8.7
	Clindamycin	CMC	18323-49-9	425	$C_{18}H_{33}ClN_2O_5S$		2.16	7.6
	Erythromycin	ETM	114-07-8	733.9	$C_{37}H_{67}NO_{13}$	2000	3.06	8.9
Fluoroquinolones (FQs)	Ciprofloxacin	CFC	85721-33-1	331.3	$C_{17}H_{18}FN_3O_3$	30,000	0.28	6.09/8.76
Sulfonamides (SAs)	Sulfamethoxazole	SMX	723-46-6	253.3	$C_{10}H_{11}N_3O_3S$	610	0.89	1.85/5.6/5.9
Diaminopyrimidines (DPs)	Trimethoprim	TMP	738-70-5	290.3	$C_{13}H_{18}N_4O_3$	400	0.91	3.23/6.76

Source: [1-4]

SM Table 5. Properties of the sediments of Ishmi River basin

Season	Location	pH ($CaCl_2$)	TN (%)	TH (%)	TS (%)	TOC (%)	$CaCO_3$ (%)	IC	OC	Al (mg kg^{-1})	Fe (mg kg^{-1})	Ca (mg kg^{-1})	K (mg kg^{-1})	Mg (mg kg^{-1})	Na (mg kg^{-1})
Spring 2023	TR1	7.65	0.06	0.55	0.12	2.43	15.46	1.85	0.58	26305	37101	72074	7307	31119	283.53
	LR1	6.47	0.94	1.74	0.36	11.30	11.44	1.37	9.93	17600	19128	59809	3932	13252	295.61
	TR2	6.9	0.75	1.57	0.18	6.85	10.58	1.27	5.58	56632	47522	58826	12845	27470	609.67
	IR1	6.76	0.43	0.95	0.22	5.76	12.93	1.55	4.21	20539	26793	64324	5248	19310	229.41
	IR2	6.8	0.65	1.22	0.18	6.40	12.09	1.45	4.95	25842	31523	55369	6776	22285	279.39
	IR3	6.97	0.24	0.74	0.11	3.74	13.81	1.66	2.08	25455	32867	60088	7158	25664	249.47
Summer 2023	TR1	7.57	0.05	0.02	0.11	2.55	15.74	1.89	0.67	29889	35123	66401	9852	31205	301.48
	LR1	6.49	1.26	2.23	0.34	12.73	8.28	0.99	11.74	29738	25685	45000	6923	12137	408.56
	TR2	7.47	0.18	0.84	0.11	2.62	10.63	1.28	1.34	40581	42179	44940	12588	32775	424.06
	IR1	7.3	0.44	1.00	0.22	5.34	12.04	1.44	3.89	28435	33047	56566	8159	24052	295.56
	IR2	7.47	0.23	0.78	0.18	3.69	13.02	1.56	2.13	29393	33382	59124	8944	25634	293.01
	IR3	7.52	0.22	0.79	0.12	3.31	13.58	1.63	1.68	34312	38557	57932	10657	30359	366.54
Spring 2024	TR1	8.35	0.06	0.31	0.11	2.14	12.67	1.52	0.62	38228	33951	57901	21410	9314	439.20
	LR1	6.37	0.02	0.29	0.17	11.43	11.19	1.34	10.09	9319	11177	47854	8111	2210	214.09
	TR2	7.05	0.40	0.48	0.18	5.49	13.11	1.57	3.92	41520	37334	56479	30762	11926	518.85
	IR1	6.54	0.84	0.52	0.23	7.97	13.77	1.65	6.32	24898	24440	62951	17766	7172	370.35
	IR2	6.51	1.45	0.84	0.25	5.17	9.66	1.16	4.01	30846	30197	52958	20699	8274	412.34
	IR3	7.32	0.21	0.29	0.13	3.67	15.25	1.83	1.84	32879	31257	63362	26783	10523	580.61
Summer 2024	TR1	7.94	0.04	0.02	0.15	2.83	15.67	1.88	0.95	27611	31947	75885	33674	8133	493.92
	LR1	6.52	0.82	0.75	0.21	8.31	8.35	1.00	7.31	54972	39725	43707	23804	11971	604.04
	TR2	7.43	0.23	0.41	0.16	3.44	12.36	1.48	1.95	47815	43059	52637	38162	14682	640.96
	IR1	7.32	0.21	0.30	0.20	3.93	14.10	1.69	2.24	21828	28824	61632	24991	4731	329.35
	IR2	7.21	0.54	0.45	0.22	5.89	13.13	1.57	4.32	23333	30853	59469	24579	5019	396.55
	IR3	7.39	0.63	0.51	0.19	5.83	12.49	1.50	4.33	29363	38158	55369	32230	6815	517.25

*pH in 1:2.5 sediment:0.01 M $CaCl_2$

SM Table 6. Calculated K_d of in both aqueous and sediment detected compounds at each location and season

Location	Season	Compound K_d (mL g^{-1})							
		NPX	IBU	AETM	ATM	CMC	CFC	TMP	SMX
TR1	Spring 2024					971.2	92.74		
	Summer 2024						61.87	39.25	
LR1	Spring 2023	6.18	27.29						
	Summer 2023	1.67	4.13		369.2		587		
	Spring 2024	18.89	7.65			289.6	5504.9		62.87
	Summer 2024	4.27	6.34	57.8			6796.5	78.7	
TR2	Spring 2023	21.70	6.35						
	Summer 2023	10.24	7.04				42.47		
	Spring 2024	16.32	8.83	81.8			1030.4		
	Summer 2024	2.89	15.34			12.75	477.2		67.56
IR1	Spring 2023	8.71	24.87						
	Summer 2023	0.42	2.09				74.98		
	Spring 2024	24.83				169.6	8534.4	3142.7	
	Summer 2024	4.13	0.17			3.06	1701.9		54.23
IR2	Spring 2023	4.09	23.94						
	Summer 2023	2.27	2.30						
	Spring 2024	14.64		1741		5.33	5293.7	775.9	
	Summer 2024	2.50	1.26	180.7			1591.9	52.76	195.7
IR3	Spring 2023	5.04	7.22						
	Summer 2023	3.89	0.70				13.92		
	Spring 2024	1.20		12.50		116.3		883.7	
	Summer 2024			178.1			910.5	70.63	197.3

SM Table 7. Correlation coefficient (R) between K_d and sediment properties

Compound	Adj. R^2 (%OC)	Adj. R^2 pH ($CaCl_2$)	D_{ow}	$CaCO_3$	Al (mg kg^{-1})	Fe (mg kg^{-1})	Ca (mg kg^{-1})	K (mg kg^{-1})	Mg (mg kg^{-1})	Na (mg kg^{-1})
AETM	0.734*	-0.085	-0.011	-0.369	-0.867*	-0.306	-0.308	-0.242	-0.609*	-0.605*
CFC	0.565**	-0.811***	0.837***	-0.105	-0.119	-0.636*	-0.394*	-0.389*	-0.384*	-0.113
CMC	0.678*	-0.194	0.15	-0.249	-0.335	-0.61*	-0.179	-0.477	-0.134	-0.11
IBU	0.206	-0.544**	0.609**	-0.144	0.311*	0.247	-0.129	0.133	-0.049	0.208
NPX	0.259	-0.461**	0.444**	-0.326*	0.423*	0.095	-0.029	0.259	-0.153	0.104
SMX	0.961**	-0.169	0.286	-0.04	0.687	0.351	-0.271	-0.18	-0.282	-0.077
TMP	0.227	-0.129	0.095	-0.248	0.499	-0.087	-0.249	-0.373	-0.112	-0.248

*p < 0.05, **p < 0.01,***p < 0.001

SM Table 8. Multiple regression analysis models for prediction of K_d for AETM, CFC, CMC, IBU, and NPX

Compound	Predictor	RMSE[a]	Adj. R^2	Regression equation only for significant parameters
AETM	OC, Alt, Mgt, Na_t	24.1	0.891	K_d = -338.339 + 224.488 (OC) - 0.064 (Al_t) + 0.155 (Mg_t) + 0.717 (Na_t)
CFC	OC, pH, D_{ow}, Fe_t, Ca_t, K_t, Mg_t	629.1	0.889**	K_d = 25784.102 - 2080.813 (pH) - 627.1 (OC) + 4897.223 (D_{ow}) - 0.115 (Fe_t) - 0.061 (Ca_t) + 0.005 (K_t) - 0.061 (Mg_t)
CMC	OC, Fe_t	72.8	0.604	K_d = 103.97 + 20.88 (OC) - 0.003 (Fe_t)
IBU	pH, D_{ow}, Al_t	6.72	0.53*	K_d = 15.49 - 2.285 (pH) + 0.115 (D_{ow}) + 6.357 * 10^{-5} (Al_t)
NPX	pH, D_{ow}, $CaCO_3$, Al_t	5.18	0.549**	K_d = 4.774 - 4.462 (pH) + 2.191 (D_{ow}) + 1.085 ($CaCO_3$) + 4.794 * 10^{-4} (Al_t)

*p < 0.05, **p < 0.01, ***p < 0.001, [a]Root Mean Square Error (RMSE)

SM Table 9. In situ (calculated) and predicted K_d values of NPX, IBU, AETM, CMC, and CFC calculated using the developed models

Compound K_d (mL g^{-1})									
NPX		IBU		AETM		CFC		CMC	
In situ	Predicted	In situ	Predicted	In situ	Predicted	In situ	Predicted	In situ	Predicted
6.18	14.47	27.29	40.60	57.82	72.61	92.74	175.3	971.2	15.02
1.67	15.98	4.13	39.62	81.84	103.8	61.87	164.8	289.6	281.1
18.89	15.23	7.65	50.00	174.1	165.8	587.0	1170.7	12.75	15.59
4.27	26.89	6.34	38.74	180.7	200.0	6796.5	2316.4	169.6	162.6
21.70	19.22	6.35	17.98	12.50	18.27	5504.9	5116.8	3.06	64.31
10.24	4.21	7.04	4.97	178.1	181.7	42.47	244.0	5.33	97.11
16.32	12.12	8.83	12.42			1030.4	1269.0	116.3	48.66
2.89	9.91	15.34	5.91			477.2	638.8		
8.71	7.60	24.87	21.50			74.98	16.92		
0.42	1.53	2.09	6.49			8534.4	3656.9		
24.83	17.56	0.17	5.76			1701.9	2427.6		
4.13	0.39	23.94	19.99			5293.6	5189.5		
4.09	8.25	2.30	4.26			1591.9	1372.6		
2.27	1.44	1.26	7.71			13.92	-348.7		
14.64	17.16	7.22	13.67			910.2	116.7		
2.50	1.27	0.70	4.03						
5.04	6.48								
3.89	3.99								
1.20	6.93								

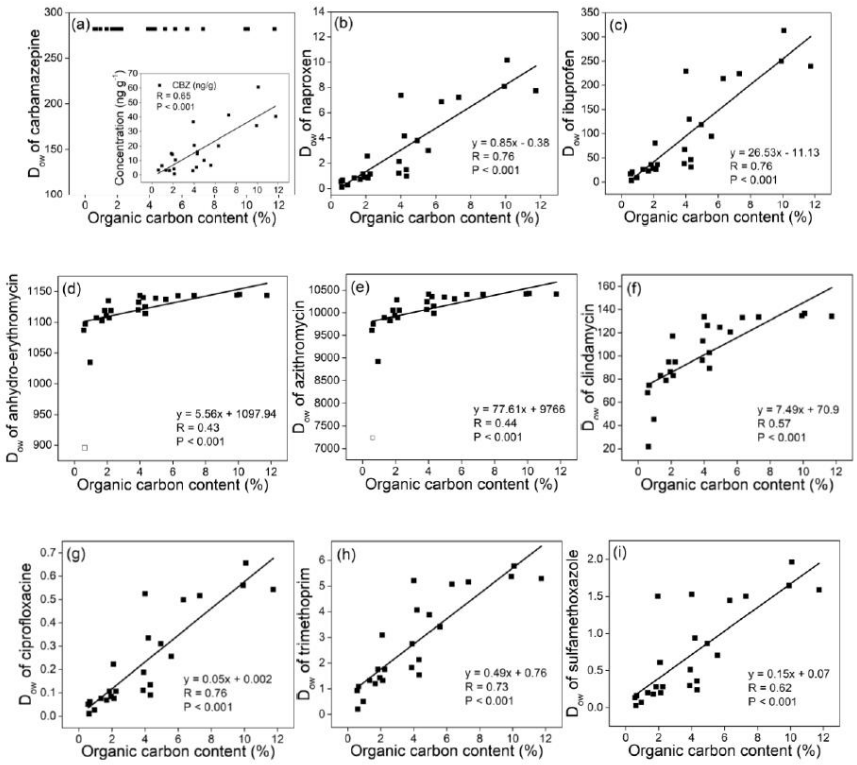

SM Fig. 1 Relation between the calculated D_{ow} with oganic carbon content of the sediments for (a) carbamazepine (also the relation for the carbamazepine detected concentrations); (b) naproxen; (c) ibuprofen; (d) anhydro-erythromycin; (e) azithromycin; (f) clindamycin; (g) ciprofloxacine; (h) trimethoprim; and (i) sulfamethoxazole

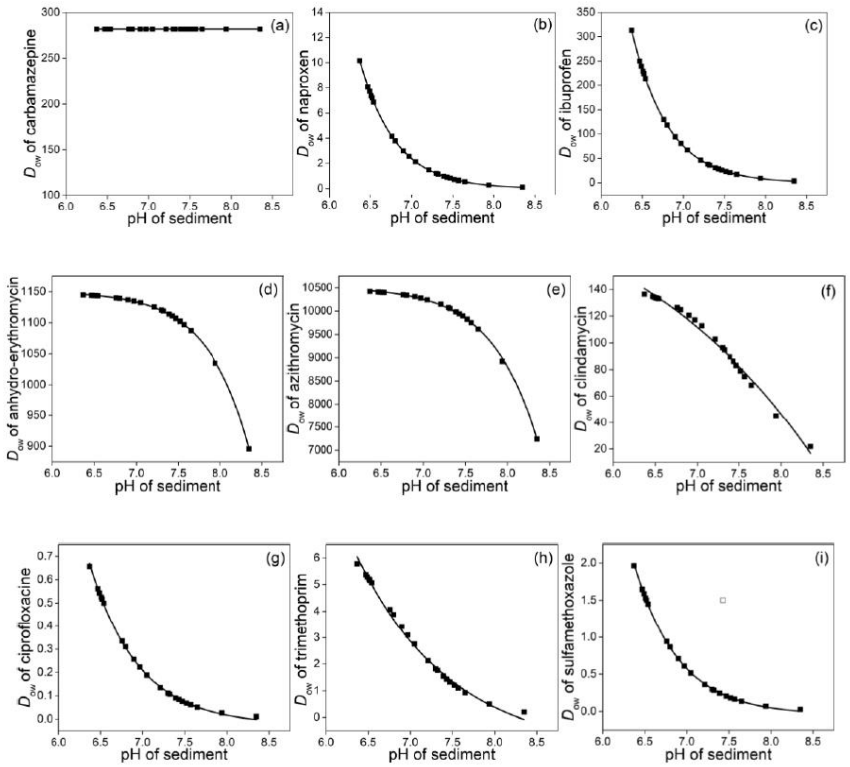

SM Fig. 2 Relation between the calculated D_{ow} with pH of the sediments for (a) carbamazepine; (b) naproxen; (c) ibuprofen; (d) anhydro-erythromycin; (e) azithromycin; (f) clindamycin; (g) ciprofloxacine; (h) trimethoprim; and (i) sulfamethoxazole

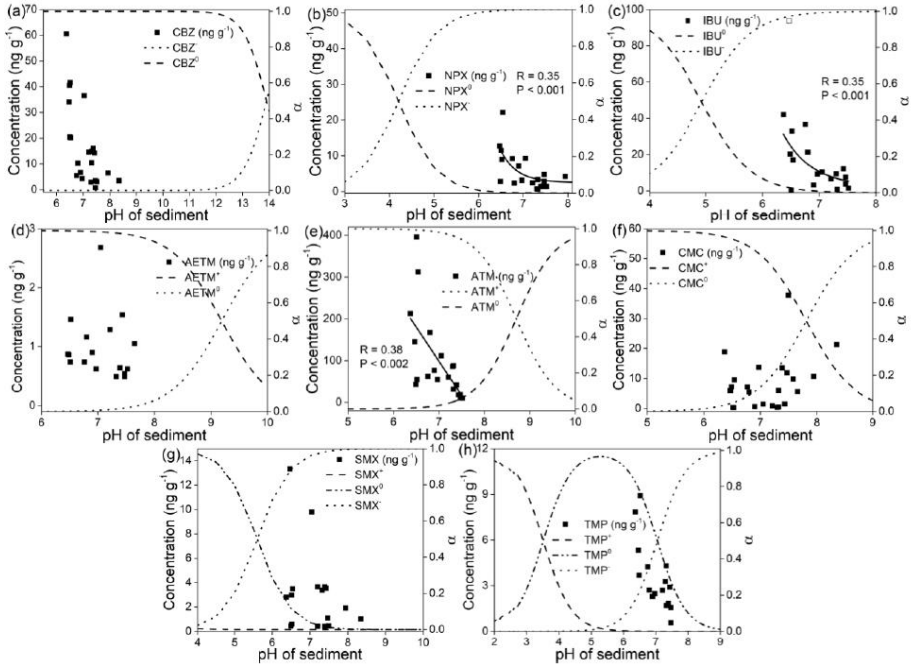

SM Fig. 3 Relation between the detected concentrations with pH of sediment for (a) carbamazepine; (b) naproxen; (c) ibuprofen; (d) anhydro-erythromycin; (e) azithromycin; (f) clindamycin; (g) sulfamethoxazole; and (h) trimethoprim

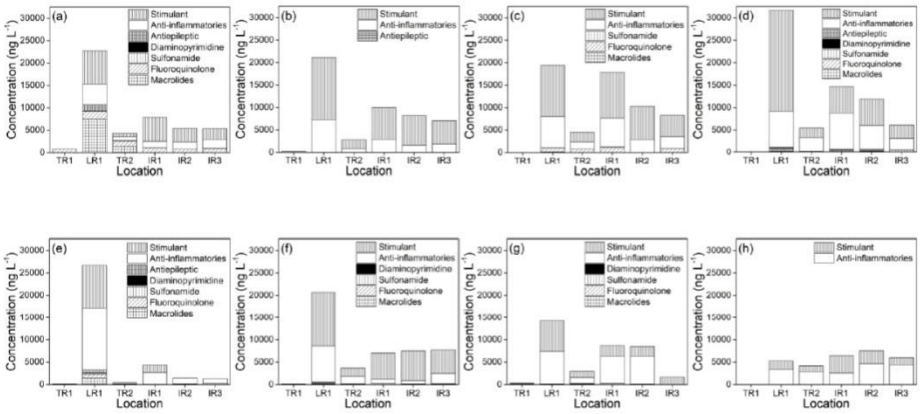

SM Fig. 4 Pharmaceutical concentrations in waters for (a) and (e) winter; (b) and (f) spring; (c) and (g) summer; and (d) and (h) autumn seasons of the years 2023 and 2024

SM Table 10. Statistical results for selected pharmaceuticals in water samples from the Ishmi River basin (2023-2024)

Compound	Factors	Year 2023				Year 2024			
		d.f.	MS	F	*P* level	d.f.	MS	F	*P* level
AETM	Season					2	[a]*H* = 3.51		[a]0.173
	Location					5	[a]*H* = 7.32		[a]0.198
	Season x Location					10	[a]n.a.		
ATM	Season	2	[a]*H* = 0.04		[a]0.979	2			
	Location	5	[a]*H* = 34.63		[a]**<0.001**	5			
	Season x Location	10	[a]n.a.			10			
CMC	Season					2	7408.326	4.366	**0.028**
	Location					5	3409.539	2.009	0.125
	Season x Location					10	3885.717	2.29	0.060
CFC	Season	2	$2.708*10^6$	108.472	**<0.001**	2	[a]*H* = 1.24		[a]0.54
	Location	5	520791.436	20.858	**<0.001**	5	[a]*H* = 11.23		[a]**0.047**
	Season x Location	10	142111.385	5.691	**<0.001**	10	[a]n.a.		
SMX	Season	2	83162.911	44.586	**<0.001**	2	[a]*H* = 6.25		[a]**0.044**
	Location	5	21232.7	11.383	**<0.001**	5	[a]*H* = 6.26		[a]0.28
	Season x Location	10	18466.033	9.9	**<0.001**	10	[a]n.a.		
TMP	Season	2	[a]n.a.			2	33.316	0.382	0.687
	Location	5	[a]*H* = 10.60		[a]0.060	5	1576.089	18.079	**<0.001**
	Season x Location	10	[a]n.a.			10	867.65	9.953	**<0.001**
Total	Season	2	$1.661*10^7$	58.703	**<0.001**	2	[a]*H* = 3.00		[a]0.223
	Location	5	$1.001*10^7$	35.38	**<0.001**	5	[a]*H* =5.19		[a]0.393
	Season x Location	10	$6.683*10^6$	23.619	**<0.001**	10	[a]n.a.		

[a]Kruskal–Wallis tests

SM Table 11. Statistical results for selected pharmaceuticals in sediment samples from the Ishmi River basin (2023-2024)

Compound	Factors	Year 2023				Year 2024			
		d.f.	MS	F	*P* level	d.f.	MS	F	*P* level
CBZ	Season	1	17.12	1.895	0.193	1	464.09	14.903	**0.002**
	Location	5	767.7	85.01	**<0.001**	5	1000.801	32.139	**<0.001**
	Season x Location	5	26.08	2.888	0.061	5	106.834	3.43	**0.037**
NPX	Season	1	81.016	8.448	**0.013**	1	1017.861	80.903	**<0.001**
	Location	5	31.387	3.273	**0.042**	5	403.008	32.032	**<0.001**
	Season x Location	5	19.48	2.031	0.145	5	222.344	17.672	**<0.001**
IBU	Season	1	2469.868	13.108	**0.003**	1	36.569	1.623	0.225
	Location	5	1775.002	9.42	**<0.001**	5	775.155	34.648	**<0.001**
	Season x Location	5	809.369	4.295	**0.017**	5	71.558	3.198	**0.045**
AETM	Season	1	1.901	2.565	0.135	1	0.169	0.836	0.378
	Location	5	0.268	0.362	0.864	5	2.438	12.019	**<0.001**
	Season x Location	5	0.272	0.367	0.861	5	0.715	3.526	**0.034**
ATM	Season	1	19036.076	92.399	**<0.001**	1	139716.686	326.011	**<0.001**
	Location	5	5556.092	26.968	**<0.001**	5	27615.56	64.437	**<0.001**
	Season x Location	5	4099.168	19.897	**<0.001**	5	17707.405	41.317	**<0.001**
CMC	Season	1	275.574	1.97	0.185	1	[a]$H = 0.08$		[a]0.77
	Location	5	256.419	1.833	0.180	5	[a]$H = 2.08$		[a]0.15
	Season x Location	5	107.714	0.77	0.558	5	[a]n.a.		
CFC	Season	1	95767.3	24.5	**<0.001**	1	6	$3.04*10^{31}$	**<0.0001**
	Location	5	239888.7	61.3	**<0.001**	5	$1.11*10^{-30}$	5.64	**0.006**
	Season x Location	5	7266.3	1.9	0.175	5	$1.11*10^{-30}$	5.64	**0.006**
SMX	Season	1	21.54	1.294	0.277	1	32.507	5.856	**0.032**
	Location	5	30.319	1.821	0.182	5	11.604	2.09	0.137
	Season x Location	5	29.158	1.752	0.197	5	16.649	2.999	0.055
TMP	Season	1	10.48	7.232	**0.019**	1	767.281	140.75	**<0.001**
	Location	5	11.053	7.628	**0.002**	5	202.084	37.07	**<0.001**
	Season x Location	5	0.868	0.599	0.701	5	250.332	35.805	**<0.001**
Total	Season	1	252930.224	50.115	**<0.001**	1	862208.857	1287.128	**<0.001**
	Location	5	383021.318	75.891	**<0.001**	5	484267.683	722.927	**<0.001**
	Season x Location	5	23224.299	4.601	**0.014**	5	113047.77	168.76	**<0.001**

[a]Kruskal–Wallis tests

References

1. Chen K, Zhou JL (2014) Occurrence and behavior of antibiotics in water and sediments from the Huangpu River, Shanghai, China. Chemosphere 95:604-612
2. Li Y, Ding J, Zhang L, Liu X, Wang G (2019) Occurrence and ranking of pharmaceuticals in the major rivers of China. Sci Total Environ 696:133991
3. Moreno-Gonzalez R, Rodriguez-Mozaz S, Gros M, Barcelo D, Leon VM (2015) Seasonal distribution of pharmaceuticals in marine water and sediment from a Mediterranean coastal lagoon (SE Spain). Environ Res 138:326-344
4. Zhang DQ, Hua T, Gersberg RM, Zhu J, Ng WJ, Tan SK (2013) Carbamazepine and naproxen: fate in wetland mesocosms planted with Scirpus validus. Chemosphere 91:14-21

3. Publication 2: Sustainable removal of aqueous naproxen using a ternary magneto-biochar-clay composite: Competition with carbamazepine and influence of dissolved organic matter

Published in *Chemical Engineering Journal Advances* as: Sustainable removal of aqueous naproxen using a ternary magneto-biochar-clay composite: Competition with carbamazepine and influence of dissolved organic matter

DOI: 10.1016/j.ceja.2025.100784

Main Text of Publication 2 from page 77

Supplementary Material of Publication 2 from page 87

3.1. Main Text of Publication 2

Chemical Engineering Journal Advances 23 (2025) 100784

Contents lists available at ScienceDirect

Chemical Engineering Journal Advances

journal homepage: www.sciencedirect.com/journal/chemical-engineering-journal-advances

Sustainable removal of aqueous naproxen using a ternary magneto-biochar-clay composite: Competition with carbamazepine and influence of dissolved organic matter

Aleksandër Peqini [a,b,*], Paul N. Diagboya [c], Ferdi Brahushi [b], Rolf-Alexander Düring [a]

[a] Institute of Soil Science and Soil Conservation, Research Centre for BioSystems, Land Use and Nutrition (iFZ), Justus Liebig University Giessen, Heinrich-Buff-Ring 26, 35392 Giessen, Germany
[b] Department of Environment and Natural Resources, Faculty of Agriculture and Environment, Agricultural University of Tirana, 1029 Tirana, Albania
[c] Environmental fate of chemicals and remediation (EnFaCRe) laboratory, Department of Environmental Management and Toxicology, University of Delta, PMB 2090 Agbor, Nigeria

ARTICLE INFO

Keywords:
Feldspar
Grape cluster stalk
Naproxen
Magnetite
Carbamazepine
Adsorption

ABSTRACT

Low-cost magneto-biochar-clay (MBC) composite adsorbent prepared by a combination of synthesized Fe_3O_4, biochar (from grape cluster stalk), and feldspar clay was tested for naproxen removal from simulated and real contaminated aqueous solutions. Preliminary sorption results for naproxen and other contaminants showed higher removal efficiency of the MBC than the pristine materials. Naproxen adsorption optimum solid-liquid ratio was at 0.5 g/L and the adsorption equilibrium was attained in 720 min on this composite, while the optimum adsorption was achieved at solution pH of 2.5. The process was endothermic and better described by the Sips adsorption isotherm model. Adsorptive pore filling, electrostatic and hydrophobic interactions between the composite surfaces and the naproxen species were the main mechanisms of naproxen uptake. In a competitive adsorption study with carbamazepine, the two compounds showed higher competition at lower solution pH values. With increase in dissolved organic matter concentration in water, naproxen and carbamazepine sorption reduced significantly. The composite retained high removal efficiency (≥99 %) after five consecutive adsorption cycles. Naproxen removal efficiency in real environmental water (river water) containing low naproxen concentration (50 μg/L) was quite high (≈ 93 %). Based on this study, the composite is sustainable, cost-efficient, and potentially applicable for naproxen and carbamazepine removal from surface waters.

1. Introduction

The ubiquitous presence of emerging contaminants, especially the pharmaceutically active compounds in surface water bodies is alarming; this is mostly so in low- to middle-income countries due to non-existent or poor wastewater treatment technologies [1]. Major input sources of pharmaceuticals include effluents from pharmaceutical plants, human and veterinary hospital effluents, excretion of semi/un-metabolized pharmaceuticals by humans and animals, as well as discharges from the municipal sewage system [2]. These compounds pose several risks to the ecosystem and human health because some of them have poor degradability and can bioaccumulate, this leads to longer exposure time in the environment which can result in drug resistant microbial species, and most have been reported to have adverse effects on non-target species [3].

Naproxen, a nonsteroidal anti-inflammatory drug (NSAID) is one of the frequently detected pharmaceuticals in the environment, particularly in surface waters with concentrations ranging from ng/L to μg/L [1, 4–7]. The frequent detection of naproxen in water may be related to its continuous discharge and low removal efficiency (<15 %) by conventional water treatment processes [8]. Naproxen is preferred in the treatment of osteoarthritis, rheumatoid arthritis, fever, and pain. Its widespread preference and use is attributed to several factors, including rapid absorption, long duration of action, high binding affinity to plasma proteins, lower vascular risk, and easy purchase without prescription [9]. Naproxen adverse effects to ecosystems and biota are mainly attributed to the toxicity of its metabolites including hydroperoxide, ketone, alcohol, etc. These metabolites (hydroperoxide, ketone) are

* Corresponding author at: Institute of Soil Science and Soil Conservation, Research Centre for BioSystems, Land Use and Nutrition (iFZ), Justus Liebig University Giessen, Heinrich-Buff-Ring 26, 35392 Giessen, Germany.
E-mail address: aleksander.peqini@umwelt.uni-giessen.de (A. Peqini).

https://doi.org/10.1016/j.ceja.2025.100784

Available online 3 June 2025

reported to have more toxicity than the parent compound to *Vibrio fischeri* and *Daphnia magna* [10]. Naproxen has adverse effects on gastrointestinal and renal activity of zebrafish and its embryos [8,11]. A concentration higher than 1 g/L has been reported to cause genotoxic effects in microorganisms such as *Bacillus thuringiensis* [12]. Carbamazepine, used in epileptic cases, also considered in this study is one of the most detected pharmaceuticals in water bodies [1]. Carbamazepine is another important and commonly used medication, and its photolytic metabolites are reportedly toxic to bacteria (*Vibrio fischeri*), algae (*Pseudokirchneriellasubcapitata*), and *Daphnia magna* [13]. The acute toxicity of this compound to fish, such as the Rainbow Trout (*Oncorhynchus mykiss*) makes it a very harmful compound for aquatic systems [14]. Therefore, it is of high importance to remove these compounds from water.

Pharmaceuticals could be removed from water *via* different techniques, including adsorption, physico-chemical/biological processes, or their combinations. The adsorption process has several advantages compared to the most techniques due to easy handling and operation, sustainability (when obtained from agro-organic waste), formation of zero-to-little harmful by-product, and cost-effectiveness. Several agro-organic wastes have been studied for naproxen removal from water, such as grape branches [15], rice straw [16], peanut shells [17], sheep manure [18], palm date and orange peel [19], bamboo [20], and wild plum kernels [3]. Major shortcomings of most natural adsorbents include bleeding of the adsorbents, low adsorption efficiencies, low durability/stability, and cumbersome post-adsorption separation of adsorbents from water. Thus the elimination of these flaws is the focus of most recent studies, and synergistic combination of two or more low-cost materials such as biomass, clays and magnetic nanoparticles have been proposed to overcome these [21–23]. It has been confirmed that biochar and clay combination increases the surface area, adsorption sites, improves the porosity, and adsorbent stability and reusability compared to the starting materials [24–27]. Irrespective of these attributes, post-adsorption (after adsorption process) separation of adsorbent from treated water remains a challenge. Recently, magnetization of adsorbents has been proposed and studied, and it has been found to make adsorbents easy to handle, the process simple to operate, and it saves cost [22,28]. Thus, the aim of the study was to prepare a low-cost adsorbent from agrowaste that can be magnetically separated from treated water post-adsorption.

In the current study, grape cluster stem bio-waste collected from a farm in Albania was used to prepare the composite. Due to favorable climatic conditions, grape cluster is a major agro-waste in Albania running into several thousand tons per year and thus sufficient quantity can be obtained for water treatment purposes. As a European Union candidate country, Albania has to align its water policy with the Water Framework Directive (Directive 2000/60/EC), which requires a good ecological and chemical status for all its water bodies. Albania is a middle-income country (World Bank, 2022), and has over 30 % of its population located in the central-western region, where the Ishmi river basin is located. Notably, this area lacks functional wastewater treatment plants, raising concerns about environmental pollution. Naproxen was selected for this study because it was detected almost in all collected water samples along the Ishmi river during a two-year study (2023-2024), with concentrations ranging from 0.3 μg/L to 2.6 μg/L, and an average concentration of 1 μg/L over the study period (our unpublished preliminary data). These findings align with the national data on naproxen consumption, where monthly average usage for the years 2022, 2023, and 2024 was reported at 119.3, 156.6, and 140.6 kg, respectively. Carbamazepine was also detected with concentrations ranging from 0.17 μg/L to 1.32 μg/L, and the monthly average usage for the years 2022, 2023, and 2024 was 45.6, 36, and 46 kg, respectively. It is important to note that these amounts reflect only the reimbursed quantities by the state (Mandatory Health Insurance Fund of Albania). The connection between the detected environmental concentrations of naproxen and carbamazepine, and their consumption underscores the potential negative impact on the aquatic environment. These results highlight the need for the establishment of effective wastewater treatment infrastructure in Albania to reduce pharmaceutical presence and protect water resources. Hence, the objective of this study was to prepare magneto-biochar-clay composite using grape cluster waste, feldspar clay, and magnetic nanoparticles for the removal of naproxen and carbamazepine from water.

2. Materials and methods

2.1. Materials, pretreatments, and ternary magnetic composite preparation and characterizations

Pretreated Feldspar clay (FLC) [29] and precleaned grape cluster stalk waste (GC) were the main low-cost materials used in this study. The GC was dried at 40 °C until a constant weight was achieved, then pulverized, sieved (1000 μm size sieve), and stored. Mettler Toledo scale (ME 204), MilliQ (Purelab, UK) water at 18.2 MΩcm, pH meter (inoLab® pH 7110), and HPLC grade acetonitrile (ACN) were used in this study. Naproxen, carbamazepine, sodium azide (NaN_3), formic acid, and humic acid sodium salt were purchased from Merck-Sigma-Aldrich GmbH, Germany. Ethanol and acetic acid were purchased from Carl Roth GmbH & Co. KG (Karlsruhe, Germany). The Strata C-18 cartridges were purchased from Phenomenex, USA.

The FLC and GC were employed alongside the synthesized magnetic nanoparticles (MNP) to prepare the ternary magneto biochar-clay composites (MBC-x). The average mass of raw GC which gave the specific mass of biochar (BC) was determined by calcination of triplicate (same) mass of GC for 2 h (in limited air) at a temperature of 500 °C. The MNP was prepared *via* chemical co-precipitation [30] by mixing $FeCl_3$ (7.8 g) and $FeSO_4{\cdot}7H_2O$ (3.9 g) in 400 mL water under continuous magnetic stirring. A solution of 2.0 M NaOH was added drop-wise until the red solution turned black. The MNP in the mixture was obtained by magnetic separation or centrifugation (5 min; 2500 rpm). It was washed (6x) with MilliQ water, dried at 40 °C, weighed, and stored in an air tight container.

Two ratio combinations of MBC-x (1:2:1 and 1:3:1) were prepared using the MNP, BC and FLC. The procedure started by preparing the MNP as described above but without the separation step. The calculated raw GC mass which gave the specific BC ratio was then added before shaking at 200 rpm for 30 min, and the subsequent addition of the FLC mass to give the specific ratio. The entire mixture was further agitated for 2 h, centrifuged at 1500 rpm for 10 min, and dried at 80 °C overnight before being calcined inside a crucible, as described above. The composites (MBC-1:2:1 and MBC-1:3:1) were cooled, washed till neutral, sieved, weighed, and stored.

The individual adsorbents and the composites were characterized for their cation exchange capacity (CEC) using the sodium saturation method and point of zero charge (pHpzc) using pH-drift method [31], as well as using the Fourier transform infrared (FTIR) spectrometer (VERTEX70, Bruker Optics, Germany) for the analysis of functional groups, the X-ray diffractometer (XRD) (Empyrean spectrometer, Malvern Panalytical, Germany) to assess crystallinity, the QUADRASORBevo analyzer (Quantachrome Instruments, USA) determining specific surface area, and the scanning electron microscope (SEM, Gemini SEM 560 Zeiss, Germany) in order to depict surface morphology.

2.2. Adsorption experiments

Standard stock solutions of naproxen and carbamazepine (10000 mg/L) were prepared in 50:50 ACN:MilliQ and stored at 4 °C, while the working solutions were prepared from the stock solution in MilliQ with 100 mg/L NaN_3, (biocide). To eliminate the co-solvent effect, the ACN amount in solution was kept at <0.1 %. Preliminary batch sorption experiments were carried out using 20 mg of either BC, FLC, MNP, or MBC (separately) in 10 mL of 1 mg/L of naproxen solution. Other

separate preliminary tests were performed using 20 mg mass in 15 mL of 2 mg/L terbuthylazine, 15 mL of 5mg/L Pb(II), and 30 mL of 5 mg/L Cu (II). Considering the ease of separation of the MBC 1:2:1 composite from water impacted by the magnetic property and its high adsorption performance compared to other tested materials, the MBC 1:2:1 composite was employed in the detailed batch adsorption study. Each batch experiment used 5 mg mass (except for mass effect study) of adsorbent in 10 mL of 2.5 mg/L naproxen solution (except for concentration effect study) at pH of 4.5 ± 0.1 (except for the study of pH effect) using 20 mL brown glass vials incubated for 1440 min (except for kinetics study) at 200 rpm and 20 °C (except for temperature effect study). The solution pH adjustment was carried out using 0.2 M HCl or NaOH. The effects of several adsorption parameters such as adsorbent mass from 5-40 mg, time from 1-1440 min, solution pH from 2.5-10, naproxen concentration from 1-20 mg/L, and ambient temperature from 20-40 °C were investigated. Naproxen desorption was performed after equilibrium at 20 °C in order to get more insight to the adsorption mechanism. The desorption process was carried out using the composite that was magnetically separated from the naproxen solution, dried overnight at 40 °C, and the vials with the same residual composites were refilled with the same background solution/biocide (without naproxen). The competition with carbamazepine was assessed with 5 mg adsorbent mass, at varying solution pH (2.5-10) and 2.5 mg/L concentration for both compounds. The effect of dissolved organic matter (DOM) with humic acid sodium salt (5-100 mg/L) and a concentration of 2.5 mg/L each naproxen and carbamazepine, using 5 mg adsorbent at a solution pH of 4.5 ± 0.1, was evaluated. The sorption with pristine river water (pH 4.5 ± 0.1) with 2.5 mg/L naproxen and carbamazepine, and 5 mg adsorbent mass was also evaluated. The composite's reusability was assessed using 5 mg of the used-adsorbent and naproxen solution concentration of 2.5 mg/L. The adsorbed naproxen was desorbed by shaking in 10 mL of ethanol twice (200 rpm for 1 h) and rinsed in MilliQ water under the same conditions, before drying overnight and reusing. Five cycles of reusability were carried out. The composite's applicability and removal efficiency was evaluated in river water (collected from the Ismi river in Albania), which was spiked with similar environmental naproxen concentrations (50 μg/L). For the naproxen determination in this last experiment, samples were concentrated by using C-18 Strata cartridges and extracted with 2 mL ACN:acetic acid (80:20, v:v). After each experiment, the solutions were filtered with 1 μm glass fiber filters, and analyte concentration remaining in solution was measured using HPLC-DAD.

2.3. Naproxen and carbamazepine determination

A previously reported analytical method for the determination of naproxen and carbamazepine determination [32] was applied. Naproxen and carbamazepine were analyzed by an Agilent 1200 HPLC system (Agilent Technologies Inc., USA), equipped with a reverse-phase, C18 column (3 μm, 120 Å, 2.1 × 150 mm), column oven, autosampler, quarternary pump, and a DAD detector . The device was operated at 35 °C with an injection volume of 20 μL. The mobile phase consisted of a mixture of acetonitrile:0.2 % formic acid in water (60:40, v:v) at a flow rate of 0.3 mL/min. The wavelengths of 230 nm and 285 nm, and 8 min run time (3.38 and 2.1 min retention time) were employed for naproxen and carbamazepine, respectively. The naproxen and carbamazepine calibration curves exhibited a linear range with r^2 of 1 using concentrations between 0.05 and 20 mg/L, and 0.5 – 20 mg/L in 100 mg/L biocide (NaN_3) for naproxen and carbamazepine, respectively. Using blanks, naproxen and carbamazepine sorption on the vials walls, caps, and filters were found to be negligible.

2.4. Data treatment and adsorption model fittings

The amounts (mg/g) of naproxen and carbamazepine adsorbed (q_e) were calculated from Eq. 1 (SM Table 2). Kinetics of naproxen sorption was evaluated using the nonlinear forms of the pseudo-first-order (PFO) (SM Table 2 Eq. 2), pseudo-second-order (PSO) [33] (SM Table 2 Eq. 3), and the intra-particle diffusion (IPD) [34] (SM Table 2 Eq. 4) models. The Langmuir (SM Table 2 Eq. 5), Freundlich (SM Table 2 Eq. 6), and the Sips non-linear adsorption isotherm (SM Table 2 Eq. 7) models were fitted to the equilibrium adsorption data and used to describe the naproxen uptake process. The dimensionless equilibrium constant K^0 (L/g) was calculated from Eq. 8 (SM Table 2), while the thermodynamic parameters were determined from Eq. 9 and 10 (SM Table 2) using equilibrium adsorption data at 293.15, 303.15, and 313.15 K. The model fittings and models' parameters were obtained using the OriginPro 2015 software (OriginLab Corporation, USA). All equations and parameters are shown in SM Table 2.

3. Results and discussions

3.1. Characterization of adsorbents

The characterization results of the starting materials adsorbents and composites are presented in Figs. 1 and 2 and SM Table 1. The pHpzc was first determined because an adsorbent's pHpzc is an important property that determines its surface charge state at varying solution pH (SM Fig. 1). The surface charge density is positive below the pHpzc, thus, the adsorbent attract negatively charged ions, while above the pHpzc, the charge is negative and the surface attracts positive ions. The pHpzc (SM Table 1) of the BC was quite alkaline (pHpzc of 10.0) unlike those of the MNP and FLC which were near neutral and slightly acidic, respectively. The MBC composites exhibited similarly high pHpzc values (mean value of 9.3) as the BC, and this suggests that the BC component of the composite has a particularly strong effect on its property. The alkaline pHpzc values are in agreement with reported values for other biochar composites [30,35]. Evaluation of the cation exchange capacity (CEC) values (SM Table 1) of the composites indicated average percentage decreases of ≈48 and 16 %, respectively, in comparison to the BC and MNP values, but these values were significantly higher than the FLC value. The BET specific surface area values (SM Table 1 and Fig. 1d) of the composites were not substantially different from the BC values but significantly lower than that of the MNP, thus highlighting the dominant contribution of the BC in the composite.

The FTIR spectra (Fig. 1b) scanned between 4000 and 500 cm^{-1} for the precursor adsorbents and the composites showed that the major functional groups associated with the precursor adsorbents were transferred to the composites. For instance, the FLC and BC peaks around 1035 cm^{-1} attributed to Si-O in-plane bending vibrations, as well as the FLC peaks at 730 and 525 cm^{-1} ascribed to Si-O-Si bridging bonds in SiO_2 and Al-OH/Al-O deformations, respectively [30], were observed in the composites although with slight shifts. The signature Fe_3O_4 MNP Fe-O peak at ≈560 cm^{-1} was also noticeably transferred to the composites; indicating the presence of magnetic property in the composites [36]. The composites' peaks between 1585 and 1420 cm^{-1} are characteristic of C=O, C=C aromatic stretching rings, and amide-I groups, while those at ≈3200 cm^{-1} for all adsorbents were attributed to –OH groups possibly from water [34,37,38].

Evaluation of the crystallinity using the XRD (Fig. 1c) expressed the presence of the signature FLC peaks ascribed to microcline, quartz, and feldspar minerals at 2θ of 22.0, 26.6, 27.9°, respectively, as well as the partial triclinic feldspar mineral peak at 30.7°. Typical Fe_3O_4 spinal structures were present at 2θ of 30.3, 35.5, 43.1, 57.1, and 62.7. Similar to the FTIR spectra, these unique XRD peaks of the FLC and MNP were transferred to the composites, an indication that there were no significant lattice changes in the primary components of the composites [28,30]. The morphological structure of these adsorbents observed *via* the SEM (Fig. 2a–f) showed that the composites (Fig. 2e-f) were truly a combination of materials by exhibiting the honey comb porous nature of the BC (Fig. 2b) as well as the spinal MNP (Fig. 2d), thus, confirming a successful composite preparation.

Preliminary naproxen sorption experiments, conducted to evaluate

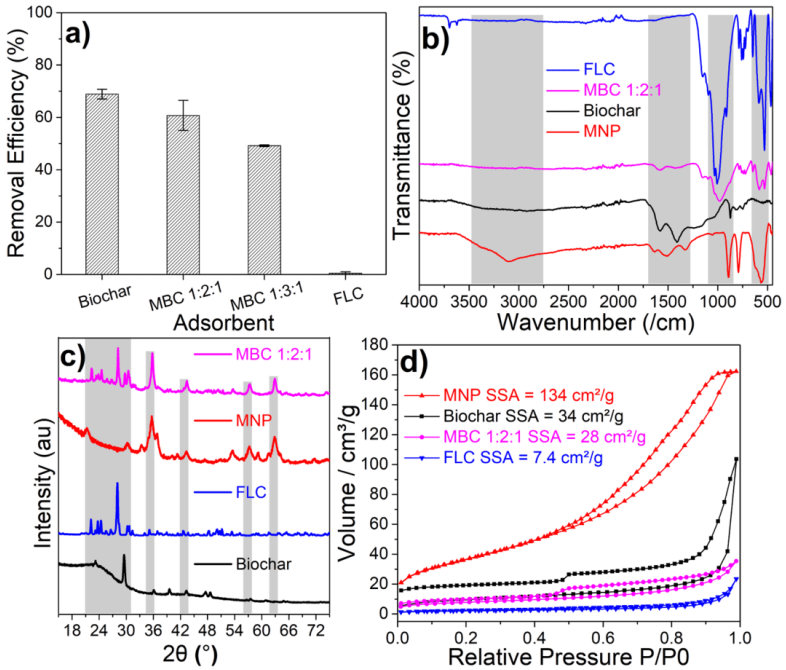

Fig. 1. (a) Preliminary experiment showing naproxen removal efficiencies of the starting materials and composite; (b) comparative FT-IR spectra peaks of the starting materials and composite; (c) XRD diffractograms of the starting materials and composite; and (d) nitrogen adsorption/desorption isotherms (showing the BET specific surface areas).

and compare the sorption potentials of the starting materials and composites showed highest removal efficiency in the BC with 68.8 % removal, followed by MBC 1:2:1 and MBC 1:3:1 with 60.7 % and 49.1 %, respectively (Fig. 1*a*). FLC exhibited very low removal efficiency (<0.5 %). Due to the lack of magnetic properties in the BC, the MBC 1:2:1 was selected as the best performing adsorbent to be used for determining the optimized sorption parameters. Further preliminary sorption tests using two inorganic contaminants (Cu(II) and Pb(II)) and another organic contaminant (terbuthylazine) (SM Fig. 2) showed that the MBC 1:2:1 composite exhibited the highest removal efficiency compared to other adsorbents with ≈95.7, 99.7, and 76.6 % for Cu(II), Pb(II), and terbuthylazine, respectively.

3.2. Mass optimization, sorption kinetics, and effect of pH

The adsorbent dosage directly impacts the amount of contaminant adsorbed due to changing availability and access to adsorption sites as more or less particles interact with the contaminants in solution [39]. Thus, the composite's adsorbent dosage optimization was carried out in a mass range of 5-40 mg in 10 mL (0.5-4 g/L) of 1 mg/L naproxen solution at 1440 min incubation (Fig. 3a). It was observed that with increasing adsorbent dose, the amount of naproxen adsorbed was decreased from 1.71 mg/g to 0.20 mg/g. The removal efficiency also exhibited similar trend, gradually decreasing from 90 % to 85 % with increase in mass. This diminution in the percentage naproxen adsorbed at higher adsorbent loading may be ascribed to an increased aggregation of the adsorbents which resulted in the subsequent unavailability of adsorption sites and reduced adsorption [16]. Based on the obtained data, 5 mg (0.5 g/L) of the adsorbent was selected as the optimum mass for naproxen adsorption.

The sorption rate trend of naproxen on the MBC 1:2:1 composite was carried out using 5 mg adsorbent in 10 mL of 2.5 mg/L naproxen solution. The results, depicted in SM Fig. 4a, showed a fast naproxen uptake from the composite in the first 180 min, which corresponds to naproxen uptake on the richly available vacant adsorption sites as well as its diffusion from the solution phase to the pores at the beginning of the process [22]. Thereafter, the adsorption process was gradual until equilibrium which was reached at about 720 min. The uptake process here was mainly characterized by the slow diffusion of naproxen into the micropores [40,41]. Subsequent experiments were carried out over 1440 min because at this time, a stable equilibrium was well established.

Three adsorption kinetics models (PFO, PSO, and IPD) were employed in evaluating the naproxen uptake process and their fitting curves and estimated models' parameters are presented in SM Fig. 4a and Table 1, respectively. The PSO model exhibited a higher correlation coefficient (r^2) and smaller chi-square (χ^2) values, with better correlated calculated q_e value than the PFO model. These values imply that the PSO model fit better to the rate data and indicate that the adsorption process was mainly controlled by sharing or exchange of valence electrons which resulted in attractive interactions including electrostatic and hydrophobic interactions between the adsorbent surfaces and the naproxen species [21,42]. In addition, an evaluation of the IPD model C (mg/g) parameter, which is a measure of the estimated surface concentration of the contaminant, indicated that less than 15 % of total adsorption occurred on the composite's surface; the bulk of the naproxen uptake were within the pores [43,44]. The multi-linear IPD plot (SM Fig. 4a) indicates that more than one stage is involved in naproxen adsorption: surface adsorption, and within the pores of the composite.

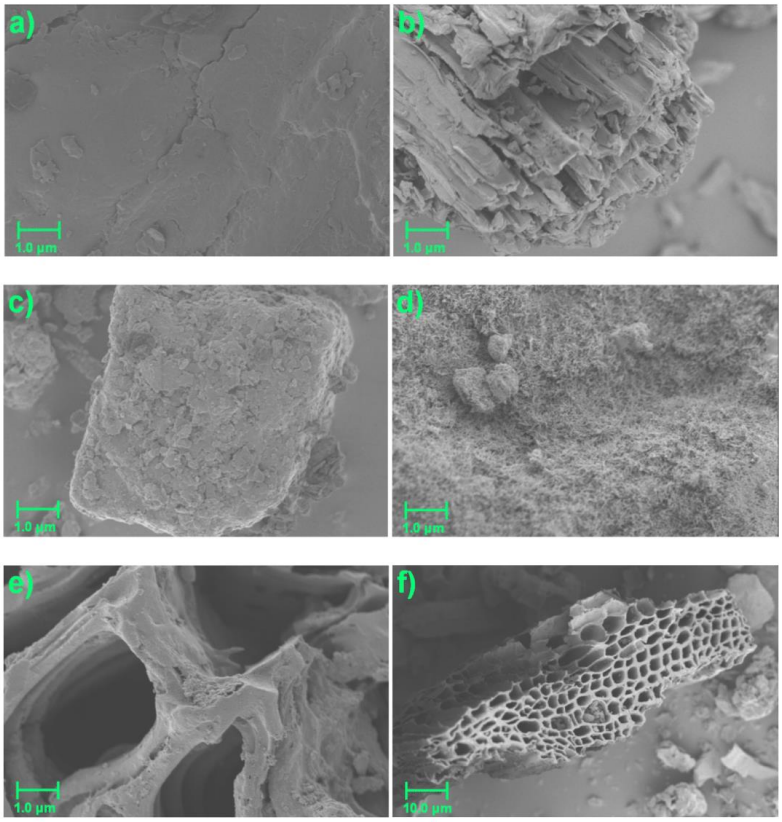

Fig. 2. SEM electron micrographs of (a) biomass; (b) biochar; (c) feldspar; (d) magnetic nanoparticles; (e) MBC 1:2:1; and (f) MBC 1:3:1.

Table 1
Kinetic model parameters for naproxen adsorption on MBC 1:2:1.

Kinetic model	Parameter	Naproxen MBC 1:2:1
PFO	q_e (mg g^{-1})	2.427
	k_1 (min^{-1})	0.008
	r^2	0.87
	χ^2	0.11
PSO	q_e (mg g^{-1})	2.768
	k_2 (g mg^{-1} min^{-1})	0.004
	r^2	0.93
	χ^2	0.058
IPD	C (mg g^{-1})	0.433
	k_i (g g^{-1} min$^{1/2}$)	0.073
	r^2	0.948
	χ^2	0.043
Experimental	mg/g	2.889

Naproxen is at first adsorbed through surface functional groups until saturation, and then diffused in the composite's porous sites [3].

Solution pH is recognized as a major interfering factor in contaminants uptake because it affects the degree of speciation of the contaminant as well as the adsorbent sites charge [35]. Hence, taking into account the physico-chemical properties of the naproxen molecule (SM Table-3), the effect of solution pH on the naproxen uptake by the MBC 1:2:1 composite was tested over five different solution pH (2.5, 4.5, 6.5, 8, and 10), and the adsorption trend is depicted in Fig. 3b. Naproxen has a dissociation constant (*pKa*) of 4.2 [45], and may be anionic or neutral depending on the deprotonation (H^+) of the carboxylic group [46]. Thus, at low solution pH, the neutral form predominates due to negligible deprotonation of the carboxylic group of the naproxen molecule, and uptake process is *via* hydrophobic interaction between the composite surface and aromatic rings of naproxen molecule, as well as through hydrogen bonds between the carboxylic group and composite's functional groups [46]; this is the reason for the higher uptake recorded at lower pH values. At pH 4.5, the adsorption is mainly *via* electrostatic interaction between the positively charged composite surface and anionic naproxen (pHpzc = 9.2) [17,20]. However, as pH increases, the composite's surface becomes progressively deprotonated and less positive, naproxen becomes increasingly anionic resulting in increased water solubility, weaker and fewer electrostatic interactions (electrostatic repulsion), and lower naproxen uptake. It is assumed that the naproxen uptake did not reduce to zero due to uptake or trapping of the naproxen molecules within the composite's pores.

3.3. Equilibrium adsorption at varying temperatures and adsorption isotherm modeling

Equilibrium adsorption of naproxen on MBC 1:2:1 composite at varying concentrations (1–20 mg/L), and temperatures (20, 30, and 40

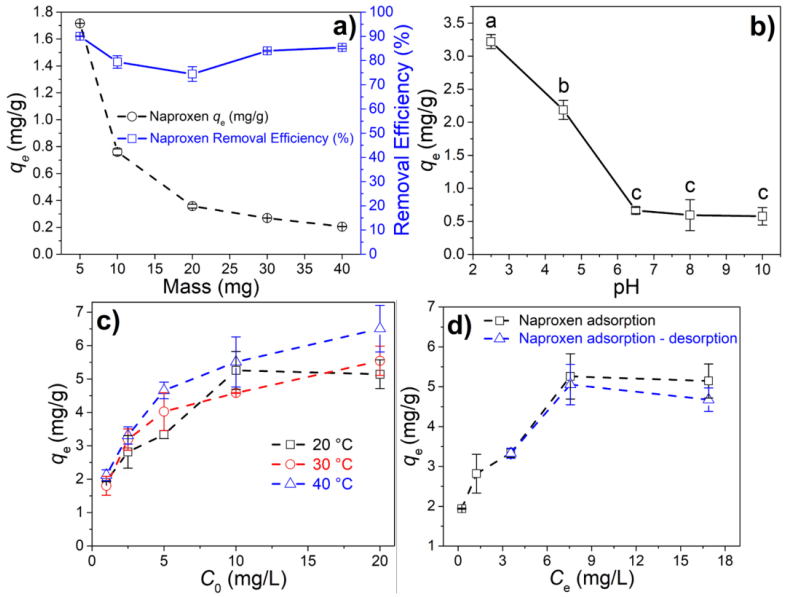

Fig. 3. (a) Adsorption trend and removal efficiency at varying MBC 1:2:1 dosage; (b) adsorption trend at varying naproxen solution pH; (c) effect of concentration and temperature on naproxen uptake; and (d) naproxen desorption at 20 °C.

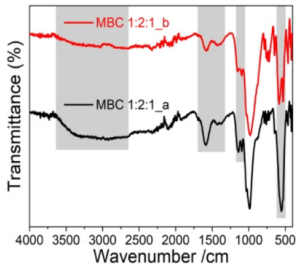

Fig. 4. Comparison of pre-adsorption (before adsorption process, MBC 1:2:1_b) and post-adsorption (after adsorption process, MBC 1:2:1_a) FTIR spectra.

°C), was studied and the trends in mg/g and percentages are given in Fig. 3c and SM Fig. 3, respectively. The trends showed increasing amounts of naproxen sorption as the concentration increased until equilibrium was attained at 10 mg/L concentration (Fig. 3c). Similar trends have been reported in the literature [16,46]. This increased uptake at higher concentration may be attributed to two sorption phenomena: multi-layer adsorption resulting from by π-π interactions and the behavior of naproxen molecules as concentration increased [27,31]. On one hand, due to the presence of electron-deficient π-bonds on the benzene ring structures of the naproxen molecule, it is possible for π-π interaction to occur between adsorbed naproxen and another naproxen molecule in solution leading to multi-layer adsorption at higher concentrations [31]. In addition, at higher concentrations, the potential for the transfer of naproxen molecules from the saturated composite's external surfaces to the inner pore surfaces becomes higher leading to the observed enhanced adsorption [27]. Evaluating the equilibrium data in terms of efficiency of naproxen uptake showed a decreasing efficiency trend as concentration increased (SM Fig. 3), and this may be ascribed to the limited active adsorption sites at fixed composite mass, thus, relative to the increasing concentration of naproxen, the efficiency will be progressively lower.

Evaluating the effect of ambient temperature on naproxen uptake showed a slightly increased uptake with higher temperature (Fig. 3c). Similar trend has been reported by other authors studying biochar based adsorbents [46,47], and this trend was attributed to the energy input into the system at higher temperature which was helpful in breaking the repulsive force (activation energy) hindering naproxen adsorption. The increase in adsorption at higher temperatures might be due to the increment of naproxen mobility (which enhances further migration into the adsorbent pores), as a result of breaking hydrogen bonds (water – COOH), and solute hydrophobicity (which may favor the hydrophobic interactions between naproxen and the composite) [46]. In addition, at high temperatures, the porosity and pore volume may have been increased, thus improving naproxen uptake [16]. This naproxen uptake trend suggested that the process was endothermic, thus the data was evaluated to obtain the thermodynamic variables (Table 2) and describe the process appropriately. The positive ΔH confirmed that the process was endothermic, thus an increase in temperature would result in an increase in naproxen uptake. The negative ΔG and its increasing magnitude with temperature indicate that the adsorption process is spontaneous and becomes more favorable at high temperatures, while the ΔS (> 0) suggested an increased randomness (mobility) of the naproxen molecules on the composite's external surface at equilibrium [18].

Further evaluation of the naproxen equilibrium adsorption data were obtained by fitting three adsorption isotherm models (Langmuir, Freundlich, and Sips) to the data as depicted in SM Fig. 4b-d with the model parameters shown in Table 2. Analysis of the fitting parameters, r^2 and χ^2, showed that the Sips model described the equilibrium data better than the Freundlich and Langmuir models. This suggests that naproxen uptake process comprised of complex interactions occurring

Table 2
Naproxen adsorption isotherm model parameters and calculated thermodynamics parameters for naproxen uptake.

Adsorption isotherm model	Parameter	293.15 K 20 °C	303.15 K 30 °C	313.15 K 40 °C
Langmuir	Q_o (mg/g)	5.241	5.309	6.185
	β	1.135	1.396	1.524
	r^2	0.721	0.93	0.812
	χ^2	0.594	0.14	0.567
Freundlich	$1/n$	0.245	0.236	0.233
	K_F	2.734	2.88	3.444
	r^2	0.866	0.95	0.99
	χ^2	0.285	0.099	0.03
Sips	q_{max} (mg/g)	6.726	6.148	8.516
	$1/n$	0.305	0.35	0.265
	K_S (L/mg)	0.053	0.131	0.034
	r^2	0.82	0.951	0.991
	χ^2	0.381	0.098	0.025
Thermodynamics	ΔG° (kJ/mol)	-17.14	-18.25	-19.08
	ΔH°(kJ/mol)	11.29	11.29	11.29
	ΔS° (J/mol/K)	97.1	97.1	97.1

on heterogeneous composite surfaces of unequal affinity for the naproxen molecule in solution [27]. Some of these interactions have been suggested above and include electrostatic interactions, π-π interactions leading to multi-layer adsorption, as well as possible hydrogen bonding, and pore filling or entrapment within the composite pores.

3.4. Adsorption mechanisms

Considering the FTIR spectra results, the composite properties, speciation of naproxen, and adsorption trends, possible mechanisms of naproxen adsorption onto the composite were proposed (Fig. 5). An examination of the naproxen post-adsorption effect (after adsorption process) on the FTIR spectra (Fig. 4) showed that the broad peak around 3200 /cm which was attributed to the –OH groups exhibited the highest change in intensity after the adsorption process (region 3600 – 2600 /cm), indicating that the –OH groups of the composite were the main contributors to the naproxen adsorption process *via* electrostatic interactions and H-bonding; the composite's adsorption site acts as the H-donor while the deprotonated naproxen molecules is the H-acceptor. Similar FTIR trend has been reported [3] for naproxen adsorption on biochar. Taking into account that the adsorption conditions were at solution pH 4.5 and the composite's pHpzc of 9.2, these interactions occur due to the positive charge of the composite and the negatively charged naproxen ions. Furthermore, the FTIR spectra showed that the aromatic stretching vibrations corresponding to the C=O and C=C groups (peaks between 1585 and 1420 /cm) showed higher intensities. This response of the C=C bond indicates the presence of π-π interactions between the benzene rings of naproxen with the graphitic planes of the carbonaceous structure of the composite [48]. On the other hand, that of C=O groups, suggests n-π interactions between the oxygen electron pairs (n-electron donors) of hydroxyl groups of naproxen with composite's electron-depleted sites [3,40]. Another peak that showed enhanced vibration after the adsorption was the magnetic Fe–O (≈ 560 /cm), indicating an interaction of $–COO^-$ of naproxen molecules with Fe–OH impregnated on the MBC 1:2:1 composite surface [28]. Also, the desorption of adsorbed naproxen on MBC 1:2:1 composite at 20 °C using the same background electrolyte/biocide solution (Fig. 3d) showed a low desorption especially at low naproxen adsorption concentrations (<3 mg/L). This data suggests a high entrapment of naproxen on the pores of the composite, thus, supporting and confirming the IPD model *C* (mg/g) parameter, which showed that the bulk of the naproxen uptake process occurred within the composite's pores.

3.5. Competitive sorption of naproxen and carbamazepine and effect of dissolved organic matter

The effect of solution pH on naproxen and carbamazepine uptake from single and binary solutions was tested under the same conditions (as described in section 3.2), and the adsorption trends are given in Fig. 6*a*. Carbamazepine has two dissociation constants (*pKa*) values of 2.3 (ketone group) and 13.9 for the $–CONH_2$ (amine) group [49]. Thus, at all tested solution pH values, it existed as neutral compound. Under these conditions, carbamazepine adsorption onto the composite mostly involved hydrophobic, π–π interactions and hydrogen bonding [50]. In addition, the post FTIR spectra of composite after single carbamazepine sorption, showed same region response as post-naproxen-sorption spectra, indicating that same sites were responsible for their adsorption (SM Fig. 5). Due to the positive charge of the composite (pH <pHpzc), cation-π interactions may occur with the π-system (benzene ring) of carbamazepine [51]. From the adsorption trends in the binary system, it was observed that at the solution pH <4.5, both compounds had high sorption though naproxen sorption was higher. This sorption trend could result from strong hydrophobic interactions and the highly porous and heterogeneous nature of the composite [3]. Interestingly, with increasing solution pH the sorption of carbamazepine surpasses that of naproxen both in single and binary solution though the amounts

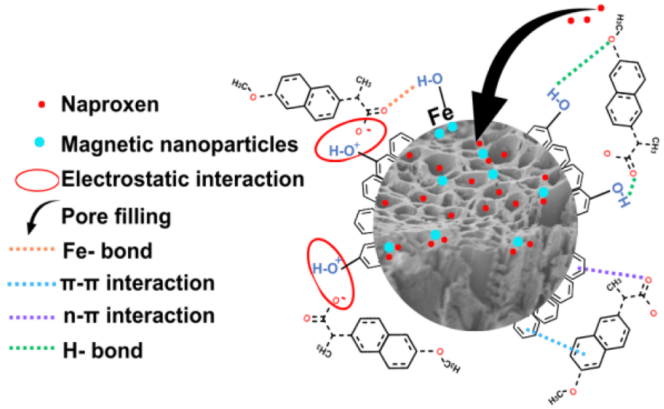

Fig. 5. Proposed adsorption mechanisms of naproxen onto MBC 1:2:1 composite in a SEM electron micrograph (magnification: 10 μm).

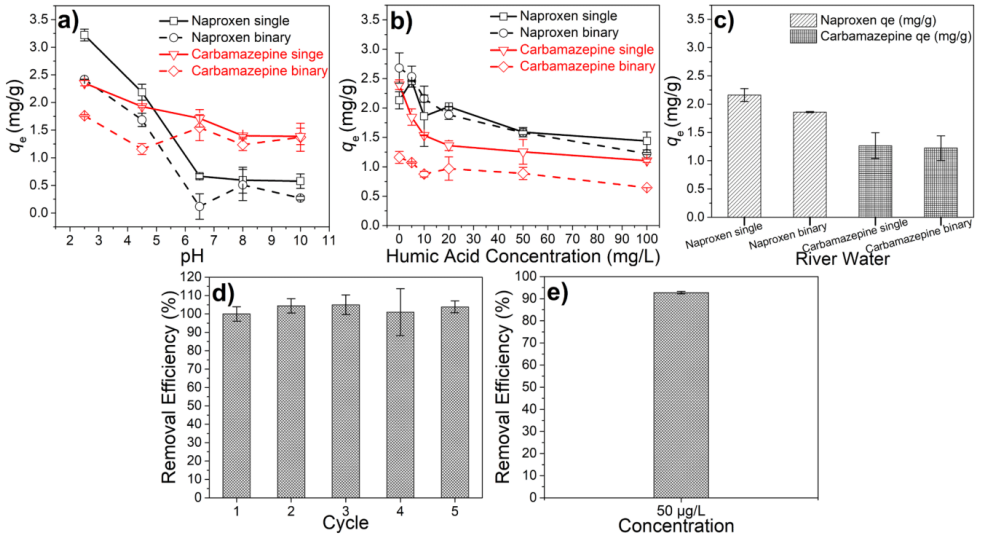

Fig. 6. (a) Competitive adsorption of naproxen and carbamazepine, (b) effect of dissolved organic matter on naproxen and carbamazepine sorption, and (c) adsorption of naproxen and carbamazepine in river water; (d) comparative reusability of naproxen over 5-cycles, and (e) removal efficiency with Ishmi river water at 50 µg/L *naproxen concentration.*

adsorbed were lower than at low pH. This trend suggests strong competition between naproxen and carbamazepine at lower pH but at the higher pH range the competition was weak and carbamazepine sorption exceeded naproxen.

The presence of DOM in wastewater effluents directly impacts and is considered as the main limiting factor in organic compounds sorption [52]. Therefore, the effect of DOM on naproxen and carbamazepine sorption onto the composite was tested over five different humic acid concentrations (5-100 mg/L), while the concentrations of naproxen and carbamazepine remained fixed at 2.5 mg/L. The sorption trends depicted in Fig. 6*b* showed that at very low DOM concentration (5 mg/L), the uptake of naproxen in single solution slightly improved from 2.13 to 2.46 mg/g. After this, a gradual naproxen sorption decrease was observed, reaching 1.44 mg/g at 100 mg/L DOM concentration. Similarly, in binary system, naproxen showed a similar decreasing trend. This trend may be related to the discussion above; the pHpzc of the composite had a value of 9.2, and at solution pH of 4.5, the composite net charge is positive and naproxen exists as a deprotonated molecule, indicating a significant electrostatic interaction. Also at the same pH conditions (pH 4.5), humic acid substances are negatively charged, thus as humic acid adsorb onto the composite surface, the adsorption of naproxen (mainly negatively charged) would decrease due to repulsion forces [53]. Carbamazepine in the single system showed an immediate decrease in sorption with increasing humic acid concentration from 5-20 mg/L, with initial decrease of 1.84 and 1.36 mg/g, respectively. After this, a slight decrease was observed, reaching 1.1 mg/g at 100 mg/L humic acid concentration. The relatively high presence of oxygen containing functional groups such as –COOH, –OH, and C=O in humic acid, could result in complex formation with biochar and probably with carbamazepine, indicating a high competition between these groups and carbamazepine for the composite's active adsorption sites and hydrophobic interactions, thus decreasing the amount of adsorbed carbamazepine on the composite [54,55]. Meanwhile, carbamazepine sorption in binary system (with naproxen) was lower compared to that of single system, indicating a higher competition. The composite sorption potential for naproxen and carbamazepine at 2.5 mg/L concentrations, 5 mg mass, and solution pH of 4.5 in single and binary systems was tested in river water, and the results are given in Fig. 6*c*. The composite showed similar sorption capacities as 20 mg/L DOM concentration (total organic carbon of river water = 25.7 mg/L), with 2.16 and 1.85 mg/g for single and binary systems for naproxen, and 1.26 and 1.22 mg/g for single and binary systems for carbamazepine, respectively.

3.6. Reusability

The reusability of the MBC 1:2:1 was investigated in five adsorption cycles and the results are presented in Fig. 6*d*. In addition, the naproxen uptake by the composite using environmentally relevant concentration was also tested with Ishmi river (Albania) water (spiked with 50 µg/L) and the results are given in Fig. 6e. The removal efficiency for naproxen in the first cycle was adjudged to be 100 %. After that, during the four subsequent cycles, the removal efficiency remained around ≈100 % (compared to the first cycle), thus, no significant difference was observed. Interestingly, the results with Ishmi river water, using environmentally relevant naproxen concentration showed a removal efficiency of ≈92.8 %. Therefore, these results confirm that MBC 1:2:1 composite is potentially applicable and useful for naproxen and carbamazepine removal from water.

4. Conclusions

The adsorption of the pharmaceutical compound- naproxen was investigated onto a ternary magneto-biochar-clay composite (MBC 1:2:1), made from a combination of grape cluster biomass, feldspar clay, and Fe_3O_4. Characterization data indicated that the composite physicochemical properties such as pHpzc, CEC, BET surface area, morphology, and the functional groups presence were mainly impacted by biochar presence. Naproxen adsorption process was endothermic, and better described by Sips adsorption isotherm model. Adsorptive pore filling, electrostatic and hydrophobic interactions between the composite surfaces and the naproxen species were the main mechanisms of naproxen

uptake. The composite exhibited very good removal efficiency after five consecutive adsorption cycles as well as in real environmental water (river water) containing low naproxen concentration. Therefore, the prepared composite is sustainable, cost-efficient, and potentially applicable for naproxen removal from natural waters.

Competing interests

The authors have no relevant financial or non-financial interests to disclose.

Funding

This research did not receive any specific grant from funding agencies in the public, commercial, or not-for-profit sectors.

CRediT authorship contribution statement

Aleksandër Peqini: Writing – review & editing, Writing – original draft, Visualization, Validation, Software, Methodology, Investigation, Formal analysis, Conceptualization. **Paul N. Diagboya:** Writing – review & editing, Writing – original draft, Validation, Software, Project administration, Methodology, Formal analysis. **Ferdi Brahushi:** Writing – review & editing, Supervision, Project administration, Methodology, Funding acquisition, Conceptualization. **Rolf-Alexander Düring:** Writing – review & editing, Supervision, Resources, Project administration, Methodology, Funding acquisition, Conceptualization.

Declaration of competing interest

The authors declare that they have no known competing financial interests or personal relationships that could have appeared to influence the work reported in this paper.

Acknowledgements

We acknowledge the support of Deutsche Bundesstiftung Umwelt (DBU), Germany and the Erasmus+ program, for the support of the research fellowships to A Peqini, and the support of the Alexander von Humboldt Foundation, Germany, for the award of Georg Forster experienced research fellowship to PN Diagboya. Also, we acknowledge the support of the Department of Chemistry at JLU Giessen for technical assistance with the composite characterization.

Supplementary materials

Supplementary material associated with this article can be found, in the online version, at doi:10.1016/j.ceja.2025.100784.

Data availability

Data will be made available on request.

References

[1] J.L. Wilkinson, et al., Pharmaceutical pollution of the world's rivers, Proc. Natl. Acad. Sci. U S A (8) (2022) 119.
[2] K. Kümmerer, The presence of pharmaceuticals in the environment due to human use–present knowledge and future challenges, J. Environ. Manage. 90 (8) (2009) 2354–2366.
[3] O. Paunovic, et al., Ionisable emerging pharmaceutical adsorption onto microwave functionalised biochar derived from novel lignocellulosic waste biomass, J. Colloid Interface Sci. 547 (2019) 350–360.
[4] B.F. Da Silva, et al., Occurrence and distribution of pharmaceuticals in surface water, suspended solids and sediments of the Ebro river basin, Spain, Chemosphere 85 (8) (2011) 1331–1339.
[5] M. Petrovic, et al., Determination of 81 pharmaceutical drugs by high performance liquid chromatography coupled to mass spectrometry with hybrid triple quadrupole-linear ion trap in different types of water in Serbia, Sci. Total Environ. 468-469 (2014) 415–428.
[6] A. Lolic, et al., Assessment of non-steroidal anti-inflammatory and analgesic pharmaceuticals in seawaters of North of Portugal: occurrence and environmental risk, Sci. Total Environ. 508 (2015) 240–250.
[7] M. Papageorgiou, C. Kosma, D. Lambropoulou, Seasonal occurrence, removal, mass loading and environmental risk assessment of 55 pharmaceuticals and personal care products in a municipal wastewater treatment plant in Central Greece, Sci. Total Environ. 543 (Pt A) (2016) 547–569.
[8] T. Ding, et al., Biodegradation of naproxen by freshwater algae Cymbella sp. and Scenedesmus quadricauda and the comparative toxicity, Bioresour. Technol. 238 (2017) 164–173.
[9] D. Wojcieszynska, U. Guzik, Naproxen in the environment: its occurrence, toxicity to nontarget organisms and biodegradation, Appl. Microbiol. Biotechnol. 104 (5) (2020) 1849–1857.
[10] M. Della Greca, et al., Phototransformation and ecotoxicity of the drug Naproxen-Na, Environ. Chem. Lett. 1 (4) (2003) 237–241.
[11] Q. Li, et al., Acute toxicity and histopathological effects of naproxen in zebrafish (Danio rerio) early life stages, Environ. Sci. Pollut. Res. Int 23 (18) (2016) 18832–18841.
[12] D. Gorny, et al., Naproxen ecotoxicity and biodegradation by Bacillus thuringiensis B1(2015b) strain, Ecotoxicol. Environ. Saf 167 (2019) 505–512.
[13] E. Donner, et al., Ecotoxicity of carbamazepine and its UV photolysis transformation products, Sci. Total. Environ. 443 (2013) 870–876.
[14] Z.H. Li, et al., Acute toxicity of carbamazepine to juvenile rainbow trout (Oncorhynchus mykiss): effects on antioxidant responses, hematological parameters and hepatic EROD, Ecotoxicol. Environ. Saf 74 (3) (2011) 319–327.
[15] J. Georgin, et al., Woody residues of the grape production chain as an alternative precursor of high porous activated carbon with remarkable performance for naproxen uptake from water, Environ. Sci. Pollut. Res. Int 29 (12) (2022) 16988–17000.
[16] S. Bhattacharya, et al., Thermal, Chemical and ultrasonic assisted synthesis of carbonized Biochar and its application for reducing Naproxen: Batch and Fixed bed study and subsequent optimization with response surface methodology (RSM) and artificial neural network (ANN), Surf. Interfaces 26 (2021) 101378.
[17] F. Tomul, et al., Peanut shells-derived biochars prepared from different carbonization processes: Comparison of characterization and mechanism of naproxen adsorption in water, Sci. Total Environ. 726 (2020) 137828.
[18] M. Fatih Dilekoglu, M. Yapici, Adsorption of naproxen pharmaceutical micropollutant from aqueous solutions on superior activated carbon synthesized from sheep manure: Kinetics, thermodynamics, and mechanism, J. Mol. Liq. 381 (2023) 121839.
[19] Z. Dashti, et al., Effects of lignin on biochar from pyrolysis: emphasis on removing naproxen as pharmaceutical pollutants in wastewater, Clean Technol. Environ. Policy (2024).
[20] T.D. Pham, et al., Adsorption characteristics of ciprofloxacin and naproxen from aqueous solution using bamboo biochar, Biomass Convers. Biorefinery 15 (2) (2023) 3071–3082.
[21] Z. İlbay, et al., Isolation of naproxen from wastewater using carbon-based magnetic adsorbents, Int. J. Environ. Sci. Technol. 12 (11) (2015) 3541–3550.
[22] Z. Anfar, et al., Microwave assisted green synthesis of Fe2O3/biochar for ultrasonic removal of nonsteroidal antiinflammatory pharmaceuticals, R. Soc. Chem. 10 (2020) 11371–11380.
[23] P.N Diagboya, et al., Clay-carbonaceous material composites: Towards a new class of functional adsorbents for water treatment, Surf. Interfaces 19 (2020) 100506.
[24] M. Arif, et al., Synthesis, characteristics and mechanistic insight into the clays and clay minerals-biochar surface interactions for contaminants removal-A review, J. Clean. Prod. 310 (2021) 127548.
[25] A. Maged, et al., Synergistic mechanisms for the superior sorptive removal of aquatic pollutants via functionalized biochar-clay composite, Bioresour. Technol 387 (2023) 129593.
[26] Y. Yao, et al., Characterization and environmental applications of clay–biochar composites, Chem. Eng. J. 242 (2014) 136–143.
[27] B.I. Olu-Owolabi, et al., Utilizing eco-friendly kaolinite-biochar composite adsorbent for removal of ivermectin in aqueous media, J. Environ. Manage 279 (2021) 111619.
[28] B. Zhang, et al., One-pot synthesis of MnFe2O4 functionalized magnetic biochar by the sol-gel pyrolysis method for diclofenac sodium removal, J. Clean. Prod. 381 (2022) 135210.
[29] P.N. Diagboya, et al., Comparative empirical evaluation of the aqueous adsorptive sequestration potential of low-cost feldspar-biochar composites for ivermectin, Colloids Surf. A: Physicochem. Eng. Asp. (2021) 127930.
[30] P.N. Diagboya, E.D. Dikio, Scavenging of aqueous toxic organic and inorganic cations using novel facile magneto-carbon black-clay composite adsorbent, J. Clean. Prod. 180 (2018) 71–80.
[31] B.I. Olu-Owolabi, et al., Empirical aspects of an emerging agricultural pesticide contaminant retention on two sub-Saharan soils, Gondwana Res. 105 (2022) 311–319.
[32] L.M. Madikizela, L. Chimuka, Synthesis, adsorption and selectivity studies of a polymer imprinted with naproxen, ibuprofen and diclofenac, J. Environ. Chem. Eng. 4 (4) (2016) 4029–4037.
[33] P.N. Diagboya, S.O. Akpotu, E. Osabohien, Ordered mesoporous silica to the rescue: A potential anti-contamination ally for pesticide capture in soil, Colloids Surf. A: Physicochem. Eng. Asp. 715 (2025) 136634.
[34] J. Junck, et al., Mechanistic interpretation of the sorption of terbuthylazine pesticide onto aged microplastics, Environ. Pollut. 345 (2024) 123502.

[35] P.R. Sera, et al., Potential of valourized Moringa oleifera seed waste modified with activated carbon for toxic metals decontamination in conventional water treatment, Bioresour. Technol. Rep. 16 (2022) 100881.
[36] R.P. Mohubedu, et al., Magnetic valorization of biomass and biochar of a typical plant nuisance for toxic metals contaminated water treatment, J. Clean. Prod. 209 (2019) 1016–1024.
[37] F. Güzel, et al., Performance of grape (Vitis vinifera L.) industrial processing solid waste–derived nanoporous carbon in copper(II) removal, Biomass Convers. Biorefinery 11 (4) (2020) 1363–1373.
[38] I. Villaescusa, et al., Removal of copper and nickel ions from aqueous solutions by grape stalks wastes, Water. Res 38 (4) (2004) 992–1002.
[39] S.O. Akpotu, et al., Designer composite of montmorillonite-reduced graphene oxide-PEG polymer for water treatment: enrofloxacin sequestration and cost analysis, Chem. Eng. J. 453 (1) (2023) 139771.
[40] B. Czech, et al., Engineered biochars from organic wastes for the adsorption of diclofenac, naproxen and triclosan from water systems, J. Clean. Prod. 288 (2021) 125686.
[41] E.B. AttahDaniel, et al., Adsorption investigation of a composite of metal-organic framework and polyethylene oxide hydrogel, Proc. Inst. Mech. Eng. N: J. Nanomater. Nanoeng. Nanosyst. (2023), https://doi.org/10.1177/23977914231195748(0), p. 23977914231195748.
[42] X. Feng, et al., Enhanced adsorption of naproxen from aquatic environments by β-cyclodextrin-immobilized reduced graphene oxide, Chem. Eng. J. 412 (2021) 128710.
[43] C.Y. Abasi, P.N.E. Diagboya, E.D. Dikio, Layered double hydroxide of cobalt-zinc-aluminium intercalated with carbonate ion: preparation and Pb(II) ion removal capacity, Int. J. Environ. Stud. 76 (2) (2018) 251–265.
[44] A.N. Ebelegi, et al., Covalently bonded polyamidoamine functionalized silica used as a Pb(II) scavenger from aqueous solution, J. Environ. Chem. Eng. 7 (4) (2019) 103214.
[45] V.M. Vulava, et al., Sorption, photodegradation, and chemical transformation of naproxen and ibuprofen in soils and water, Sci, Total, Environ. 565 (2016) 1063–1070.
[46] H.E. Reynel-Avila, et al., Assessment of naproxen adsorption on bone char in aqueous solutions using batch and fixed-bed processes, J. Mol. Liq. 209 (2015) 187–195.
[47] B.I. Olu-Owolabi, et al., Fractal-like concepts for evaluation of toxic metals adsorption efficiency of feldspar-biomass composites, J. Clean. Prod. 171 (2018) 884–891.
[48] C. Jung, et al., Competitive adsorption of selected non-steroidal anti-inflammatory drugs on activated biochars: Experimental and molecular modeling study, Chem. Eng. J. 264 (2015) 1–9.
[49] D. Shan, et al., Preparation of ultrafine magnetic biochar and activated carbon for pharmaceutical adsorption and subsequent degradation by ball milling, J. Hazard. Mater. 305 (2016) 156–163.
[50] D. Chen, et al., Activated biochar derived from pomelo peel as a high-capacity sorbent for removal of carbamazepine from aqueous solution, RSC Adv. 7 (87) (2017) 54969–54979.
[51] S. Jemutai-Kimosop, et al., Insights on adsorption of carbamazepine onto iron oxide modified diatomaceous earth: Kinetics, isotherms, thermodynamics, and mechanisms, Environ. Res 180 (2020) 108898.
[52] R. Guillossou, et al., Influence of dissolved organic matter on the removal of 12 organic micropollutants from wastewater effluent by powdered activated carbon adsorption, Water, Res 172 (2020) 115487.
[53] Y. Gao, M.A. Deshusses, Adsorption of clofibric acid and ketoprofen onto powdered activated carbon: effect of natural organic matter, Environ. Technol. 33 (15-16) (2011) 1719–1727.
[54] L. Lin, W. Jiang, P. Xu, Comparative study on pharmaceuticals adsorption in reclaimed water desalination concentrate using biochar: Impact of salts and organic matter, Sci, Total, Environ. 601-602 (2017) 857–864.
[55] H. Zhong, et al., Efficient adsorption removal of carbamazepine from water by dual-activator modified hydrochar, Sep. Purif. Technol. 353 (2025).

3.2. Supplementary Material of Publication 2

Supplementary Material

Sustainable removal of aqueous naproxen using a ternary magneto-biochar-clay composite: competition with carbamazepine and influence of dissolved organic matter

Aleksandër Peqini[1, 2*], Paul N. Diagboya[3], Ferdi Brahushi[2], Rolf-Alexander Düring[1]

[1]Institute of Soil Science and Soil Conservation, Research Centre for BioSystems, Land Use and Nutrition (iFZ), Justus Liebig University Giessen, Heinrich-Buff-Ring 26, 35392 Giessen, Germany

[2]Department of Environment and Natural Resources, Faculty of Agriculture and Environment, Agricultural University of Tirana, 1029 Tirana, Albania

[3]Environmental fate of chemicals and remediation (EnFaCRe) laboratory, Department of Environmental Management and Toxicology, University of Delta, Agbor, Nigeria

*Corresponding author.

E-mail: aleksander.peqini@umwelt.uni-giessen.de

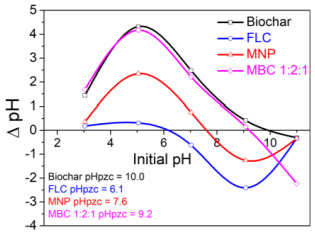

SM Fig. 1 pHpzc of biochar, FLC, MNP, and MBC 1:2:1 composite

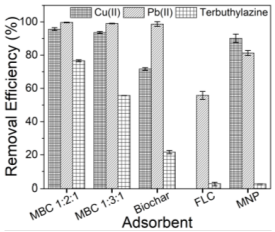

SM Fig. 2 Removal efficiency for Cu(II), Pb(II), and terbuthylazine

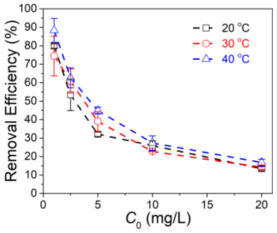

SM Fig. 3 Removal efficiency for naproxen at increasing concentration and temperature on MBC 1:2:1 composite

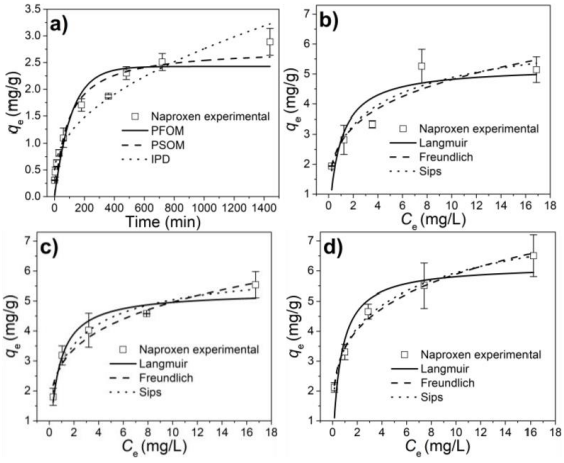

SM Fig. 4 (a) Naproxen adsorption rate trend and kinetics model fittings on the naproxen adsorption rate data; (b) adsorption isotherm models at 20°C, (c) at 30 °C, and (d) at 40 °C

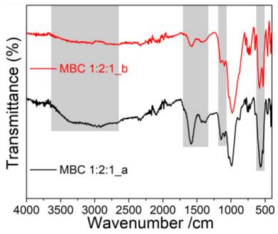

SM Fig. 5 Carbamazepine post-adsorption FTIR spectra of MBC 1:2:1

SM Table 1. Physicochemical characterization of adsorbents

Adsorbent	pHpzc	CEC (cmol/kg)	BET Specific Surface Area (m^2/g)
Biochar	10.0	50.1	34
MNP	7.6	34	134
FLC	6.1	5.3	7.4
MBC 1:2:1	9.2	28.4	28
MBC 1:3:1	9.4	23.2	32

SM Table 2. Data treatment equations

Equation	Description	Parameters	Equation number
$q_e = (C_O - C_e)v/m$	Amount of analyte adsorbed (mg/g)	m, v, q_e, C_o, C_e, are the composite mass (g), volume of analyte solution (L), equilibrium amount of analyte adsorbed (mg/g), initial and final analyte concentrations (mg/L), respectively	1
$q_t = q_e(1 - e^{-k_1 t})$	Pseudo-First Order (PFO) kinetics model [1]	t, q_t, and k_1 are time (min), naproxen adsorbed at time- t (mg/g), and PFO model rate constant, respectively	2
$q_t = \frac{q_e^2 k_2 t}{1 + q_e k_2 t}$	Pseudo-Second Order (PSO) kinetics model	k_2 is the PSO model rate constant	3
$q_e = k_{IPD} t^{1/2} + C$	Weber-Morris intraparticle diffusion (IPD)	k_{IPD} and C are the IPD model rate constant, and the amount of surface adsorbed naproxen (mg/g), respectively	4
$q_e = \frac{Q_O b C_e}{1 + b C_e}$	Langmuir adsorption isotherm model [2]	Q_o (mg/g) and b (L/mg) are the maximum adsorption capacity per gram (mg/g) and energy-related parameter (L/mg), respectively	5
$q_e = k_f C_e^n$	Freundlich adsorption isotherm model [3]	k_f (L/g) and n are Freundlich model constant and the Freundlich linearity parameter (dimensionless), respectively	6
$q_e = \frac{Q_o (K_S C_e)^n}{1 + (K_S C_e)^n}$	Sip's adsorption isotherm model	K_S (L/mg) and n are Sip's model constant and the Sip's exponent, respectively	7
$K^0 = K_L * 1000$	Dimensionless equilibrium constant	K_L is Langmuir constant	8
$LnK^0 = \frac{\Delta S^o}{R} - \frac{\Delta H^o}{RT}$	Thermodynamic parameters	ΔS^o, ΔH^o, T, and R are entropy change (J/mol/K), enthalpy change (kJ/mol), Temperature (K), and ideal gas constant (J/K/mol), respectively	9
$\Delta G^o = -RTLnK^0$	Van't Hoff equilibrium	ΔG^o is the Gibb's free energy (kJ/mol)	10

*All similar parameters are defined only once

SM Table 3. Physico-chemical properties of naproxen

Compound (formula)/CAS number	Molecular Structure	Molecular Weight (g/mol)	Log K_{ow}	Log D_{ow}	pK_a
Naproxen ($C_{14}H_{14}O_3$)/22204-53-1	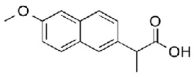	230.27	3.2*	1.7*	4.2

Source: [4], *At pH = 7

3

References

1. Junck, J., et al., *Mechanistic interpretation of the sorption of terbuthylazine pesticide onto aged microplastics.* Environmental Pollution, 2024. **345**: p. 123502.
2. Langmuir, I., *The constitution and fundamental properties of solids and liquids.* J. Amer. Chem. Soc., 1916. **38**: p. 2221–2295.
3. Freundlich, H.M.F., *Über die adsorption in lösungen.* Zeitschrift für Physikalische Chemie, 1906. **57A**: p. 57A, 385-470.
4. Vulava, V.M., et al., *Sorption, photodegradation, and chemical transformation of naproxen and ibuprofen in soils and water.* Sci Total Environ, 2016. **565**: p. 1063-1070.

4. Publication 3: Enhancing Biosorbent Stability, Performance Efficiency, and Cost-effectiveness: A Ternary Magnetic Composite for Sequestration of Multiple Toxic Metals from Water

Published in *Langmuir Journal* as: “Enhancing Biosorbent Stability, Performance Efficiency, and Cost-effectiveness: A Ternary Magnetic Composite for Sequestration of Multiple Toxic Metals from Water”

DOI: 10.1021/acs.langmuir.5c01248

Main Text of Publication 3 from page 92

Supplementary Information of Publication 3 from page 101

4.1. Main Text of Publication 3

LANGMUIR

Open Access

pubs.acs.org/Langmuir Article

Enhancing Biosorbent Stability, Performance Efficiency, and Cost-effectiveness: A Ternary Magnetic Composite for Sequestration of Multiple Toxic Metals from Water

Aleksandër Peqini,* Paul N. Diagboya, Seit Shallari, Ferdi Brahushi, and Rolf-Alexander Düring

Cite This: *Langmuir* 2025, 41, 15022−15030 Read Online

ACCESS | Metrics & More | Article Recommendations | Supporting Information

ABSTRACT: Innovative low-cost magneto-biochar-clay (MBC 1:2:1 and MBC 1:3:1) composite adsorbents formed by a one-step combination of magnetic nanoparticles (MNP), biochar (from grape cluster stalk), and feldspar clay were employed for Cd(II), Cr(VI), and Cu(II) removal from simulated contaminated aqueous solution. The composites expressed higher cation exchange capacity and BET surface area compared to the feldspar clay, as well as characteristic biobased functional groups such as hydroxyls, carboxyls, and amides. The optimum removal efficiency was achieved at a 0.66 g/L solid-to-liquid ratio, and the equilibrium was attained at 720 min for all three ions. The adsorption process was via electrostatic interactions as well as adsorption within the pores (>90% of total adsorption). Surface functional groups involved in the adsorption process are −OH, $-COO^-$, and −C−N. An increase of Cu(II) concentration in solution enhanced Cr(VI) removal efficiency by 86 and 79% on MBC 1:2:1 and MBC 1:3:1, respectively, while reducing Cd(II) uptake by 65 and 52%, respectively. The equilibrium data was described by the Langmuir and Langmuir−Freundlich adsorption isotherm models. Higher temperature slightly enhanced Cd(II) adsorption, while no temperature impact was observed for Cr(VI) and Cu(II) adsorption. The adsorbent reusability study confirmed that the removal efficiency for Cr(VI) remained high after five cycles, while for Cd(II) and Cu(II) only during the first adsorption cycle. Thus, the MBC composite is a cost-effective and efficient adsorbent and, due to its magnetic properties, can easily be applied as a water treatment adsorbent for Cr(VI) removal from water.

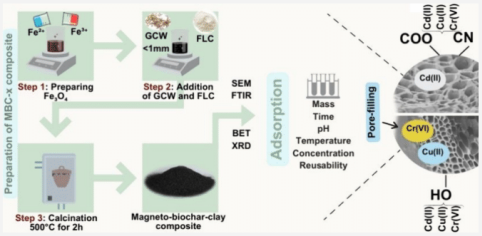

1. INTRODUCTION

In 2022, the World Health Organization reported that 3.5 billion people lack access to clean water, while 2.2 billion of these do not have access to clean potable water.[1] Environmental pollutants, especially in water, are introduced via various anthropogenic activities, including agricultural, industrial, domestic, and other personal activities.[2−5] A widely detected group of pollutants in the aqueous environment includes toxic metals. Toxic metals include Pb(II), Hg(II), Cd(II), As(III), Cr(VI), and Cu(II), and they are known to pose serious health risks to humans and other biota. For instance, Cd(II) is reported to be toxic to the kidney, cause bone demineralization, and may impair lung function and increase the risk of lung cancer, while Cr(VI) causes lung and skin cancer, and is neurotoxic.[6,7] Cu(II) is an essential element for biota but in excess amounts has been linked to the generation of highly reactive oxidative hydroxyl radicals, which damages the cells and DNA.[8] Hence, it is vital to eliminate these toxic metals from water.

Several wastewater treatment techniques abound for contaminant removal from water, including chemical oxidation, precipitation, adsorption, biological techniques, and their combinations. Among these techniques, the simple, cost-efficient, environmentally friendly, and easy-to-handle adsorption is the most sought-after.[9,10] There are several kinds of adsorbents such as synthetic nano- and mesoporous materials,[11,12] clays,[13,14] and biomass-based adsorbents.[15,16] With appropriate treatment (e.g., calcination, pyrolysis) of this side-stream biomass and the availability of low-cost materials like clays, the adsorption technique is very promising. Application of low-cost agricultural biomass in this manner improves environmental aesthetics and reduces their adverse environmental effects, such as greenhouse gas emissions, leaching to soil and ground/surface water, potential fire sources, etc. Irrespective of the several advantages associated with biomass-derived materials, their application as the sole adsorbent suffers from several drawbacks, including low adsorption of

Received: March 14, 2025
Revised: May 4, 2025
Accepted: May 22, 2025
Published: June 2, 2025

https://doi.org/10.1021/acs.langmuir.5c01248
Langmuir 2025, 41, 15022−15030

contaminants, bleeding of the adsorbents, low stability, low pore size and surface area, and difficulty in adsorbent removal from treated water postadsorption.[17] Hence, biomass adsorbents in synergistic combinations with other low-cost materials such as clays and nanoparticles have been studied.[18−21] Most of the combinations have been aimed at enhancing the composite's adsorption capacity and stability. Yet, another challenge is the separation of the adsorbents from large volumes of water postpurification. One proposed method of handling this is through magnetizing the adsorbent, thus eliminating the need for cumbersome and energy-demanding filtration postpurification.[22] In the presence of a strong magnetic field, the magnetized adsorbents are pulled aside in a solid−liquid separation process, leaving the purified water on one side and the contaminant-filled adsorbent on the other.

In this study, grape cluster stem biowaste was obtained from a farm in Albania. Grape cluster waste runs in several tons yearly, and it should be put to alternative use to improve environmental aesthetics and reduce pollution. In addition, as Albania prepares to join the EU, there is a requirement for aligning its water policy with the Water Framework Directive (Directive 2000/60/EC), which requires the achievement of a good ecological and chemical status for all water bodies. The National Environment Agency of Albania reported in 2022 that the water quality of two out of six basins in Albania (Ishmi and Seman), evaluated through physicochemical parameters, resulted in a bad quality. Also, during a 1 year assessment in four different seasons of the Ishmi basin, Cd, Cr, and Cu were commonly detected (with 0.00015, 0.0043, and 0.00245 mg/L for Cd, Cr, and Cu, respectively (own data)). Thus, using a magnetic low-cost adsorbent prepared from local materials could help in reducing pollution and attaining the water standards set by the EU Directive on the protection of groundwater against pollution and deterioration (Directive 2006/118/EC) and Directive on environmental quality standards (Directive 2008/105/EC). Therefore, the study aimed to prepare cost-efficient magnetic adsorbents from feldspar clay and commonly available grape cluster biomass for the removal of three toxic metals (Cd(II), Cr(VI), and Cu(II)) from water.

2. MATERIALS AND METHODS

2.1. Materials and Pretreatment. Previously described pretreated feldspar clay (FLC)[13] was employed in this study. Grape cluster stalk waste (GCW) was obtained from local vineyards in a central area of Albania. The GCW was washed with distilled water, dried (40 °C) to a constant weight, pulverized to fineness, sieved through a 1000 μm mesh sieve, and stored. Milli-Q (Purelab, UK) water at 18.2 MΩcm, Mettler Toledo scale (ME204), and pH meter (inoLab pH 7110) were used throughout the study. Analytical grade reagents were used throughout, including cadmium nitrate tetrahydrate (Merck, Germany), anhydrous copper chloride (Merck, Germany), potassium dichromate (Merck, Germany), iron(III) chloride (Sigma-Aldrich, Germany), and iron(II) sulfate heptahydrate (Carl Roth, Germany). Standard stock solutions (1000 mg/L each) of Cd(II), Cr(VI), and Cu(II) were prepared in Milli-Q water from the above chemicals and stored, while the working solutions were prepared from these stocks.

2.2. Adsorbents and Magnetic Composite Preparations and Characterizations. The adsorbents used in this study were pristine Feldspar clay (FLC), biochar (BC), magnetic nanoparticles (MNP), and biochar-clay composites (MBC-*x*). The chemical coprecipitation of pure MNP was carried out by mixing $FeCl_3$ (7.8 g) and $FeSO_4 \cdot 7H_2O$ (3.9 g) in 400 mL Milli-Q water at room temperature under continuous magnetic stirring,[18] followed by dropwise addition of 2.0 M NaOH until the red/gray solution becomes black marking the completion of the MNP precipitation. The mixture was centrifuged for 5 min (2500 rpm), washed 6 times with Milli-Q, dried (40 °C), and weighed before storing it in an airtight container.

Pristine BC was obtained from the GCW by calcination of a known weight of GCW for 2 h in limited oxygen on a furnace ramped up at a temperature of ∼14 °C/min until 500 °C. The crucible was allowed to cool to room temperature in the furnace, sieved through to 1000 μm mesh sieve, washed 6 times with Milli-Q, dried (40 °C), and weighed before storing in an airtight container.

From the recorded weights of BC and MNP, the required masses to prepare MBC of ratios 1:2:1 and 1:3:1 were determined. From the adjusted weights, the MNP was prepared as described above but stopped before the centrifugation step, and then the adjusted GCW mass was added with shaking for 30 min at 200 rpm, followed by the addition of the adjusted FLC mass with further shaking for 2 h. The mixture was centrifuged (1500 rpm) for 10 min, dried overnight at 80 °C, and calcined in a crucible, as described above. The final composite materials were cooled, sieved, washed, weighed, and stored. The composites were labeled MBC-1:2:1 and MBC-1:3:1. Other variants of the MBC (with higher BC/FLC/MNP) were prepared, but since the ultimate goal of the composite(s) was to adsorb pollutants optimally while preserving the lowest possible magnetic property for easy removal of the adsorbent from water postadsorption, the two reported variants were the best in terms of better magnetic property and lower preparation cost.

The BC, FLC, MNP, and MBC composites were characterized by analytically determining their point of zero charge (pHpzc) using pH-drift method[23] and cation exchange capacity (CEC) using the sodium saturation method,[24] while the functional groups were determined using the Fourier transform infrared (FTIR) spectrometer (VERTEX70, Bruker Optics, Germany), crystallinity using X-ray diffractometer (XRD) (Empyrean spectrometer, Malvern Panalytical, Germany), specific surface area and porosity using a QUADRASORBevo analyzer (Quantachrome Instruments, USA), and surface morphology using a scanning electron microscope (SEM, Gemini SEM 560 Zeiss, Germany) with an energy-dispersive X-ray probe (EDX).

2.3. Sorption Experiments. Preliminary batch sorption experiments using monocontaminant and tricontaminant solutions were comparatively carried out using the BC, FLC, MNP, and MBC adsorbents. The results showed enhanced performances of the MBC 1:2:1 and MBC 1:3:1 composites; thus, these were employed in the detailed sorption study. Typically, each batch experiment employed 20 mg of mass of adsorbent in 30 mL of 5 mg/L contaminant solution (except where otherwise stated) at pH of 5.5 ± 0.1 (except for the effect of pH) in 50 mL plastic centrifuge tubes incubated for 1440 min (except where stated) at 200 rpm and 20 °C. The pH of the working solutions was adjusted with 0.2 M HCl/NaOH, where required. The effects of the following sorption parameters[25] were examined: adsorbent mass (10−50 mg), time (1−1440 min), solution pH,[3−6] contaminants concentration (1−20 mg/L), and experimental temperature (20, 30, and 40 °C). The reusability study was carried out using 20 mg of used adsorbent and solution metal concentrations of 0.5−10 mg/L. The adsorbed metals were desorbed by shaking in 30 mL of 0.2 M HCl twice (200 rpm for 1 h) and then in Milli-Q under the same conditions, before drying overnight and reusing. Five cycles of reusability were carried out. After each experiment, the samples were filtered with 0.45 μm PTFE filters, and metals in the filtrate were measured using an inductively coupled plasma−optical emission spectrometer (ICP-OES, Varian 720-ES).

2.4. Sorption Data Analysis. The amounts (mg/g) of cations adsorbed (q_e) were calculated from eq 1, where C_o, C_e, v, and m are the initial and final concentrations (mg/L) of metal cations in solutions, experimental solution volume (mL), and mass (g) of adsorbent, respectively.

$$q_e = (C_o - C_e)v/m \quad (1)$$

https://doi.org/10.1021/acs.langmuir.5c01248
Langmuir 2025, 41, 15022−15030

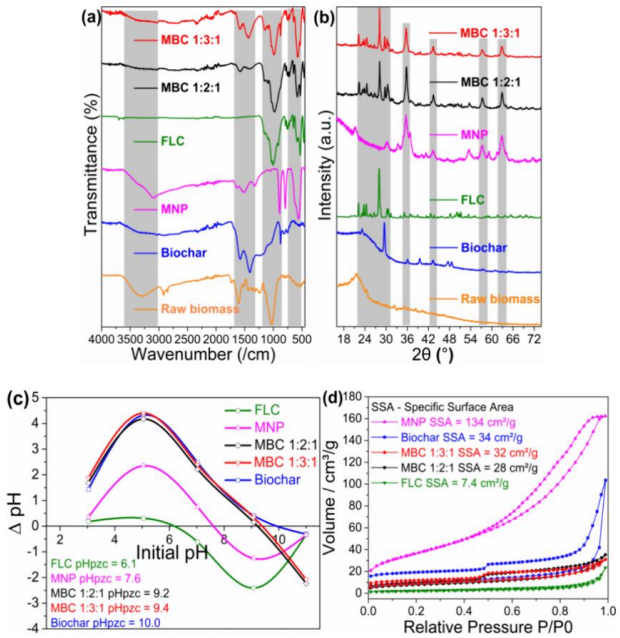

Figure 1. Characterization results of the biochar, FLC, MNP, MBC 1:2:1, and MBC 1:3:1 showing (a) FT-IR spectra peaks; (b) XRD diffractograms; (c) pHpzc; and (d) nitrogen adsorption/desorption isotherms (showing BET specific surface areas).

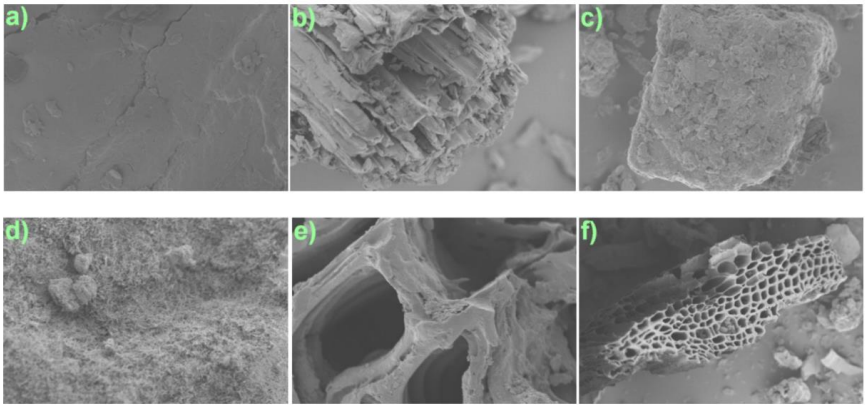

Figure 2. SEM electron micrographs of (a) biomass (magnification: 1 μm); (b) biochar (1 μm); (c) feldspar (1 μm); (d) magnetic nanoparticles (1 μm); (e) MBC 1:2:1 composite (1 μm); and (f) MBC 1:3:1 composite (10 μm).

The nonlinear forms of the pseudo-first-order (PFOM)[26] (eq 2), pseudo-second-order (PSOM) (eq 3), and the intraparticle diffusion (IPD) (eq 4)[27] models were employed to explain the experimental rate data. The model quantities q_e and q_t are the amounts adsorbed (mg/g) at equilibrium and time t, and k_1 (/min) and k_2 (g/μg/min) are the rate constants of the PFOM and PSOM, respectively. The K_i (g/μg min$^{1/2}$) is the rate parameter of the IPD control stage, and C (μg/g) is the estimated surface concentration of cations on the adsorbent surface.

$$q_t = q_e(1 - e^{-k_1 t}) \tag{2}$$

$$q_t = \frac{q_e^2 k_2 t}{1 + k_2 q_e t} \tag{3}$$

$$q_t = K_i t^{1/2} + C \tag{4}$$

https://doi.org/10.1021/acs.langmuir.5c01248
Langmuir 2025, 41, 15022−15030

The equilibrium sorption data were fitted with nonlinear adsorption isotherm models of the Langmuir (eq 5), Freundlich (eq 6), and Langmuir–Freundlich (eq 7) type, where the models' parameters Q_0 or q_{max} (mg/g) are the maximum adsorption capacity per unit weight of adsorbent, b is the Langmuir constant, K_F is the Freundlich isotherm constant, $1/n_F$ is the Freundlich isotherm linearity parameter, and K_{lf} and n are a constant and the dimensionless exponent of Langmuir–Freundlich, respectively.

$$q_e = \frac{Q_o b C_e}{1 + bC_e} \tag{5}$$

$$q_e = K_F C_e^{1/n_F} \tag{6}$$

$$q_e = \frac{q_{max} K_{lf} C_e^n}{1 + K_{lf} C_e^n} \tag{7}$$

The equilibrium constant K_d (L/g) (eq 8) and thermodynamic parameters (enthalpy ΔH° (kJ/mol) (eq 9), entropy ΔS° (J/mol/K) (eq 9), and Gibbs free energy ΔG° (kJ/mol) (eq 10) were calculated using the equilibrium sorption data at 293.15, 303.15, and 313.15 K, where R is the universal gas constant. All fittings and models' parameters were generated using the OriginPro2015 software (OriginLab Corporation, USA).

$$K_d = \frac{q_e}{C_e} \tag{8}$$

$$\ln K_d = \frac{\Delta S^\circ}{R} - \frac{\Delta H^\circ}{RT} \tag{9}$$

$$\Delta G^\circ = -RT \ln K_d \tag{10}$$

3. RESULTS AND DISCUSSIONS

3.1. Characterization of Adsorbents. The main aim for the composite fabrication was to prepare an adsorbent that is economical, environmentally friendly, easy to separate from water post-treatment, and more effective in water treatment than any of the precursor materials. Hence, selected physical and chemical properties (Figures 1 and 2 and Table 1) of the precursor and composite adsorbents were analyzed and described here to prove that the composites meet these critical requirements. The results in Table 1 showed that the biochar exhibited a high or very alkaline pHpzc (Figure 1c), unlike the MNP and the feldspar, which expressed near-neutral and slightly acidic values, respectively. The final MBC composites exhibited pHpzc values that were closer to the major bulk material in the composite (biochar): the more biochar present, the higher the pHpzc value. The average composite pHpzc value was 9.3, and this pHpzc value was in line with those reported for clay-biochar composites.[15,18] The pHpzc is one important parameter that indicates the adsorbent's surface charge state in solution pH: below the pHpzc value, the average surface charge density is positive and the adsorbent would likely attract negatively charged ions, while it is negative above the pHpzc value and the surface would attract positive ions.[27]

Table 1. Physiochemical Characterization of Adsorbents

adsorbent	pHpzc	CEC (cmol/kg)	BET specific surface area (m^2/g)
biochar	10.0	50.1	34
MNP	7.6	34	134
FLC	6.1	5.3	7.4
MBC 1:2:1	9.2	28.4	28
MBC 1:3:1	9.4	23.2	32

The values of the cation exchange capacity (CEC) (Table 1) of the composites showed an average decrease of ∼48 and 16%, respectively, when compared to the biochar and the MNP but higher than the feldspar. In addition to the low cost and higher stability of the composites, an average CEC of 24 mequiv/100g was considered effective. Similar to the CEC, the BET (Table 1 and Figure 1d) values were lower for the composites compared to those of the biochar and the MNP. The textural properties measured via nitrogen adsorption–desorption isotherms at 77 K (Figure 1*d*) showed majorly IV isotherms with a sharp inflection usually occurring around relative pressures (P/P_0) of 0.5–0.9.

Prediction and comparison of the major functional groups associated with the precursor and the final composites were done by monitoring the peaks between 4000 and 500/cm for biochar, MNP, FLC, MBC 1:2:1, and MBC 1:3:1 as shown in the FTIR spectra in Figure 1a. The peak around 1035/cm of the FLC and biomass were attributed to Si–O in-plane bending vibrations, while those at 730 and 525/cm of FLC were attributed to the Si–O–Si bridging bonds in SiO_2 and Al–OH/Al–O deformations, respectively.[18] These peaks were observed in the composites, though with slight shifts indicating the transfer of functional constituents from the precursors to the composites. Another major peak transferred to the composites is the characteristic magnetic Fe–O peak (around 560/cm) of the MNP; its presence is indicative of the magnetic property in the composites.[22] The peaks between 1585 and 1420/cm, especially in the composites, are characteristic of C═O, C═C aromatic stretching rings, and amide-I groups, while those around 3200/cm of all materials (except FLC) were attributed to the presence of −OH groups.[26−29]

The degree of crystallinity measured through XRD (Figure 1b) showed the presence of characteristic FLC peaks for microcline, quartz, and feldspar minerals at 2θ of 22.0, 26.6, and 27.9°, respectively, with a partly triclinic feldspar mineral peak at 30.7°. Typical Fe_3O_4 MNP spinal structures were observed at 2θ values of 30.3, 35.5, 43.1, 57.1, and 62.7. Similar to the FTIR spectra, these crystal peaks in the FLC and MNP were observed in the composites, showing that there were no phase changes in the basic lattices of the FLC and MNP within the final composites.[18]

The morphologies of the precursor and final materials were examined via SEM (Figure 2a–f). The SEM of the raw biomass exhibited spongy amorphous surfaces (Figure 2a), which became less spongy with nonregular porous surfaces upon calcination to the biochar (Figure 2b), while the MNP exhibited spinal structures (Figure 2d). However, the morphologies of both MBC composites (Figure 2e,f) showed almost regular surfaces with shaped pores in the form of a honeycomb, confirming a successful preparation process.

Preliminary sorption experiments carried out to ascertain and compare sorption potentials of the precursor and composites showed enhanced removal efficiency for MBC 1:2:1 and MBC 1:3:1 of ∼370, 201, and 122% for Cd(II), Cr(VI), and Cu(II), respectively, in comparison to the GCW, biochar (Figure S1a). In addition, the composites showed better removal efficiencies for Pb(II) and for a model organic compound (terbuthylazine) of 99.7 and 99.0% for MBC 1:2:1, and 76.6 and 55.7% for MBC 1:3:1, respectively (Figure S1b).

https://doi.org/10.1021/acs.langmuir.5c01248
Langmuir 2025, 41, 15022−15030

Thus, further experiments were conducted using MBC 1:2:1 and MBC 1:3:1 to obtain the optimized sorption parameters.

3.2. Optimization of Mass and pH, and Sorption Kinetics. For mass optimization of the composite adsorbents, a mass range of 10 up to 50 mg (0.33 and 1.66 g/L) was considered, using a 5 mg/L ternary contaminant solution, and the sorption trends are depicted in Figure 3a,b. Results showed

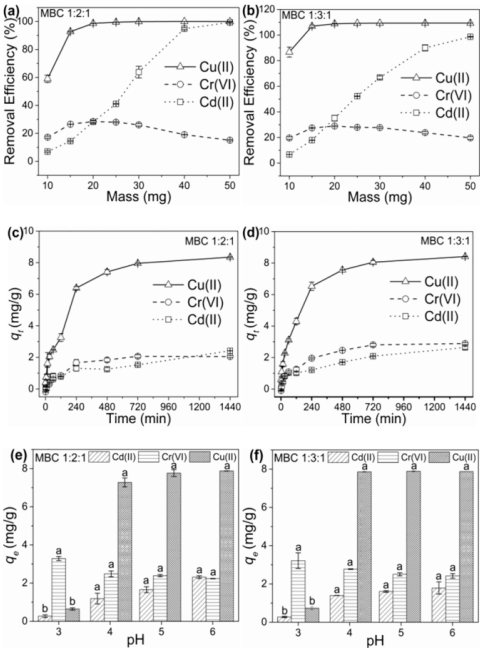

Figure 3. Adsorption trends at varying masses of (a) MBC 1:2:1 and (b) MBC 1:3:1; adsorption rate trend on (c) MBC 1:2:1 and (d) MBC 1:3:1; and adsorption trend at varying solution pH for (e) MBC 1:2:1 and (f) MBC 1:3:1.

that the Cd(II) and Cu(II) removal efficiency increased with a higher adsorbent mass. This was ascribed to the presence of numerous active exchangeable sites for these cations and the greater surface area of the adsorbents with increasing adsorbent mass.[30,31] For the Cr(VI) anion, however, the removal efficiency rose initially with an increase in adsorbent mass, but beyond the 20 mg mass, there was a downward deflection. A similar trend was reported for the coadsorption of Cd(II) and Cr(VI),[32] and this may be attributed to the antagonistic effect between the two ions in solution during coadsorption. The results showed that the mass for optimum removal efficiency for all three cations was 20 mg; thus, this amount was selected for further experiments. At the 20 mg mass of MBC 1:2:1 and MBC 1:3:1, the optimum adsorption for Cd(II) was 2.3 and 2.9 mg/g, respectively. These values for Cr(VI) were 2.3 and 2.4 mg/g, while those for Cu(II) were 7.6 and 8.3 mg/g, accordingly.

The sorption rate trends for Cd(II), Cr(VI), and Cu(II) ions on the composites are presented in Figure 3c,d. Both composites showed fast ion uptake over the first 240 min, and this may be attributed to the presence of plenty of empty active adsorption sites on the adsorbent surfaces.[33] This initial fast adsorption was followed by a slower increase in trend up to 720 min, which was ascribed to the filling of the remaining composite adsorption sites and intraparticle diffusion of cations within the composites.[34] Though a significant portion of the adsorption of the contaminants (≥85%) occurred before 240 min, equilibrium was attained for both composites at 720 min. Therefore, further tests were carried out at 720 min. The mass and rate experiments showed that the affinity of the composites for Cu(II) ions was far higher than for Cd(II) and Cr(VI); the general trend was Cu(II) > Cd(II) ≥ Cr(VI).

Another important parameter in evaluating the efficiency of a new adsorbent is its response to pH changes. This is vital because it directly affects both the metal ions' speciation and composite surface charge.[35] Therefore, the influence of solution pH on the adsorption process by the MBC composites was evaluated and is presented in Figure 3e,f. The significantly low ($p < 0.05$) sorption for Cd(II) and Cu(II) observed in the acidic conditions (pH 3) may be ascribed to partial protonation of the functional groups, and the competition between H^+ (or H_3O^+) and metal, both cations for the negatively charged adsorption sites on the MBC composites.[33] Thus, by increasing the solution pH, the proton concentration decreases and the adsorption sites become progressively negative, resulting in a lower competition between protons and cations and more electrostatic

Table 2. Kinetic Model Parameters for MBC 1:2:1 and MBC 1:3:1 Adsorption

kinetic model	parameter	Cd(II) MBC 1:2:1	Cd(II) MBC 1:3:1	Cr(VI) MBC 1:2:1	Cr(VI) MBC 1:3:1	Cu(II) MBC 1:2:1	Cu(II) MBC 1:3:1
PFO	q_e (mg g^{-1})	1.831	2.249	2.049	2.760	8.141	8.031
	k_1 (min^{-1})	0.005	0.004	0.005	0.006	0.005	0.007
	r^2	0.701	0.806	0.946	0.962	0.965	0.967
	χ^2	0.145	0.129	0.038	0.044	0.334	0.299
PSO	q_e (mg g^{-1})	2.120	2.482	2.389	3.162	9.454	9.103
	k_2 (g mg^{-1} min^{-1})	0.003	0.003	0.002	0.002	0.0007	0.001
	r^2	0.779	0.875	0.942	0.980	0.968	0.981
	χ^2	0.107	0.083	0.041	0.023	0.308	0.174
IPD	C (mg g^{-1})	0.220	0.251	0.124	0.231	0.816	1.198
	k_i (g g^{-1} $min^{1/2}$)	0.055	0.065	0.064	0.085	0.234	0.236
	r^2	0.910	0.953	0.830	0.891	0.883	0.875
	χ^2	0.043	0.031	0.122	0.130	1.135	1.150
experimental	mg/g	2.413	2.636	2.048	2.888	8.348	8.414

https://doi.org/10.1021/acs.langmuir.5c01248
Langmuir 2025, 41, 15022−15030

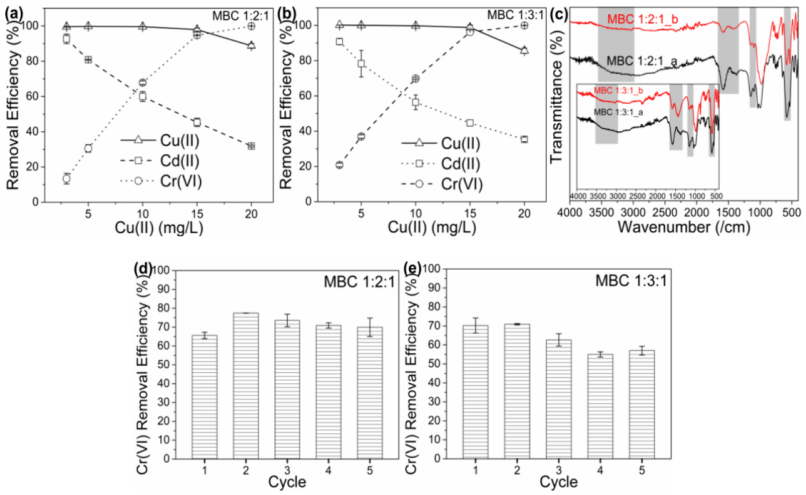

Figure 4. (a) Effect of the initial concentration of Cu(II) on Cd(II) and Cr(VI) removal efficiency on MBC 1:2:1; (b) on MBC 1:3:1 [adsorbent mass: 20 mg in 30 mL solution using 1 mg/L Cd(II), 3 mg/L Cr(VI), and 3−20 mg/L of Cu(II), pH = 5.4 at 200 rpm]; (c) pre- and postadsorption FTIR spectra of the composites; (d) reusability of Cr(VI) on MBC 1:2:1; and (e) on MBC 1:3:1.

interactions with Cd(II) and Cu(II) on both composites.[36] The optimum pH for adsorption of Cd(II) and Cu(II) was at pH 6. However, for Cr(VI) anions, which exist as $HCrO_4^-$ at low pH,[37] the adsorption was higher at pH 3 as a result of electrostatic attraction between $HCrO_4^-$ and positively charged adsorbent surfaces, especially at pH 3.[11] Thus, the optimum adsorption of Cr(VI) occurred at pH 3.

In evaluating the removal kinetics of Cd(II), Cr(VI), and Cu(II) by MBC 1:2:1 and MBC 1:3:1, the PFOM, PSOM, and IPD kinetic models were employed. The fitting plots and model parameters are given in Figure S2a−f and in Table 2, respectively. In general, by comparing the PFOM and PSOM correlation coefficients (r^2) and chi-square (χ^2), the PSOM exhibited better trends with values closer to unity and smaller, respectively. These show that the model fits the rate data and indicates that the adsorption process was controlled by the valence electron exchange between surface adsorption sites and metal ions, possibly leading to electrostatic interactions.[22,38,39] The IPD model was evaluated to gain insight into the particulate nature (surface-to-pore relationship) of the adsorption process on the MBC composites. The C (mg/g) parameter of this model, which is an indication of the extent of surface adsorption, was lower than the experimental values (<10% of total adsorption) for both composites, suggesting that metal ions adsorption within the pores of the composites played some role in the adsorption process.

3.3. Effect of Initial Concentration and Coexisting Metal Ions. The effect of initial concentration results (Figure 4a,b) showed that increasing initial Cu(II) concentration in solution enhanced Cr(VI) removal efficiency by 86 and 79% on MBC 1:2:1 and MBC 1:3:1, respectively, while reducing Cd(II) uptake by 65 and 52%, respectively. Thus, in a ternary metal solution of Cr(VI), Cu(II), and Cd(II), increasing the Cu(II) concentration would enhance Cr(VI) uptake while reducing the adsorption of Cd(II). Interestingly, it was also observed that as the concentration increased, the Cr(VI) removal attained ∼100% efficiency, while the Cu(II) efficiency decreased from ∼100 to ∼90%. This may be due to the Cu(II) adsorption site occupation (displacement of adsorbed ions) by Cr(VI) as concentrations increased. This suggests that increasing the adsorbed positive charge on the adsorbent surface leads to higher electrostatic interaction with the Cr(VI) anion, possibly in a multilayer. A similar trend has been reported earlier.[40]

The adsorption mechanism in a multicomponent system could be explained based on ionic properties (Table S1). The higher adsorption of Cu(II) may be attributed to its smaller hydrated radius and higher electronegativity (highest standard reduction potential) compared to Cd(II) and Cr(VI); this results in easier access into the pores and greater electrostatic interactions with the composite adsorption sites.[21,41] To determine the interactions in a ternary system, the relative metal i adsorption R_i(%) (eq 11)[32] was employed, as given in Table S2.

$$R_i = \frac{\text{metal } i \text{ adsorption capacity with the coexistence of metal } j \text{ and } k}{\text{metal } i \text{ adsorption capacity without coexistence of metal } j \text{ and } k} \times 100 \quad (11)$$

Based on this parameter, if R_i > 100%, then the interactive effect of mixed ions is synergistic, while R_i < 100% means there were antagonistic reactions. However, R_i = 100% shows noninteractive behavior. From the results (Table S2), Cd(II) exhibited a synergistic and antagonistic effect for MBC 1:2:1 and MBC 1:3:1, respectively, while Cu(II) and Cr(VI) exhibited synergistic effects for both composites.

The effect of the metal adsorption on the FTIR spectra was examined and is depicted in Figure 4c. The peaks at around 3200/cm, which were attributed to the −OH groups, showed enhanced vibration after adsorption, indicating strong interaction with the metal ions.[21,42] The −OH groups might

https://doi.org/10.1021/acs.langmuir.5c01248
Langmuir 2025, 41, 15022−15030

have served as electron donors for Cr(VI) reduction to Cr(III) while being oxidized to carboxyl groups.[43] This was confirmed by the corresponding carboxyl peak increase at 1585/cm after adsorption. Another source of electrons for Cr(VI) reduction might have been iron oxide (Fe°) ions present in the composites.[37,42,44] Amide-I groups at around 1420/cm exhibited higher vibrations and shifted after adsorption, indicating that these groups were active in the metal ion adsorption process.

3.4. Effect of Temperature on Sorption and Adsorption Isotherm Modeling. The adsorption of Cd(II), Cr(VI), and Cu(II) on the MBC composites at fixed solution concentrations of Cd(II) (1 mg/L) and Cr(VI) (1 mg/L), and at varying concentrations (3−20 mg/L) of Cu(II) at three different temperatures (20−40 °C), are given in Figure S4a−f. The sorption trends showed that with increasing Cu(II) concentration, Cd(II) sorption decreased (Figure S4a,b), especially at low temperature (20 °C). The slightly higher Cd(II) and Cu(II) (only on MBC 1:3:1) uptake at higher temperatures may be attributed to the endothermic nature of the process. On the other hand, no significant change in the sorption of Cr(VI) was observed as the temperature was varied (Figure S4c−f). The calculated thermodynamic parameters showed that $\Delta G° < 0$, $\Delta S° > 0$, and $\Delta H° > 0$ for MBC 1:3:1 (Table 3), indicating a spontaneous and endothermic process.

Table 3. Sorption Thermodynamic Parameters for Cu(II) on MBC 1:3:1

temperature	$\Delta G°$ (kJ/mol)	$\Delta H°$(kJ/mol)	$\Delta S°$ (J/mol/K)
293.15 K (20 °C)	−3.95	10.10	47.95
303.15 K (30 °C)	−4.41		
313.15 K (40 °C)	−4.91		

The negative $\Delta G°$ values implied that the adsorption process is spontaneous. Moreover, the $\Delta G°$ decreases with temperature increase, suggesting that higher temperature conditions favor the adsorption process, thus enhancing the spontaneity of the process.[45] This was supported by the positive $\Delta H°$ (10.10 kJ/mol) value, which indicated an endothermic process. Additionally, the positive $\Delta S°$ value (47.95 J/mol/K) signaled an increase in randomness at the solid-solution interface as the process proceeded toward equilibrium.

Due to the higher affinity of the composites for Cu(II), the Cu(II) adsorption isotherm models were evaluated at fixed Cd(II) and Cr(VI) concentrations, 1 and 3 mg/L, respectively, at three different temperatures (20, 30, and 40 °C). The employed model parameters (Langmuir, Freundlich, and Langmuir−Freundlich) are shown in Table 4 (Figure S3a−f). The r^2 (≥0.87) and χ^2 (≤12.06) values suggested that the Langmuir adsorption isotherm model fit the data better than the Freundlich model, and this is an indication that the Cu(II) adsorption process occurred on similar adsorption sites and in a monolayer. The relatively good fits of the Langmuir−Freundlich model ($r^2 \geq 0.87$; $\chi^2 \leq 12.28$) corroborate the idea that the adsorption occurred on heterogeneous adsorption sites but with a similar affinity or energy for Cu(II).

3.5. Reusability and Cost Implications. The reusability of the MBC composite, an economic indicator of its applicability, was performed, and the results of five cycles are shown in Figure 4d,e. The average removal efficiency of the composites for Cd(II) and Cu(II) in the first cycle was ∼20 and 87%, respectively. In subsequent adsorption cycles, no significant removal of these cations was observed; thus, the reuse of these composites for both cations was not possible. This may be ascribed to the strong attachments of these cations to the composite's adsorption in the first cycle. However, Cr(VI) adsorption of the composites exhibited relatively constant efficiencies through the consecutive cycles (Figure 4d,e) with slight decreases (<10%) in efficiency for the MBC 1:3:1 toward the fifth cycle. The recorded Cr(VI) removal efficiencies in the fifth cycle were 70 and 57% for MBC 1:2:1 and MBC 1:3:1, respectively. The subsequent inability of the composites to adsorb Cd(II) and Cu(II) but enhanced Cr(VI) adsorption is an indication of cooperative adsorption after the first cycle. Thus, the used composites may be reusable for Cr(VI) removal from water.

The cost implication of applying the MBC composites was estimated as reported by others for similar adsorbents[46,47] by considering the cost of all precursor materials, treatments (energy and chemicals), and post-treatments (washing, drying, packaging, and transport) based on the reported calculation. The estimated costs per kilogram are ∼5.54 United States $ (Table S3). Considering the reusability of these adsorbents, this is far cheaper than several reported low-cost adsorbents.[46−49]

Table 4. Cu(II) Adsorption Model Parameters

		Cu(II) MBC 1:2:1			Cu(II) MBC 1:3:1		
adsorption isotherm model	parameter	20 °C	30 °C	40 °C	20 °C	30 °C	40 °C
Langmuir	Q_o (mg/g)	27.88	26.36	28.02	24.95	28.87	29.26
	β	26.12	46.33	30.55	142.16	33.07	22.58
	r^2	0.95	0.94	0.93	0.87	0.95	0.92
	χ^2	4.29	5.55	6.87	12.06	4.43	8.26
Freundlich	$1/n$	0.22	0.19	0.20	0.15	0.18	0.20
	K_F	24.97	24.82	24.99	24.93	24.82	25.07
	r^2	0.81	0.91	0.76	0.84	0.64	0.69
	χ^2	19.25	9.01	24.46	15.70	35.55	31.43
Langmuir−Freundlich	q_{max} (mg/g)	27.95	30.68	28.63	29.50	27.41	28.97
	$1/n$	0.98	0.56	0.90	0.52	1.41	1.05
	K_{LF}	24.83	23.54	20.05	8.73	180.8	28.10
	r^2	0.93	0.99	0.90	0.94	0.96	0.88
	χ^2	6.43	0.42	10.04	2.36	3.87	12.28

https://doi.org/10.1021/acs.langmuir.5c01248
Langmuir 2025, 41, 15022−15030

4. CONCLUSIONS

The starting individual materials of grape cluster biomass, feldspar clay, and Fe_3O_4 were successfully combined into ternary magneto-biochar-clay composites in MBC 1:2:1 and MBC 1:3:1. This was confirmed by following higher cation exchange capacity and BET surface area values compared to feldspar clay. Similarly, characteristic properties of the individual starting materials, such as unique infrared and XRD peaks as well as the basic crystalline structure of the feldspar, were transferred to the MBC composite. These adsorbents were applied in simultaneous aqueous multimetal ions (Cd(II), Cr(VI), and Cu(II)) adsorption. Preliminary data showed enhanced MBC adsorption efficiency in comparison to the individual adsorbents. The average enhanced efficiencies of both composites for Cd(II), Cr(VI), and Cu(II) were ∼370, 201, and 122%, respectively. The adsorption processes were mainly controlled by electrostatic interactions and adsorption on the pores. The surface functional groups involved in the process are −OH, $-COO^-$, and −C−N. The Cu(II) ion was the most adsorbed, and equilibrium was achieved in 720 min for all three metal ions. The optimal pH of adsorption for Cd(II) and Cu(II) was recorded at solution pH 6, while at pH 3 for Cr(VI). Cooperative adsorption was observed between Cu(II) and Cr(VI) in a multimetal solution, while Cd(II) adsorption decreased. Generally, the process was spontaneous but endothermic and was described by Langmuir and Langmuir−Freundlich adsorption isotherm models. The composites showed good removal efficiency for Cd(II) and Cu(II) during the first adsorption cycle and for Cr(VI) even after five consecutive cycles; thus, the composite is a low-cost, easy-to-handle, feasible, and sustainable adsorbent for application in water treatment.

■ ASSOCIATED CONTENT

Supporting Information

The Supporting Information is available free of charge at https://pubs.acs.org/doi/10.1021/acs.langmuir.5c01248.

Removal efficiency of metal ions and terbuthylazine on MBC 1:2:1, MBC 1:3:1, biochar, FLC, and MNP; kinetics modeling of rate data; isotherm model fittings for equilibrium data; effect of temperature on adsorption; ionic properties of Cd(II), Cr(VI) and Cu(II); interactions of metal ions in ternary systems; cost analysis of MBC 1:2:1/MBC 1:3:1 production (PDF)

■ AUTHOR INFORMATION

Corresponding Author

Aleksandër Peqini − *Institute of Soil Science and Soil Conservation, Research Centre for BioSystems, Land Use and Nutrition (iFZ), Justus Liebig University Giessen, Giessen 35392, Germany; Department of Environment and Natural Resources, Faculty of Agriculture and Environment, Agricultural University of Tirana, Tirana 1029, Albania*; Email: aleksander.peqini@umwelt.uni-giessen.de

Authors

Paul N. Diagboya − *Environmental fate of chemicals and remediation (EnFaCRe) laboratory, Department of Environmental Management and Toxicology, University of Delta, PMB 2090 Agbor, Nigeria*; orcid.org/0000-0003-2982-433X

Seit Shallari − *Department of Environment and Natural Resources, Faculty of Agriculture and Environment, Agricultural University of Tirana, Tirana 1029, Albania*

Ferdi Brahushi − *Department of Environment and Natural Resources, Faculty of Agriculture and Environment, Agricultural University of Tirana, Tirana 1029, Albania*

Rolf-Alexander Düring − *Institute of Soil Science and Soil Conservation, Research Centre for BioSystems, Land Use and Nutrition (iFZ), Justus Liebig University Giessen, Giessen 35392, Germany*

Complete contact information is available at: https://pubs.acs.org/10.1021/acs.langmuir.5c01248

Notes

The authors declare no competing financial interest.

■ ACKNOWLEDGMENTS

We acknowledge the support of Deutsche Bundesstiftung Umwelt (DBU), Germany, for the support of the research fellowship to A.P. and the support of the Alexander von Humboldt Foundation, Germany, for the award of a Georg Forster experienced research fellowship to P.N.D. Also, we acknowledge the technical assistance of Elke Schneidenwind (JLU) and the support of the Department of Chemistry at JLU Giessen for technical assistance with the composite characterization.

■ REFERENCES

(1) WHO, U.N.C.s.F.U.a.W.H.O. *Progress on household drinking water, sanitation and hygiene 2000−2022: special focus on gender*; WHO **2023**.

(2) Vaikosen, E. N.; et al. GC-MS fragmentation patterns of sprayed endosulfan and its sulphate metabolite in samples of Theobroma cacao L from a field kinetic study. *Eur. J. Mass Spectrom (Chichester)* **2019**, *25* (4), 362−371.

(3) Adedayo Adesina, O.; et al. Periodic characterization of alkylnaphthalenes in stack gas and ambient air around a medical waste incinerator. *Environ. Sci. Pollut Res. Int.* **2017**, *24* (27), 21770−21777.

(4) Nagajyoti, P. C.; Lee, K. D.; Sreekanth, T. V. M. Heavy metals, occurrence and toxicity for plants: a review. *Environmental Chemistry Letters* **2010**, *8* (3), 199−216.

(5) Oderinde, A.; Diagboya, P. Sorption of competing heavy metals on Laterite. *Federal Polytechnic Ilaro J. Pure Appl. Sci.* **2023**, *5* (1), 1−9.

(6) Wise, J. P., Jr.; et al. Current understanding of hexavalent chromium [Cr(VI)] neurotoxicity and new perspectives. *Environ. Int.* **2022**, *158*, No. 106877.

(7) Sharma, P.; et al. Health hazards of hexavalent chromium (Cr (VI)) and its microbial reduction. *Bioengineered* **2022**, *13* (3), 4923−4938.

(8) Jan, A. T.; et al. Heavy Metals and Human Health: Mechanistic Insight into Toxicity and Counter Defense System of Antioxidants. *Int. J. Mol. Sci.* **2015**, *16* (12), 29592−630.

(9) Crini, G.; Lichtfouse, E. Advantages and disadvantages of techniques used for wastewater treatment. *Environmental Chemistry Letters* **2019**, *17* (1), 145−155.

(10) Wang, Q.; et al. Recent development of natural polysaccharide-modified biochar on adsorption of pollutants from wastewater: Preparation, characterization, mechanisms and applications. *Sep. Purif. Technol.* **2024**, *343*, No. 127142.

(11) Nkutha, C. S.; et al. Application of eco-friendly multifunctional porous graphene oxide for adsorptive sequestration of chromium in

aqueous solution. *Water Environment Research* **2020**, *92* (7), 1070−1079.
(12) Zanele, Z. P.; et al. Metals and Antibiotics as Aqueous Sequestration Targets for Magnetic Polyamidoamine-Grafted SBA-15. *Langmuir* **2021**, *37* (32), 9764−9773.
(13) Diagboya, P. N.; et al. Comparative empirical evaluation of the aqueous adsorptive sequestration potential of low-cost feldspar-biochar composites for ivermectin. *Colloids Surf., A* **2022**, *634*, No. 127930.
(14) Akpotu, S. O.; et al. Engineered Geomedia Kaolin Clay-Reduced Graphene Oxide−Polymer Composite for the Remediation of Olaquindox from Water. *ACS Omega* **2022**, *7*, 34054−34065.
(15) Sera, P. R.; et al. Potential of valourized Moringa oleifera seed waste modified with activated carbon for toxic metals decontamination in conventional water treatment. *Bioresource Technology Reports* **2021**, *16*, No. 100881.
(16) Okoli, C. P.; Diagboya, P. N.; Anigbogu, I. O.; Olu-Owolabi, B. I.; Adebowale, K. O.; et al. Competitive biosorption of Pb(II) and Cd(II) ions from aqueous solutions using chemically modified moss biomass (Barbula lambarenensis). *Environ. Earth Sci.* **2016**, *76* (1), 1−10.
(17) Diagboya, P. N.; et al. Clay-carbonaceous material composites: Towards a new class of functional adsorbents for water treatment. *Surfaces and Interfaces* **2020**, *19*, No. 100506.
(18) Diagboya, P. N.; Dikio, E. D. Scavenging of aqueous toxic organic and inorganic cations using novel facile magneto-carbon black-clay composite adsorbent. *Journal of Cleaner Production* **2018**, *180*, 71−80.
(19) Olu-Owolabi, B. I.; et al. Utilizing eco-friendly kaolinite-biochar composite adsorbent for removal of ivermectin in aqueous media. *J. Environ. Manage* **2021**, *279*, No. 111619.
(20) Zhou, Q.; et al. Adsorption of Cu(II) and Cd(II) from aqueous solutions by ferromanganese binary oxide-biochar composites. *Sci. Total Environ.* **2018**, *615*, 115−122.
(21) Zheng, L.; et al. Single and Binary Adsorption Behaviour and Mechanisms of Cd2+, Cu2+ and Ni2+ onto Modified Biochar in Aqueous Solutions. *Processes* **2021**, *9* (10), 1829.
(22) Mohubedu, R. P.; et al. Magnetic valorization of biomass and biochar of a typical plant nuisance for toxic metals contaminated water treatment. *Journal of Cleaner Production* **2019**, *209*, 1016−1024.
(23) Olu-Owolabi, B. I.; et al. Empirical aspects of an emerging agricultural pesticide contaminant retention on two sub-Saharan soils. *Gondwana Research* **2022**, *105*, 311−319.
(24) Olu-Owolabi, B. I.; et al. Calcined biomass-modified bentonite clay for removal of aqueous metal ions. *Journal of Environmental Chemical Engineering* **2016**, *4* (1), 1376−1382.
(25) AttahDaniel, E. B.; Mtunzi, F. M.; Wankasi, D.; Ayawei, N.; Dikio, E. D.; Diagboya, P. N.; et al. Relative empirical evaluation of the aqueous sequestration of methylene blue using benzene-1, 4-dicarboxylic acid-linked lanthanum and zinc metal organic frameworks. *Water Air Soil Pollut.* **2022**, *233* (11), 33.
(26) Junck, J.; et al. Mechanistic interpretation of the sorption of terbuthylazine pesticide onto aged microplastics. *Environ. Pollut.* **2024**, *345*, No. 123502.
(27) Diagboya, P. N.; et al. Adsorptive decolorization of dyes in aqueous solution using magnetic sweet potato (Ipomoea batatas L.) peel waste. *RSC Sustainability* **2024**, *2*, 686−694.
(28) Güzel, F.; et al. Performance of grape (Vitis vinifera L.) industrial processing solid waste−derived nanoporous carbon in copper(II) removal. *Biomass Conversion and Biorefinery* **2021**, *11* (4), 1363−1373.
(29) Villaescusa, I.; et al. Removal of copper and nickel ions from aqueous solutions by grape stalks wastes. *Water Res.* **2004**, *38* (4), 992−1002.
(30) Li, Q.; et al. Removal of toxic metals from aqueous solution by biochars derived from long-root Eichhornia crassipes. *R. Soc. Open Sci.* **2018**, *5*, No. 180966.
(31) Olu-Owolabi, B. I.; Diagboya, P. N.; Ebaddan, W. C. Mechanism of Pb2+ removal from aqueous solution using a nonliving moss biomass. *Chemical Engineering Journal* **2012**, *195*−*196*, 270−275.
(32) Jain, M.; et al. Adsorption of heavy metals from multi-metal aqueous solution by sunflower plant biomass-based carbons. *International Journal of Environmental Science and Technology* **2016**, *13* (2), 493−500.
(33) Arshadi, M.; Amiri, M. J.; Mousavi, S. Kinetic, equilibrium and thermodynamic investigations of Ni(II), Cd(II), Cu(II) and Co(II) adsorption on barley straw ash. *Water Resources and Industry* **2014**, *6*, 1−17.
(34) Mabungela, N.; Shooto, N. D.; Mtunzi, F.; Naidoo, E. B.; et al. Binary adsorption studies of Cr (VI) and Cu (II) ions from synthetic wastewater using carbon from Feoniculum vulgare (fennel seeds). *Cogent Eng.* **2022**, *9* (1), 2119530.
(35) Ebelegi, A. N.; et al. Covalently bonded polyamidoamine functionalized silica used as a Pb(II) scavenger from aqueous solution. *Journal of Environmental Chemical Engineering* **2019**, *7* (4), No. 103214.
(36) Olu-Owolabi, B. I.; et al. Fractal-like concepts for evaluation of toxic metals adsorption efficiency of feldspar-biomass composites. *Journal of Cleaner Production* **2018**, *171*, 884−891.
(37) Nnadozie, E. C.; Ajibade, P. A. Adsorption, kinetic and mechanistic studies of Pb(II) and Cr(VI) ions using APTES functionalized magnetic biochar. *Microporous Mesoporous Mater.* **2020**, *309*, No. 110573.
(38) Tan, Z.; et al. Cadmium removal potential by rice straw-derived magnetic biochar. *Clean Technologies and Environmental Policy* **2017**, *19* (3), 761−774.
(39) Xikhongelo, R. V.; et al. Polyamidoamine-Functionalized Graphene Oxide−SBA-15 Mesoporous Composite: Adsorbent for Aqueous Arsenite, Cadmium, Ciprofloxacin, Ivermectin, and Tetracycline. *Ind. Eng. Chem. Res.* **2021**, *60* (10), 3957−3968.
(40) Zhao, R.; et al. Co-removal effect and mechanism of Cr (VI) and Cd (II) by biochar-supported sulfide-modified nanoscale zero-valent iron in a binary system. *Molecules* **2022**, *27* (15), 4742.
(41) Mohan, D.; Pittman, C. U., Jr.; Steele, P. H. Single, binary and multi-component adsorption of copper and cadmium from aqueous solutions on Kraft lignin−a biosorbent. *J. Colloid Interface Sci.* **2006**, *297* (2), 489−504.
(42) Zhao, R.; et al. Co-Removal Effect and Mechanism of Cr(VI) and Cd(II) by Biochar-Supported Sulfide-Modified Nanoscale Zero-Valent Iron in a Binary System. *Molecules* **2022**, *27* (15), 180966.
(43) Song, L.; et al. Enhanced synergistic removal of Cr(VI) and Cd(II) with bi-functional biomass-based composites. *J. Hazard Mater.* **2020**, *388*, No. 121776.
(44) Zhou, L.; et al. Investigation of the adsorption-reduction mechanisms of hexavalent chromium by ramie biochars of different pyrolytic temperatures. *Bioresour. Technol.* **2016**, *218*, 351−9.
(45) Deng, J.; et al. Competitive adsorption of Pb(II), Cd(II) and Cu(II) onto chitosan-pyromellitic dianhydride modified biochar. *J. Colloid Interface Sci.* **2017**, *506*, 355−364.
(46) Das, T.; Debnath, A.; Manna, M. S. Adsorption of malachite green by Aegle marmelos-derived activated biochar: Novelty assessment through phytotoxicity tests and economic analysis. *Journal of the Indian Chemical Society* **2024**, *101* (9), No. 101219.
(47) Unuabonah, E. I.; et al. Successful scale-up performance of a novel papaya-clay combo adsorbent: up-flow adsorption of a basic dye. *Desalination and Water Treatment* **2015**, *56* (2), 536−551.
(48) Akpotu, S. O.; et al. Designer composite of montmorillonite-reduced graphene oxide-PEG polymer for water treatment: Enrofloxacin sequestration and cost analysis. *Chemical Engineering Journal* **2023**, *453*, No. 139771.
(49) Akpotu, S. O.; et al. Beyond the boundaries of organics biosorption: Reusable and cost-effective millet-straw-based carboxylate-functionalized mesoporous MCM-41. *Desalination and Water Treatment* **2024**, *320*, No. 100805.

https://doi.org/10.1021/acs.langmuir.5c01248
Langmuir 2025, 41, 15022−15030

4.2. Supplementary Information of Publication 3

SUPPLEMENTARY INFORMATION

Enhancing biosorbent stability, performance efficiency, and cost-effectiveness: a ternary magnetic composite for sequestration of multiple toxic metals from water

Aleksandër Peqini[1, 2*], Paul N. Diagboya[3], Seit Shallari[2], Ferdi Brahushi[2], Rolf-Alexander Düring[1]

[1]Institute of Soil Science and Soil Conservation, Research Centre for BioSystems, Land Use and Nutrition (iFZ), Justus Liebig University Giessen, Heinrich-Buff-Ring 26, 35392 Giessen, Germany

[2]Department of Environment and Natural Resources, Faculty of Agriculture and Environment, Agricultural University of Tirana, 1029 Tirana, Albania

[3]Environmental fate of chemicals and remediation (EnFaCRe) laboratory, Department of Environmental Management and Toxicology, University of Delta, Agbor, Nigeria

[*]Corresponding author

Email: aleksander.peqini@umwelt.uni-giessen.de

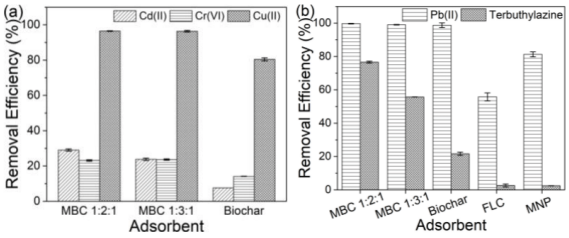

SI Fig. 1 Removal efficiency of (a) Cd(II), Cr(VI), and Cu(II) on MBC 1:2:1, MBC 1:3:1, and biochar; and (b) Pb(II) and terbuthylazine on MBC 1:2:1, MBC 1:3:1, biochar, FLC, and MNP

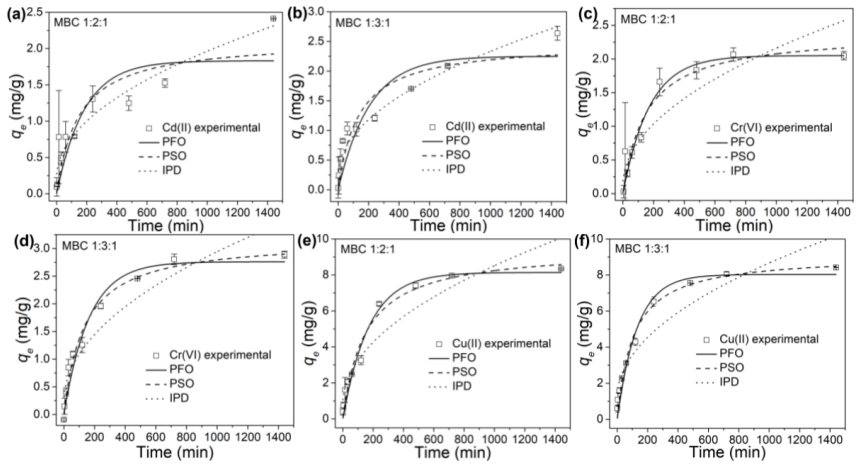

SI Fig. 2 Kinetics modeling of rate data for adsorption of (a) Cd(II) on MBC 1:2:1, (b) Cd(II) on MBC 1:3:1; (c) Cr(VI) on MBC 1:2:1 (d) Cr(VI) on MBC 1:3:1; (e) Cu(II) on MBC 1:2:1, (f) Cu(II) on MBC 1:3:1

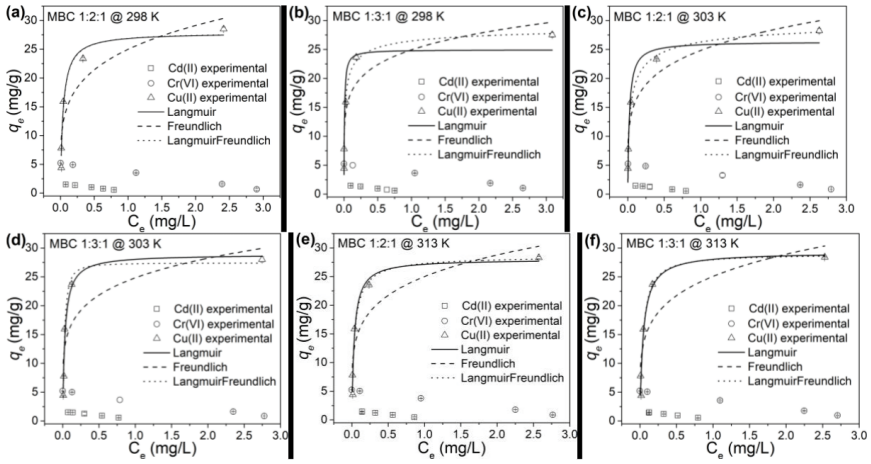

SI Fig. 3 Isotherm model fittings for Cu(II) on (a) MBC 1:2:1, (b) MBC 1:3:1 at 20 °C, (c) MBC 1:2:1, (d) MBC 1:3:1 at 30 °C, (e) MBC 1:2:1, (f) MBC 1:3:1 at 40 °C

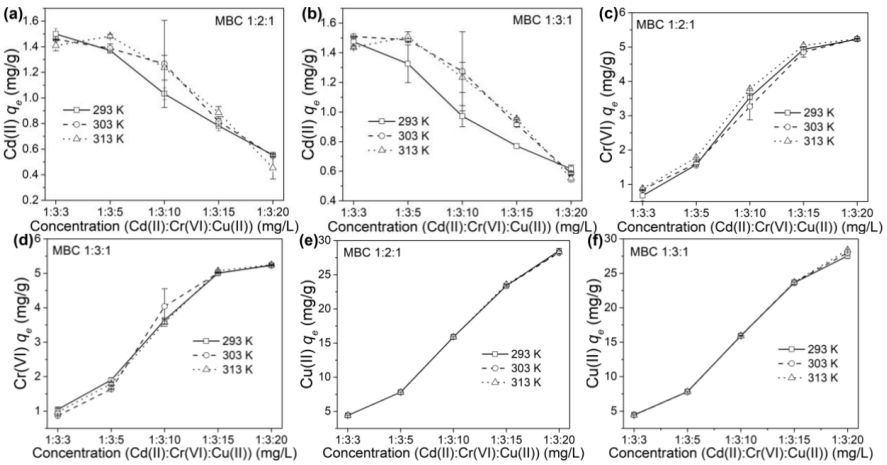

SI Fig. 4 Effect of temperature on adsorption of (a) Cd(II) on MBC 1:2:1,(b) Cd(II) on MBC 1:3:1; (c) Cr(VI) on MBC 1:2:1 (d) Cr(VI) on MBC 1:3:1; (e) Cu(II) on MBC 1:2:1, (f) Cu(II) on MBC 1:3:1

SI Table 1. Ionic properties of Cd(II), Cr(VI) and Cu(II)

Property	Cr(VI)	Cu(II)	Cd(II)
Atomic weight	51.01	63.55	112.41
Molecular weight	294.18	134.45	769.52
Electronic configuration	$[Ar]3d^5 4s^1$	$[Ar]3d^{10}4s^1$	$[Kr]4d^{10}5s^2$
Electronegativity	1.66	1.9	1.69
Ionic radii (A^0)	0.52	0.72	0.95
Hydrated radii (A^0)	4.61	4.19	4.26
Coordination number	6 & 4	2 & 4	6 & 4
Standard Reduction Pot. (V)	$Cr^{6+} + 3e^- \rightarrow Cr^{3+}$(1.1) $Cr^{3+}3e^- \rightarrow Cr$ (-0.74)	$Cu^{2+} + 2e^- \rightarrow Cu$ (0.34)	$Cd^{2+} + 2e^- \rightarrow Cd$ (-0.403)

Source: [1, 2]

SI Table 2. Interactions of metal ions in ternary systems

Metal System	MBC 1:2:1		MBC 1:3:1	
	R_i (%)	Interaction	R_i (%)	Interaction
Cadmium				
Cd(II) + Cr(VI) + Cu(II)	103	No interaction	81	Antagonistic
Chromium				
Cr(VI) + Cd(II) + Cu(II)	1510	Synergistic	29298	Synergistic
Copper				
Cu(II) + Cd(II) + Cr(VI)	109	Slightly synergistic	111	Slightly synergistic

SI Table 3. Cost analysis of MBC 1:2:1/MBC 1:3:1 production

Preparation phase		Cost assignment	Cost for ($)		Cost in stages ($)	Cost MBC 1:2:1/MBC 1:3:1 ($)
			Chemicals	Energy		
Arrangement of precursor for	Procurement (FLC)	$Cost_{AAP}$	0.125/0.1	–	0.365/0.34	5.5627/5.5154
	Transport		–	0.23		
	Packaging and storage		0.01	0.01		
Pre-treatment of precursors	Cleaning	$Cost_{PP}$	0.18/0.2	–	1.48/1.5	
	Drying		–	0.4		
	Size reduction		–	0.9		
Preparation and pyrolysis	Heating	$Cost_{Pyro}$	–	0.87	1.591/1.559	
	$FeCl_3$		0.15/0.12			
	$FeSO_4 \cdot 7H_2O$		0.014/0.012			
	Shaken			0.08		
	Centrifugation			0.027		
	Washing		0.45			
Chemical activation	NaOH treatment	$Cost_{CA}$	1.6		1.615	
	Stirring			0.015		
Others cost	Offset cost	$Cost_{Others}$	10% of $		0.5057/0.5014	

Sources: [3, 4]

4

REFERENCES

1. Jain, M., et al., *Adsorption of heavy metals from multi-metal aqueous solution by sunflower plant biomass-based carbons.* International Journal of Environmental Science and Technology, 2015. **13**(2): p. 493-500.
2. Khelifi, O., et al., *Response Surface Modeling and Optimization of Ni(II) and Cu(II) Ions Competitive Adsorption Capacity by Sewage Sludge Activated Carbon.* Arabian Journal for Science and Engineering, 2021. **47**(5): p. 5797-5809.
3. Das, T., A. Debnath, and M.S. Manna, *Adsorption of malachite green by Aegle marmelos-derived activated biochar: Novelty assessment through phytotoxicity tests and economic analysis.* Journal of the Indian Chemical Society, 2024. **101**(9): p. 101219.
4. Unuabonah, E.I., et al., *Successful scale-up performance of a novel papaya-clay combo adsorbent: up-flow adsorption of a basic dye.* Desalination and Water Treatment, 2015. **56**(2): p. 536-551.

5. List of peer-reviewed publications

The list shows all peer-reviewed publications that were published during the period of doctoral studies:

Junck, J., Diagboya, P.N., **Peqini, A.,** Rohnke, M., Düring, R-A. (2024) Mechanistic interpretation of the sorption of terbuthylazine pesticide onto aged microplastics. Journal of Environmental Pollution 345, 123502. DOI: 10.1016/j.envpol.2024.123502

> **Authors contributions: Johannes Junck:** Writing – review & editing, Writing – original draft, Visualization, Validation, Methodology, Investigation, Formal analysis, Conceptualization. **Paul N. Diagboya:** Writing – review & editing, Writing – original draft, Validation, Supervision, Resources, Project administration, Methodology, Investigation, Formal analysis, Conceptualization. **Aleksander Peqini:** Writing – review & editing, Validation, Investigation, Formal analysis. **Marcus Rohnke:** Formal analysis, Investigation, Methodology, Validation, Writing – review & editing. **Rolf-Alexander Düring:** Writing – review & editing, Supervision, Resources, Project administration, Conceptualization.

Peqini, A., Heyde, B.J., Brahushi, F., Düring, R-A. (2025) Integrated analysis of the occurrence and in situ sediment-water partitioning of selected pharmaceuticals in a riverine system. Environmental Sciences Europe 37:212, (2025). DOI: 0.1186/s12302-025-01264-w

> **AP** executed the experiments, carried out the investigation and data curation, performed formal analysis, developed methodology, validated results, and prepared the initial draft. He was also responsible for resource collection (water and sediment sampling) and securing funding. BJH contributed to conceptualization, methodology development, data analysis, and validation. He also provided software support and was actively involved in reviewing and editing the manuscript. FB contributed to conceptualization and methodology, supervised the work, supported funding acquisition, and assisted in reviewing and editing the manuscript. RAD was involved in conceptualization, methodology, and validation, provided resources, supervised the research, administered the project, supported funding acquisition, and contributed to reviewing and editing the manuscript.

Peqini, A., Diagboya, P.N., Shallari, S., Brahushi, F., Düring, R-A. (2025) Enhancing Biosorbent Stability, Performance Efficiency, and Cost-effectiveness: A Ternary Magnetic Composite for Sequestration of Multiple Toxic Metals from Water. Langmuir 41, 23, 15022-15030. DOI: 10.1021/acs.langmuir.5c01248

Aleksandër Peqini: Writing – review & editing, Writing – original draft, Visualization, Validation, Software, Methodology, Investigation, Formal analysis, Conceptualization. **Paul N. Diagboya:** Writing – review & editing, Writing – original draft, Validation, Software, Project administration, Methodology, Formal analysis. **Ferdi Brahushi:** Writing – review & editing, Supervision, Project administration, Methodology, Funding acquisition, Conceptualization. **Rolf-Alexander Düring:** Writing – review & editing, Supervision, Resources, Project administration, Methodology, Funding acquisition, Conceptualization.

Peqini, A., Diagboya, P.N., Brahushi, F., Düring, R-A. (2025) Sustainable removal of aqueous naproxen using a ternary magneto-biochar-clay composite: Competition with carbamazepine and influence of dissolved organic matter. Chemical Engineering Journal Advances 23, 100784. DOI: 10.1016/j.ceja.2025.100784

Aleksandër Peqini: Writing – review & editing, Writing – original draft, Visualization, Validation, Software, Methodology, Investigation, Formal analysis, Conceptualization. **Paul N. Diagboya:** Writing – review & editing, Writing – original draft, Validation, Software, Project administration, Methodology, Formal analysis. **Ferdi Brahushi:** Writing – review & editing, Supervision, Project administration, Methodology, Funding acquisition, Conceptualization. **Rolf-Alexander Düring:** Writing – review & editing, Supervision, Resources, Project administration, Methodology, Funding acquisition, Conceptualization.

6. List of conference contributions

The following list includes all contributions that have been presented at conferences, either as posters or oral presentations:

Peqini, A., Brahushi, F., Diagboya, P.N., Düring, R-A.: Magnetic-biochar-clay composite as an efficient adsorbent for pollutants in waters. International Conference on Agriculture and Life Sciences (ICOALS IV) 2023, Tirana, Albania. Presentation.

Peqini, A., Brahushi, F., Heinrich, A.P., Junck, J., Heyde, B.J., Düring, R-A.: Occurrence of selected pharmaceuticals in surface water of the Ishmi basin, Albania. WASSER 2024, Limburg, Germany. Poster.

Peqini, A., Diagboya, P.N., Brahushi, F., Düring, R-A.: Ternary magnetic-biochar-clay composite as efficient adsorbent for aqueous naproxen and carbamazepine: pH effect. SETAC-GLB 2024, Giessen, Germany. Poster.

Peqini, A., Diagboya, P.N., Brahushi, F., Düring, R-A.: Ternary magneto-biochar-clay composite as efficient adsorbent for aqueous naproxen and carbamazepine from Ishmi River water in Albania. IX Scientific International Conference Conserving Soils and Water 2024, Varna, Bulgaria. Poster.

Peqini, A., Brahushi, F., Düring, R-A.: In situ partitioning of selected anti-inflammatory agents in the water-sediment system: effect of pH. SETAC-GLB 2025, Dessau, Germany. Poster.

Peqini, A., Heyde, BJ., Brahushi, F., Düring, R-A.: In situ partitioning of selected antibiotics in the water-sediment system: effect of pH. International Conference on Agriculture and Life Sciences (ICOALS V) 2025, Tirana, Albania. Presentation.

Peqini, A., Finis, LM., Brahushi, F., Düring, R-A.: Potential applications of biochar from organic waste in Albania, with a focus on irrigation water treatment. International Conference on Agriculture and Life Sciences (ICOALS V) 2025, Tirana, Albania. Poster.

Peqini, A., Heyde, BJ., Brahushi, F., Düring, R-A.: In situ partitioning of selected antibiotics in the water-sediment system: effect of pH. International Scientific Conference ``Conserving Soils and Water 2025``, Varna, Bulgaria. Poster.

7. Acknowledgements

At the beginning of my PhD journey, I had doubts about whether I would be able to achieve meaningful results. This uncertainty stemmed from my transition from researching environmental pesticides to exploring the field of pharmaceuticals. Adapting to this new area required me to start learning about their applications, effects, and behavior. This transition was made possible thanks to the continuous support and guidance of my PhD supervisors, Prof. Dr. Rolf-Alexander Düring and Prof. Dr. Ferdi Brahushi**.**

I am sincerely grateful to Prof. Dr. Düring for his willingness to host and supervise my research, and for always being available for discussions, his door was truly always open. My heartfelt thanks also go to my other supervisor, Prof. Dr. Brahushi for his valuable insights, suggestions, and thoughtful, reflective discussions.

This study would not have been possible without the support of the Deutsche Bundesstiftung Umwelt (DBU). I thank Mr. Alexander Bittnerfor his trust and unwavering support, and Dr. Nicole Freyer-Wille and Sonja Beiderwellen for their tireless assistance with the program, seminars, advice, and administrative matters.

I would also like to thank my colleagues for their help and for warmly welcoming me to the team. Special thanks to Andre Heinrich**,** Johannes Junck, and Benjamin Heyde for their support, valuable suggestions, and positive spirit. I am particularly grateful to Paul Diagboya for his early guidance in the lab and for patiently answering my many questions. My thanks also go to the technicians of the Soil Science Institute, Elke Schneidenwind and Elke Müller, for their dedicated work in analyzing my numerous samples of water, sediment, and biochar. I appreciate the entire Soil Science and Department of Environment and Natural Resources teams for their helpful input during seminars and presentations.

I owe my deepest gratitude to my family, my grandmother, parents, and brothers, for their unwavering support and comforting conversations.

Finally, I extend my heartfelt thanks to my girlfriend, for her patience, encouragement, and understanding through all the challenges. Your support made this journey much easier.

8. Statutory declaration

I declare that the doctoral thesis here submitted is entirely my own work, written without any unauthorized help by a third party and solely with the assistance referred to in the thesis. I have indicated in the text those texts that have been quoted from already published sources, either verbatim or by analogy and all statements based on verbally conveyed information. During the research carried out by me and referred to in the doctoral thesis, I have at all times followed the principles of good scholarly practice as defined in the Statue of Justus Liebig University Giessen for Ensuring of Good Academic Practice.

_____

Aleksandër Peqini